EFFECTS OF DEPLETION OF CHRNA5 AND/OR TP53, AND TRANSIENT AND STABLE OVEREXPRESSION OF WILDTYPE OR MUTANT TP53 ON EXPRESSION OF DLK1-MEG3 LOCUS IN MCF7 CELLS

A THESIS SUBMITTED TO
THE GRADUATE SCHOOL OF ENGINEERING AND SCIENCE OF
BILKENT UNIVERSITY
IN PARTIAL FULFILLMENT OF THE REQUIREMENTS FOR THE
DEGREE OF
MASTER OF SCIENCE
IN
MOLECULAR BIOLOGY AND GENETICS

By

Burçin İrem Arıcı

September 2022

EFFECTS OF DEPLETION OF CHRNA5 AND/OR TP53, AND TRANSIENT AND STABLE OVEREXPRESSION OF WILDTYPE OR MUTANT TP53 ON EXPRESSION OF DLK1-MEG3 LOCUS IN MCF7 CELLS

By Burçin İrem Arıcı
September 2022

We certify that we have read this thesis and that in our opinion it is fully adequate, in scope and in quality, as a thesis for the degree of Master of Science.

Özlen Konu Karakayalı (Advisor)

Onur Çizmecioğlu (Co-Advisor)

Murat Alper Cevher

Ceren Sucularlı

Approved for the Graduate School of Engineering and Science

Orhan Arıkan
Director of the Graduate School of Engineering and Science

Abstract

EFFECTS OF DEPLETION OF CHRNA5 AND/OR TP53, AND TRANSIENT AND STABLE OVEREXPRESSION OF WILDTYPE OR MUTANT TP53 ON EXPRESSION OF DLK1-MEG3 LOCUS IN MCF7 CELLS

Burçin İrem Arıcı

MSc. in Molecular Biology and Genetics

Supervisor : Özlen Konu Karakayalı

Co-advisor : Onur Çizmecioğlu

September 2022

The expression of CHRNA5 has a prominent role in lung cancer and nicotine addiction. Besides, depletion of CHRNA5 has been identified as being tumour suppressive in breast cancer. Moreover, CHRNA5 depletion causes increases in CDKN1A expression, downregulates the 14q32.31 miRNAs and decreases DLK1 expression. This thesis examined the effects of CHRNA5 and/or TP53 downregulation, as well as TP53 overexpression, on the expression of the DLK1-DIO3 region. My findings demonstrated that CHRNA5 depletion decreased the expression of the protein-coding DLK1 and the non-protein coding MEG3 genes in this locus in the presence or absence of TP53. Since these two genes have a vital role in tumour suppression and tumorigenesis, this provided more evidence for the importance of CHRNA5 in the modulation of expression in this locus in breast cancer. Since there is a relation between CHRNA5 and TP53 induction, the expression of one of the main TP53 regulators, MDM2, was also studied. Accordingly, it was found that combining CHRNA5 depletion with

TP53 depletion caused a significant decrease in expression in both the MDM2 and MDM2 sequestering elements, PDLIM7 and CDH18. Additionally, the effects of both wild-type and mutant TP53 expression levels on DLK1-MEG3 locus and CHRNA5 were investigated in stable MCF7 breast cancer cells that we have generated. I have found that even if CHRNA5 depletion induced p53 expression, TP53 overexpression did not have CHRNA5-inducing effects regardless of the functionality of TP53. However, wild-type TP53 overexpressing MCF7 cells behaved differently than mutant TP53 overexpressing cells in their DLK1 expression levels. Future research should clarify the effects of CHRNA5 depletion on DLK1-MEG3 region for a given TP53 mutation status.

Keywords: Breast cancer, cholinergic receptors, CHRNA5, 14q31.32 miRNA cluster, RNAi, TP53 signalling, stable cell line, DLK1-MEG3 region

Özet

CHRNA5 VE/VEYA TP53 DEPLESYONU VE DOĞAL TİP VE YANLIŞ ANLAMLI MUTANT TP53'ÜN GEÇİCİ VE STABİL AŞIRI İFADESİNİN MCF7 HÜCRELERİNDE DLK1-MEG3 LOKUS İFADESİNE ETKİLERİ

Burçin İrem Arıcı

Moleküler Biyoloji ve Genetik Yüksek Lisans Programı

Tez Danışmanı : Özlen Konu Karakayalı

Tez Eş Danışmanı : Onur Çizmecioğlu

Eylül 2022

CHRNA5 ifadesi akciğer kanseri ve nikotin bağımlılığında önemli bir role sahiptir. Bunun yanı sıra, CHRNA5 deplesyonu meme kanserinde tumor baskılayıcı özlleklikleri ile tanımlanmıştır. Ayrıca CHRNA5 deplesyonunun CDKN1A gen ifadesini arttırdığı ve 14q32.31 lokusunda bulunan miRNA'ları ve DLK1 geninin ifade miktarnı düşürdüğü görülmüştür. Bu çalışmada CHRNA5 tek başına ya da p53 ile birlikte siRNA ile ifadesi azaltıldığında ya da wildtype veya mutant p53 overexpresyonu sonucunda DLK1-DIO lokusunda yarattığı değişimler araştırılmıştır. Bulgularım, CHRNA5 tükenmesinin, TP53 varlığında veya yokluğunda bu lokusta protein kodlayan DLK1 ve protein kodlamayan MEG3 genlerinin ifadesini azalttığını gösterdi. Bu iki gen, tümör baskılanması ve tümör oluşumunda hayati bir role sahip olduğu için bu bulgu, meme kanserinde bu lokustaki gen ifadesinin modülasyonunda CHRNA5'in önemine daha fazla kanıt sağladı. CHRNA5 ve TP53 indüksiyonu arasında bir ilişki olduğundan, ana TP53 düzenleyicilerinden biri olan MDM2'nin ifadesi de incelenmiştir. Daha sonra, CHRNA5

tükenmesinin TP53 tükenmesi ile birleştirilmesinin, hem MDM2 hem de MDM2 ayırma elemanları, PDLIM7 ve CDH18'de ifadesinde önemli bir azalmaya neden olduğu bulundu. Ek olarak, ürettiğimiz stabil MCF7 meme kanseri hücre hatlarında hem vahşi tip hem de mutant TP53 ifade seviyelerinin DLK1-MEG3 lokusu ve CHRNA5 üzerindeki etkileri araştırıldı. CHRNA5 tükenmesi p53 ifadesini indüklese bile, TP53 aşırı ifadesinin, TP53'ün işlevselliğinden bağımsız olarak CHRNA5 indükleyici etkilere sahip olmadığı bulundu. Bununla birlikte, vahşi tip TP53 aşırı ifade eden MCF7 hücrelerinin, DLK1 ifade seviyeleri mutant TP53 aşırı ifade eden hücrelerden farklı bulundu. Gelecekteki çalışmalar, belirli bir TP53 mutasyon durumu için CHRNA5 tükenmesinin DLK1-MEG3 lokusundaki etkilerini netleştirmelidir.

Anahtar kelimeler: Meme kanseri, kolinerjik reseptörler, CHRNA5, 14q31.32 miRNA grubu, RNAi, TP53 sinyal yolağı, kararlı gen ifadesine sahip (stabil) hücre hattı, DLK1-MEG3 lokusu

To my precious family and friends...

Acknowledgements

First and foremost, I would like to express my deepest and sincere gratitude to my advisor, Assoc. Prof. Özlen Konu Karakayalı for her invaluable guidance, patience, support, and belief in me during my MSc study. I am so honoured to be her student since my undergraduate years. I believe I have been able to improve and challenge myself in my academic career because she gave me this wonderful opportunity to be one of her master's students.

I am very grateful to my co-supervisor, Asst. Prof. Onur Çizmecioğlu, who has excellent guidance and contributions with his extensive knowledge to my thesis. Thanks to him, we achieved critical steps in this study and could add different approaches that enhance the further parts of this study.

I would also like to thank my jury members, Asst. Prof. Murat Alper Cevher and Assoc. Prof. Ceren Sucularlı for accepting to be my committee members in my thesis defence, for their time to evaluate my thesis and their contributions.

I would acknowledge Şahin Lab members for sharing antibodies with us and Çizmecioğlu Lab members for sharing plasmids for this study and their knowledge on each step which I had many questions; each of them did their best whenever I had a question or needed any suggestion.

I am glad to be part of Konu Lab, and I feel fortunate to find an opportunity to have worked with them. They have always been helpful, supportive, and kind. Thanks to them, I have studied in such a friendly and pleasant environment. I could not even begin this journey without the

guidance of our former lab members, Dr Seniye Targen and Damla Güneş. I will always continue to say that I have learnt from the bests. I would also like to thank Dr Ayşe Gökçe Keşküş, who has never gotten tired of answering my endless questions, guided me to improve myself and supported me even during the most challenging times. Many thanks to Büşra Korkmaz. She has been a great friend and taught me to stay strong and be an optimist no matter what happens. I am so thankful to Melike Tombaz, Ronaldo Leka, and Farid Ahadli for their nice friendships since my undergraduate years. My sincere thanks go to Rana Acar, Moiz Aftab, Kübra Çalışır, Siber Güneş Kılınç, Güneş Tok, Rüya Tombuloğlu, Çağdaş Yanyatan, and Merve Vural. I should thank Güneş Tok and Çağdaş Yanyatan especially for their contribution to the CHRNA5 project, for helping me in the project and for their great friendship.

I would like to extend my thanks to all Bilkent University Molecular Biology and Genetics department members. All researchers, students and staff have been so helpful, friendly, and supportive all the time. As a master's student, I am so lucky to have had the opportunity to work with Melike Dinççelik Aslan, Ünal Metin Tokat, Pelin Ersan, and İrem Evcili. Pelin Makas has always endeavoured to find solutions to even minor problems in the laboratory and has always given the best advice. Seda Birkan and Sultan Turan have also made the laboratory a more manageable working environment. I would like to thank Beste Uygur for her support, for accompanying me through endless experiments and making me a more hardworking person, and Marzana Ishraq for her positive energy and understanding.

Getting through the arduous process of writing and completing my thesis would not have been possible without my family, Asiye Arıcı, Burhan Arıcı, Aysu İzel Arıcı, Serhat Aras and Merve

Zeynep Barutlu. I am eternally so grateful for their support; without them, I would not be the person I am. They have always been by my side in every decision I made.

In addition, I would like to mention Dr Ayşegül Dilsizoğlu Şenol for the inspiration she gave me and for making me want to be a scientist. I will never forget how incredible it was for me to work with her.

Lastly, I would like to thank Bilkent University Department of Molecular Biology and Genetics for giving me such an opportunity and supporting me in my graduate studies. The project in this thesis was funded by The Scientific and Technological Research Council of Turkey (TUBITAK) with grant number 114S367 and 219Z029, and I have received scholarship from TUBITAK 219Z029. Thanks to the TUBITAK BIDEB programme, I have also been awarded the BIDEB 2210/A scholarship.

Table of Contents

List of Figures

List of Tables

List of Equations

Abbreviations

ARF	**:**	Alternative reading frame
CCND1	**:**	Cyclin D1
CDH1	**:**	Cadherin 1
CDH18	**:**	Cadherin 18
CDKN1A	**:**	Cyclin dependent kinase inhibitor 1A
CHRNA5	**:**	Cholinergic receptor nicotinic alpha 5 subunit
ddH_2O	**:**	Double-distilled H_2O
DLK1	**:**	Delta like non-canonical notch ligand 1
EMT	**:**	Epithelial-to-mesenchymal transition
ER	**:**	Oestrogen receptor
EV	**:**	Empty vector
GAPDH	**:**	Glyceraldehyde 3-phosphate dehydrogenase
HER2	**:**	Human epidermal growth factor 2
IDC	**:**	Invasive ductal carcinoma
ILC	**:**	Invasive lobular carcinoma
lncRNA	**:**	Long non-coding RNA
MAP1B	**:**	Microtubule associated protein 1B
MCF-7	**:**	Michigan Cancer Foundation-7
MDA-MB-231	**:**	M.D. Anderson - Metastatic breast 231
MDM2	**:**	Mouse double minute 2 proto-oncogene
MEG3	**:**	Maternally expressed 3
METTL7A	**:**	Methyltransferase Like 7A
miR-376	**:**	hsa-miR-376a-3p
miR-495	**:**	hsa-miR-495-3p

miRNA	**:**	microRNA
MKi67	**:**	Marker of proliferation Ki-67
mRNA	**:**	messenger RNA
PDLIM7	**:**	PDZ and LIM domain 7
PFA	**:**	Paraformaldehyde
PR	**:**	Progesterone receptor
qPCR	**:**	Quantitative polymerase chain reaction
RASGRP1	**:**	RAS guanyl-releasing protein 1
RNAi	**:**	RNA interference
siRNA	**:**	Small interfering RNA
TGFBR2	**:**	Transforming growth factor β receptor type 2
TME	**:**	Tumor microenvironment
TNBC	**:**	Triple-negative breast cancer
TP53	**:**	Tumor protein P53
TPT1	**:**	Tumor protein, translationally controlled 1
VIM	**:**	Vimentin

Chapter 1

1. Introduction

1.1. Cancer

Cancer is a main nomenclature describing a disease which occurs when the cells initiate to divide abnormally and uncontrollably, with a potential for metastasis and invasion. The ability to invade and metastasise into other tissues can be considered to classify cancer cells into two major groups: malignant (cancerous) tumours and benign (noncancerous) tumours (Sarkar et al., 2013). According to a published article in 2000, cancer's six fundamental characteristics are escaping from apoptosis, tissue invasion & metastasis, limitless cell division, inducing angiogenesis, insensitivity to growth suppression, and self-maintaining growth signals (Hanahan & Weinberg, 2000). Thanks to a more comprehensive understanding of the complexity, differential progression of cancer and the importance of the tumour microenvironment (TME), two hallmarks and two enabling characteristics parameters were added; avoiding immune destruction, deregulation of energy metabolism, genome instability & mutation and inflammation induced by a tumour (Hanahan & Weinberg, 2011).

Recently, these parameters have been improved, and additional characteristics were proposed. Phenotypic plasticity and disrupted differentiation are listed as hallmarks, and non-mutational epigenetic reprogramming and microbiome are depicted as new enabling characteristics of cancer (Hanahan, 2022).

Despite novel and successful approaches and evolving research in cancer treatments, as a subgroup of noncommunicable diseases, cancer is one of the primary causes of death for approximately 10M people globally in 2020 (Sung et al., 2021). Aggressive and complex characteristics with accompanying high fatality reveal the significance of understanding carcinogenesis.

1.1.1. Breast Cancer

According to the last version of the GLOBOCAN (Global Cancer Observatory: CANCER TODAY) report, breast cancer had the highest incidence rate at 11.7% for both genders. Furthermore, it showed the highest mortality rate at 15.5% and the highest ASR (Age-Standardized Rate) score at 47.8 in females of all ages as the most diagnosed cancer type among all other cancer types in 2020 (Sung et al., 2021). In Turkey, the incidence rate is 23.9%, which is still the most observed type of cancer in females. The 15.1% mortality rate makes female breast cancer the leading cause of death due to cancer, among other cancers in women. Furthermore, a highly expected increase in global numbers of new breast cancer cases was established from 2.26M to 3.19M between 2020 and 2040 in light of information from the Global Cancer Observatory: Cancer Tomorrow data visualisation tool, as depicted in **Figure *1-1*** (Ferlay et al., 2020). Considering the high mortality rate and the possible increase in the number of patients, it can be stated that more advanced therapeutic approaches and a better understanding of breast cancer progression are necessary.

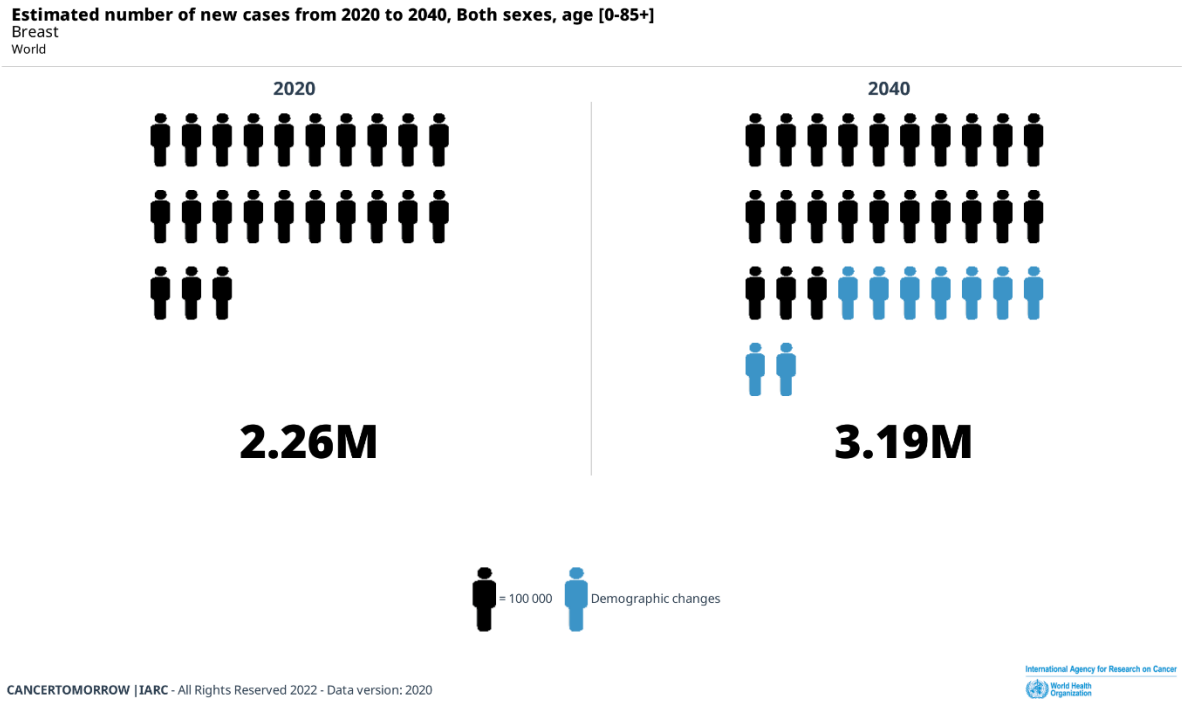

Figure 1-1. Estimated number of newly diagnosed patients between 2020-2040 in females of all ages worldwide according to Cancer Tomorrow.

(The image used in Figure *1-1* was not required copyright permission to reproduce. It was obtained from Ferlay J, Laversanne M, Ervik M, Lam F, Colombet M, Mery L, Piñeros M, Znaor A, Soerjomataram I, Bray F (2020). Global Cancer Observatory: Cancer Tomorrow. Lyon, France: International Agency for Research on Cancer. Available from: https://gco.iarc.fr/tomorrow, accessed September 5, 2022.)

1.1.2. Subtypes of Breast Cancer

Breast cancer provides dramatic phenotypic and genotypic diversity. Due to its heterogeneous structure, breast cancer is studied according to the characterisation of its subtypes to determine the most promising therapeutic approach and predict the potential prognosis of the tumour (Skibinski & Kuperwasser, 2015). Different classification methods have been used, and new approaches continue to be added.

Histological classification of breast cancer has been studied for years and divided breast cancer into two groups invasive and in situ carcinoma. These also have two major subtypes ductal and lobular carcinomas. The most frequently diagnosed subtype of breast cancer is invasive ductal carcinoma (IDC), ~80% of the breast cancer patients, followed by invasive lobular carcinoma (ILC), with a rate of ~10% (Du et al., 2018; Weigelt et al., 2008; Zhao, 2021). ILC differentiate from IDC with also molecular characteristics. E-Cadherin, CDH1 and PTEN loss is observed with strongly induced AKT signalling in ILC. In contrast, low AKT levels with intact cell adhesion morphology are observed in IDCs. Additionally, FOXA1 mutations in ILC and GATA3 mutations in IDC separate them in the regulation of ER activity (Barroso-Sousa & Metzger-Filho, 2016; Ciriello et al., 2015).

In addition to the histological and functional classification of breast cancer, molecular characterisation was proposed for examining the phenotypic diversity on gene expression level or finding a more promising prognostic approach considering this complexity (Perou et al., 2000). By this contribution, breast cancer is characterised as Luminal A & Luminal, Her2+, Basal Like, Claudin-Low and Normal Like Breast Cancers. Certain immunohistochemical (IHC) markers were used to identify molecular subgroups of breast cancer. Used markers are oestrogen receptor (ER), human epidermal growth factor 2 (HER2), progesterone receptor (PR) and Ki67 expression status (Perou et al., 2000; Sørlie et al., 2001).

The most diagnosed breast cancer subtype, among others, is Luminal A, which has positive oestrogen receptor expression status (ER+) with the lower expression of cell proliferative and prognostic marker, Ki67; therefore, it exhibits a lower growth rate and a better prognosis (Ahn et al., 2015; LI et al., 2015; Yersal, 2014). PR expression can be commonly observed in both types of luminal breast cancer; however, there is PR- Luminal B breast cancer.

Unlike the Luminal A cluster, the Luminal B subgroup also has HER2 expression characteristics (HER2+) and higher proliferation-related gene expression than Luminal A since HER2 is one of the prognostic markers, which causes the more aggressive cancer type with worse prognosis and higher growth rate (Li et al., 2016; Loi et al., 2009).

HER2-enriched (HER2+) breast cancers do not have ER or PR expression, whereas these express increased levels of HER2 with other growth factor receptor-related genes. It leads to a poor prognosis with aggressive characteristics, although it shows successful results of HER2 targeting therapeutic approaches (Cancer Genome Atlas Network, 2012; Slamon et al., 1987).

Basal-like, also called triple-negative breast cancer (TNBC), is characterised according to lack of ER, PR and HER2 expressions, yet it highly expresses basal markers. Consequently, it is unsuitable for these IHC markers, and mainly DNA damage-inducing approaches are tried due to high TP53 and BRCA1/2 mutations (Gelmon et al., 2012; Lehmann et al., 2011). TNBC is a poorly prognosed, aggressive and highly metastatic breast cancer subtype (Dent et al., 2007).

Claudin-low breast cancers were firstly considered a subcluster of TNBCs due to expressing low luminal differentiation and proliferation genes. In contrast, it has enhanced expression of epithelial-to-mesenchymal transition (EMT) genes which may cause therapeutic resistance and worse prognosis (Pommier et al., 2020; Prat et al., 2010). Recent research hypothesises it is another intrinsic subtype of breast cancer due to its low genomic instability and heterogeneous proliferative gene expression pattern among subtypes (Fougner et al., 2020).

Normal-like breast cancers have the same IHC marker expression profile as the Luminal A subtype but have high similarity with the normal breast tissue gene expression profile; therefore, it may not be included in the breast cancer subtyping (Dai et al., 2015).

1.2. TP53 Signalling

TP53 is a gene encoding tumour suppressor and transcription factor p53 protein, mostly mentioned as the "guardian of the genome" due to its major role in DNA damage response (DDR) (Lane, 1992). TP53 has remained one of the most studied genes in cancer for decades since its crucial function in several biological responses especially inducing apoptosis, DNA repair, cell cycle arrest, senescence, activation of oncogenes, changes in metabolism and mitophagy (Levine, 2020).

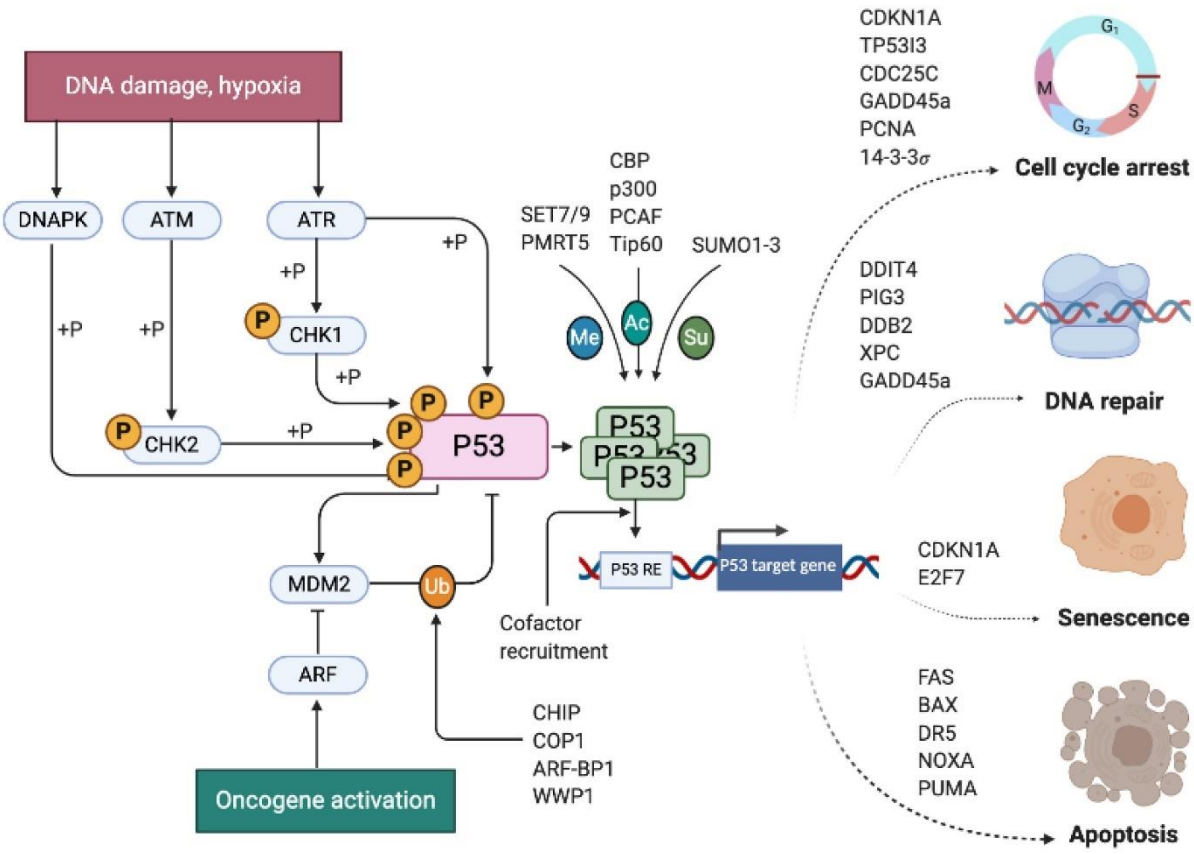

Figure 1-2. General overview of activation, regulation, and the response of p53.

(The image used in *Figure 1-2* was not required copyright permission to reproduce. It was obtained from Hernández Borrero, L. J., & El-Deiry, W. S. (2021). Tumour suppressor p53: Biology, signalling pathways, and therapeutic targeting. *Biochimica et biophysica acta. Reviews on cancer*, *1876*(1), 188556. https://doi.org/10.1016/j.bbcan.2021.188556)

P53 regulation is maintained by various post-translational modifications (PTMs) depending on presenting under normal homeostatic or stress-induced conditions. P53 is regularly degraded by MDM2/MDMX, which is an E3 ubiquitin ligase induced by wild-type p53. P53 stability is regulated under non-stressed conditions via a negative feedback loop, and in this way, p53 expression is kept at a low level (Barak et al., 1993; Kubbutat et al., 1997) (**Figure *1-2***). As another upstream regulator, ARF, or p14, inhibits ubiquitin ligase activity of MDM2 or prevents MDM2-p53 duplex formation, and leads to p53 activation and stabilisation under cellular stress conditions, specifically oncogenic stress (Llanos et al., 2001; Midgley et al., 2000).

1.2.1. Downstream Effects of TP53

As a response to any stress conditions, i.e., DNA damage, oxidative stress, hypoxia, and activation of an oncogene, p53 is stabilized by various mechanisms.

Cell cycle arrest is the most considered effect of p53 activation, among other responses. Phosphorylation of p53 on Ser20 and Ser15 residues occurred in response to stress factors, especially DDR proteins (Appella & Anderson, 2001). This p53 phosphorylation on Ser20 or ARF leads to the separation of the MDM2-p53 complex, and elevated p53 expression induces p21-RB1 signalling. P53 induces transcription of Cyclin-dependent kinase inhibitor 1A (CDKN1A), p21 protein-encoding gene (He et al., 2005). Inhibition of G_1/S phase mediators, CDK4/6, by p21 causes hypo-phosphorylation of RB protein, thus inhibiting dissociation of

RB-E2F complex and transcription of cell cycle progression genes targeted by E2F, so it causes cell cycle arrest at the G_1 phase (Giacinti & Giordano, 2006). Inhibition of DNA replication and G_2/M arrest can be modulated by p53 by interaction with PCNA and 14–3-3σ and translational modifications (Hermeking et al., 1997).

Following the cell cycle arrest, p53 initiates and regulates the DNA repair mechanism of the specific region and prevents the accumulation of oncogenic mutated genome by limiting the proliferation of the cell with cell cycle arrests. When DNA damage is maintainable for the DNA repair mechanism, p53 induces DNA repair mechanisms at the end of the cell cycle arrest by activating target genes of proper DNA repair mechanism according to the type of DNA damage (Williams & Schumacher, 2016).

If the genomic instability or the cellular stress is not sustainable for repair mechanisms, p53 can activate senescence or apoptosis. Thus, senescence and ageing are crucial roles of p53. P53 acetylation promoted by RAS and NORE1A/HIPK2 complex can lead to cellular senescence (Donninger et al., 2015; Rufini et al., 2013).

After p53 activation due to stress stimuli, p53 can induce apoptosis directly via activating transcription of PUMA and NOXA, which belong to pro-apoptotic BH3-only members of the BCL-2 protein family. PUMA and NOXA can inhibit pro-survival BCL-2 proteins (Happo et al., 2010). P53 can indirectly induce apoptosis by inducing miR34a expression, which reduces the BCL-2 level (Yamakuchi et al., 2008) and induce the genes encoding FAS and DR5, causing sensitisation to death receptor ligands (Sheikh & Fornace, 2000).

1.2.2. Turnover and stability of MDM2 in Senescence After Growth Arrest

Since one of the main focuses in this study is the regulation of TP53 through CHRNA5 depletion and its effects and leadings, MDM2 was also considered one of the critical points as its role in TP53 regulation, being one of the two main upstream elements and also having crucial effects on senescence.

CDK4 inhibition in Rb-positive cells can lead to senescence via the reduction of phosphorylated Rb in some liposarcoma cells independent of TP53 action (Kovatcheva et al., 2015). The authors had shown that when unphosphorylated Rb accumulated, this acted like a CDK4 inhibitor through deciding between quiescence and senescence as a cell fate. Interestingly in this study, MDM2 expression together with Cyclin A and ARF were reduced with unphosphorylated Rb accumulation or CDK4 inhibitor Palbociclib (PD0332991). More interestingly, they have found that the ability of MDM2 reduction to induce senescence derived from MDM2's E3 ligase activity and via TP53 binding domain based on testing MDM2 mutants and MDM2 knockdown was capable of inducing senescence in PD0332991 unresponsive cells and not treated PD0332991 untreated responsive cells. Another intriguing aspect of this study and MDM2's ability to induce is that it could be TP53-independent because E3 ligase activity and not p53 binding ability is the main culprit behind senescence induced by MDM2 loss. This study also has led to the identification of the mechanisms that gave rise to the downregulation of MDM2, whether it is transcriptional, translational or posttranslational. The authors have demonstrated that MDM2 became unstable via autoubiquitination but not by HAUSP/USP7 yet via ATRX, a chromatin remodeler; this mechanism of senescence is known as SAGA (senescence after growth arrest) (Kovatcheva et al., 2017).

Among dozens of proteins that interact with MDM2, only some of which are p53-dependent (Riley & Lozano, 2012). A recent study that knocked down selected genes from this list demonstrated that PDLIM7 and CDH18 were also involved in SAGA (Klein et al., 2018). In this study, quiescent cells that did go through senescence upon PD0332991 treatment became senescent upon knockdown of PDLIM7, suggesting that PDLIM7 was stabilizing MDM2, whose degradation was necessary for SAGA to occur. Interestingly, they also found that PDLIM7 was sequestered in cytoplasmic foci where there were CDH18 and, unlike knockdown of PDLIM7, knockdown of CDH18 prevented PD033299 induced senescence. The authors demonstrated and concluded that CDH18 sequestered PDLIM7 in cytoplasmic foci, and its absence led to higher rates of MDM2 turnover, hence senescence. Understandably, cells with low levels of CDH18 exhibited a poorer prognosis.

Accordingly, one can summarize that the downregulation of MDM2 is critical for SAGA to occur. In the quiescent state, the stability of MDM2 is regulated by PDLIM7 and CDH18, which interact in the cytoplasmic foci leaving MDM2 unprotected and auto-ubiquitinated and hence allowing the occurrence of senescence in cells in growth arrest by CDK4/6 inhibitors. This suggests that downregulation of PDLIM7 and upregulation of CDH18 may be needed for maintaining MDM2 downregulation, and this can happen in the absence of TP53.

However, in MCF7 cells, these interactions or expression levels of the MDM2-PDLIM7-CDH18 axis have not been studied and whether the depletion of TP53 by siRNA could lead to MDM2 and/or MDM2's partners that play roles in MDM2 stability and induction of SAGA. Moreover, it is not known whether siRNA against CHRNA5 that leads to growth arrest/quiescence can function as a CDK4/K inhibitor and modulate MDM2 levels.

1.2.3. Mutations of TP53

Besides being one of the most studied genes, TP53 is also the most frequently mutated gene in cancer, accounting for over 50% of all cancers and 30% of breast cancers (Bouaoun et al., 2016; Duffy et al., 2018). The most p53 mutations, 73%, are missense, point mutations located on the DNA-binding domain (DBB) and referred to as hotspots since these high frequently mutated locations (Bouaoun et al., 2016). Mutant p53 status leads to downregulation or even inhibition of downstream responses of p53, i.e., DNA repair, cell cycle arrest, autophagy and apoptosis. Even in the presence of wild-type p53 with mutant p53, the dominant negative effect can compensate for the wild-type. Due to the mutations in DBD, mutant p53 is not able to bind most elements (**Figure *1-3***).

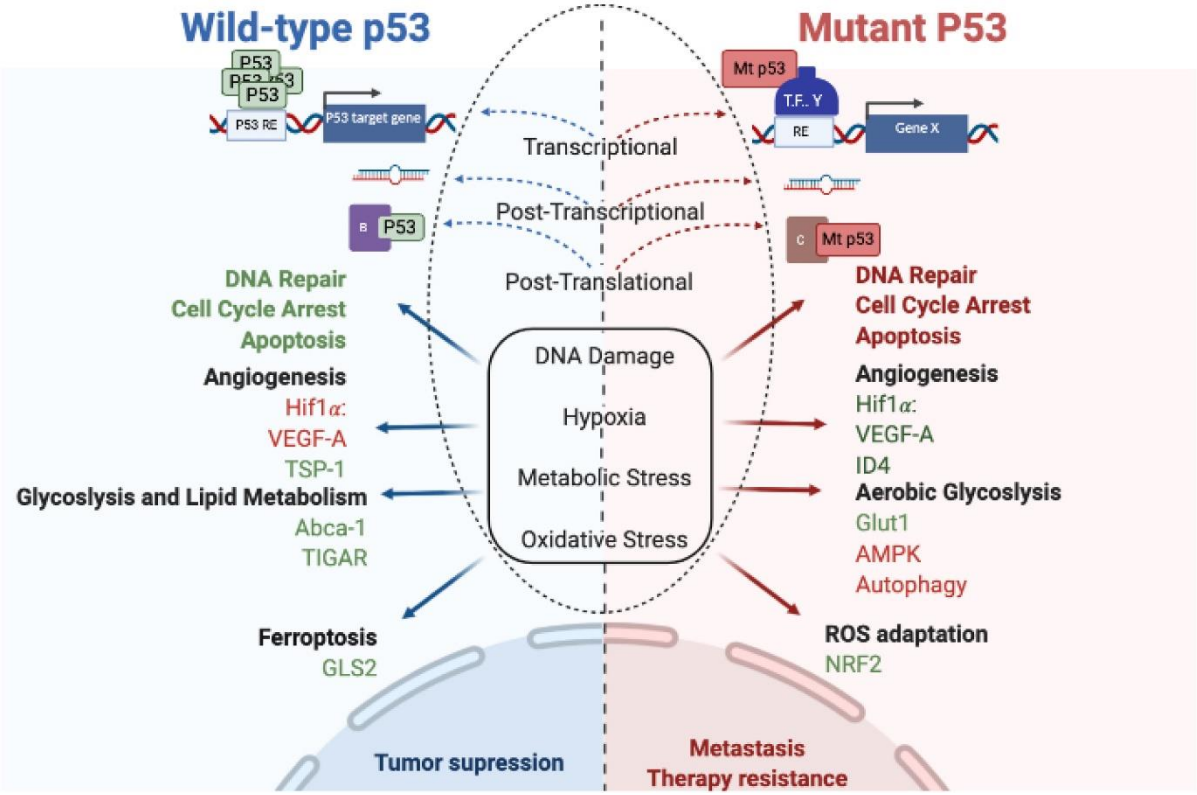

Figure 1-3. Differentiated effects of wild-type and mutant p53 regulation in cancer. Wild-type p53 function as a tumour suppressor, whereas mutant p53 leads to metastasis and resistance against therapy. Upregulated genes and responses are coloured green, and down-regulated responses and genes are coloured red.

(The image used in **Figure *1-3*** was not required copyright permission to reproduce. It was obtained from Hernández Borrero, L. J., & El-Deiry, W. S. (2021). Tumour suppressor p53: Biology, signalling pathways, and therapeutic targeting. *Biochimica et biophysica acta. Reviews on cancer*, *1876*(1), 188556. https://doi.org/10.1016/j.bbcan.2021.188556)

P53 mutations are mainly separated into two main classes depending on their structural and functional properties: the conformational mutants, e.g., R175H and R249S, and the contact site mutations, e.g., R248W and R273H. The conformational mutations change the structure of a protein by folding compared to wild-type structure, while the contact site mutation has only a small change on locus at the site where wild-type p53 binds to DNA and prevents binding (Cho et al., 1994; Hainaut & Pfeifer, 2016; Rolley et al., 1995). R175H, 248W and R273H missense, dominant-negative mutations were studied in this thesis in addition to wild-type TP53.

1.3. MicroRNAs

MicroRNAs (miRNAs) are endogenously expressed, non-coding RNAs consisting of approximately 22 bp and regulate gene expressions canonically by binding mRNAs via recognition at their 3'untranslated region (UTR). miRNAs have crucial roles in numerous biological processes, i.e., cancer, cell differentiation and apoptosis, proliferation, drug resistance and EMT processes (Hayashita et al., 2005a, 2005b; Kim et al., 2022; Matsubara et al., 2007; McManus, 2003; Peng & Croce, 2016; Tagawa et al., 2007; B. Zhang et al., 2007).

1.4. DLK1-DIO3 Region

DLK1-DIO3 region is located at 14q32 and harbours three paternally expressed genes, which are Delta-Like Ligand 1 (DLK1), Retrotransposon Gag-Like 1 (RTL1) and Iodothyronine deiodinase 3 (DIO3), and maternally expressed non-coding Maternally Expressed Gene 3 & 8 and anti-RTL1 genes in addition to 54 miRNAs (***Figure 1-4)*** In this study, we focused on the

MEG3 and DLK1 expression patterns; besides miRNAs on this locus, expression of these genes are regulated by imprinting control regions via hypermethylation and hypomethylation, respectively (Enterina et al., 2017).

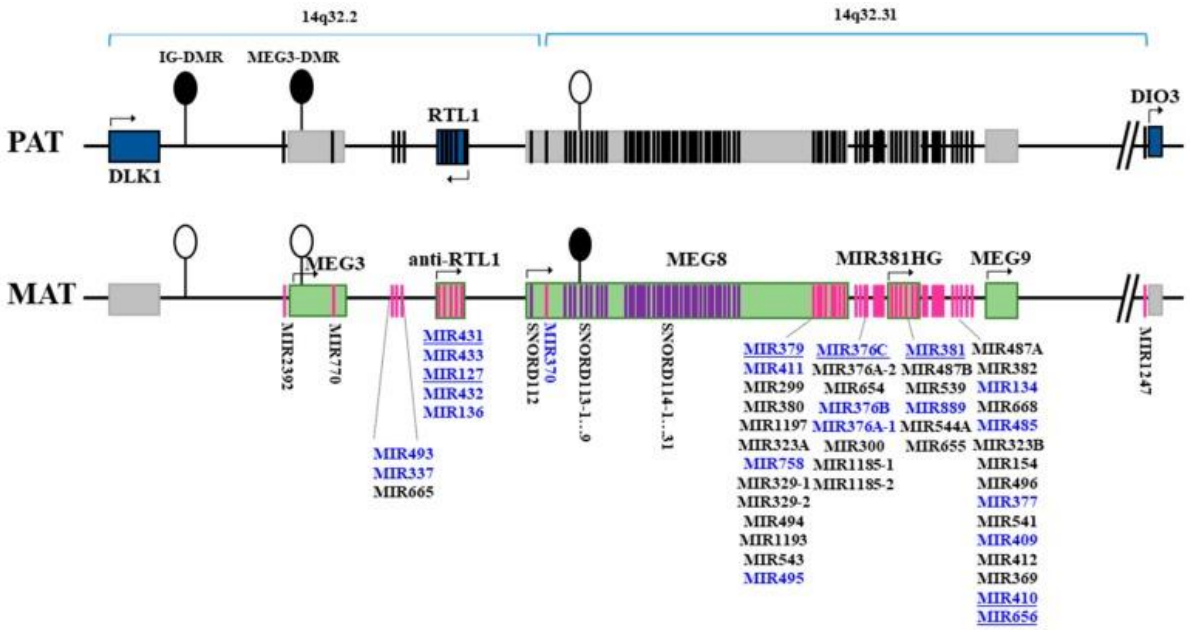

Figure 1-4. Localisation of miRNAs on DLK1-DIO3 region on human chromosome 14q32. The localisation is shown by using Human Genome Assembly GRCh38.p12. Localisation is depicted on maternal (MAT) and paternal (PAT) alleles, and genes are illustrated as rectangles and coloured according to their expression pattern. Blue: protein-coding paternally expressed genes, green: maternally expressed non-coding genes and grey: repressed genes.

(The image used in ***Figure 1-4*** was not required copyright permission to reproduce. It was obtained from Baulina, N., Osmak, G., Kiselev, I., Popova, E., Boyko, A., Kulakova, O., & Favorova, O. (2019). MiRNAs from DLK1-DIO3 Imprinted Locus at 14q32 are Associated with Multiple Sclerosis: Gender-Specific Expression and Regulation of Receptor Tyrosine Kinases Signaling. Cells, 8(2), 133. https://doi.org/10.3390/cells8020133)

Delta-Like 1 homolog (DLK1) is a paternally expressed trans-membrane protein which belongs to Epidermal Growth Factor-Like (EGF-like) family and a non-canonical Notch signalling

ligand, as it has a similar sequence and structure to Delta Ligand 1 (DLL1) which is a canonical Notch ligand. DLK1 includes six repeated EGF-Like motifs except for the conserved Delta-Serrate-LAG-2 (DSL) domain. DSL is a conserved sequence found in canonical Notch ligands and necessary for the trans-activation and cis-inhibition of the Notch receptors (Cordle et al., 2008; Gubina et al., 1999; Laborda, 2000). Two types of DLK1 isoforms are found in humans, membrane-bound (MB) and full-length cleavable (FL) isoforms, which have different functions such as large cleavable isoform can inhibit the cell differentiation in adipocytes but not the MB isoform (Mei et al., 2002). Previous studies showed that DLK1 is highly expressed in several types of tissues during foetal development, and this expression pattern is limited to a few progenitor cells after birth; this is one of the reasons why DLK1 is also named Foetal Antigen 1 (FA1) (Tornehave et al., 1993). On the other hand, high expression of DLK1 is observed in many types of cancers, i.e., breast, liver, lung, ovary, pancreas, and colon (C.-C. Huang et al., 2019; J. Huang et al., 2007; Nishina, 2012; Takagi et al., 2021; Tanimizu et al., 2004; Yanai et al., 2010). DLK1 functions as a proliferation and cell differentiation inhibitor, whereas it can enhance cell proliferation in specific cancer types in low dosage. It is shown that DLK1 expression inhibits NOTCH1 and ERK1/2 MAPK signalling in TNBC, and it leads to cell invasion and cell proliferation at the low level of DLK1 overexpression; however, at a higher level of DLK1 overexpression, it decreases both cell proliferation and invasion (M. L. Nueda et al., 2017). Expression of DLK1 leads to tumour growth, worse survival and prognosis, metastases, and increased cell proliferation, and is associated with EMT phenotype (C.-C. Huang et al., 2019; Jin et al., 2008; Takagi et al., 2021) also oppositely leads decreased cell proliferation, cell growth, and migration (Jin et al., 2008; Lee et al., 2016; M. L. Nueda et al., 2017) in different cancer types. Hence, in the most general manner, its upregulated expression might be considered a biomarker and a potential therapeutic target in different types of cancers,

and it is certain that DLK1 expression indeed inhibits differentiation and dysregulates proliferation in cancer.

Human maternally expressed gene 3 (MEG3) is a long-noncoding RNA and a tumour suppressor gene; it regulates the numerous tumour suppressor and oncogenes, including p53, RB, MYC, and TGF-beta (Ghafouri-Fard & Taheri, 2019). MEG3 regulates p53 expression level by decreasing MDM2 expression. (Zhou et al., 2007) It is shown that p53 activation required MEG3 expression by inducing MEG3 expression and its five isoforms. This functional p53 protein accumulation occurred and was not due to stress response on the cells since deletion of constructed MEG3 expression, which excluded the promoter region, did not show p53 accumulation in the cells. This accumulation without p21 expression was seen only with decreasing MDM2 levels, not with ARF-induced cells. Hence, MEG3 affects MDM2. Although MEG3 induced p53 activation led to an increase in GDF15 expression, which is a tumour suppressor, TGF-beta family member and p53 target gene (Wilson et al., 2003), by inducing GDF15-p53 binding, p21-p53 binding could not be seen in MEG3 induced cells. It is also shown that the expected cell proliferation effect of MEG3 could also occur p53-independently since MEG3 can induce GDF15 by binding its promoter. According to these, MEG3 induces the p53 expression level by repressing the MDM2 expression level. It leads to favourable binding with GDF15 over p21, so it inhibits cell proliferation and makes MEG3 considered a tumour suppressive gene (Du et al., 2018; Weigelt et al., 2008; Zhao, 2021).

Another study reveals the effects of MEG3 expression on the TGF-beta pathway (Mondal et al., 2015). In this study, the formation of RNA-DNA triplex structure was suggested as how MEG3 downregulates its target genes belonging to the TGF-beta pathway, including TGFB2, TGFBR1 & 2 and SMAD2. MEG3 functions to guide H3K27me3 mediator PRC2 (Cao et al.,

2002) by directly interacting with it. Due to the well-known function of the TGF-beta pathway on cell invasion, the effects of MEG3 downregulation were examined. In addition to significant activation of TGF-beta pathway genes, a significant amount of invasion was observed on BT-549 invasive ductal tumour cells. Additionally, repressed cell invasion was observed through MEG3 overexpression on the MDA-MB-231 cell line. Also, a different study showed that MEG3 also regulate EMT through PRC2 recruitment and TGF-beta induction as a novel function (Terashima et al., 2017).

1.5. Aims and Rationale

In this thesis, I aimed to discover whether the downregulation of the 14q32 DLK1-DIO3 imprinted region by CHRNA5 depletion is modulated by different treatments such as the presence of mimics from 14q32 miRNAs and presence or absence of wild-type TP53 and mutant protein. This region has been implicated in embryonic development, carcinogenesis, and the interaction with CHRNA5 has not been interrogated in detail in the literature. My main aim is to confirm siRNA CHRNA5 treatment downregulates DLK1 and MEG3 loci within the Dlk1-Dio3 region using qPCR and whether this downregulation is rescuable with the treatment with siRNA CHRNA5 in the presence or absence of a) 14q32.31 miRNA mimics; b) TP53 siRNA treatment. I also teste if the transient and stable overexpression vectors of TP53 expression affected DLK1, MEG3 and CHRNA5 expression

In more detail, I have the following original aims:

1. Effects of 14q32.31 miRNA mimics on DLK1-MEG3 downregulation in the presence of siRNA CHRNA5.
    a. Do miR-495-3p and/or miR-376c-3p mimic treatments rescue the DLK1 and/or MEG3 downregulation observed in CHRNA5 depletion?
    b. Are CHRNA5 siRNA modulated targets of the above-mentioned miRNAs rescued in the presence of the mimics using in silico and qPCR validation assays?

2. Effects of TP53 siRNA treatment on DLK1-MEG3 downregulation in the presence of siRNA CHRNA5.
    a. Is DLK1-MEG3 downregulation by siRNA CHRNA5 dependent on the presence or absence of TP53 in MCF7 cells?
    b. Does TP53 WT transient overexpression influence DLK1-MEG3 expression
    c. Does TP53 mutant overexpression influence DLK1-MEG3 expression?
3. Do TP53 wild-type and mutant overexpressing stable MCF7 cells behave differently than empty vector overexpressing cells with respect to DLK1-MEG3 modulation?

Chapter 2

2. Materials & Methods

2.1. Materials

2.1.1. Chemicals, Reagents and Kits

All chemicals, reagents and kits used were grouped and listed under the headings. Titles were determined according to the experimental procedure type and the study for which materials were used.

2.1.1.1. Cell Culture Solutions

The reagents and chemicals used for cell culture and maintenance were listed in **Table 2-1** with their companies and catalogue numbers.

Table 2-1. List of materials used for mammalian cell culture and maintenance.

Product Name	Company & Country	Catalogue Number
Dulbecco's Modified Eagle Medium (DMEM) Low Glucose, without L-Glutamine, with Sodium Pyruvate	Biowest, France	L0064
DMEM, with 1.0g/l Glucose and Sodium Pyruvate, without L-Glutamine, without Phenol Red	PAN-Biotech, Germany	P04-001159
Dimethyl Sulfoxide (DMSO)	AppliChem, Germany	A3672
Fetal Bovine Serum (FBS), European Grade, Heat Inactivated	Biological Industries, USA	04-127-1A
L-Glutamine, 200 mM	Cegrogen Biotech, Germany	K0100-670
3-(4,5-Dimethylthiazol-2-yl)-2,5-Diphenyltetrazolium Bromide (MTT)	Thermo Fisher Scientific, USA	M6494
MEM Non-Essential Amino Acid (NEAA) 100X, without L-Glutamine	PAN-Biotech, Germany	P08-32100

Dulbecco's Phosphate Buffered Saline (PBS), without Calcium and Magnesium	Biowest, France	L0615
Penicillin/Streptomycin, 100x	Cegrogen Biotech, Germany	P0100-790
Trypsin-EDTA	Biological Industries, USA	03-051-5B
Puromycin	Sigma-Aldrich, Germany	P8833
Dodecyl Sulphate Sodium Salt (SDS)	EMD Millipore, USA	822050

2.1.1.2. Transfection Reagents and Nucleic Acids

The reagents and oligonucleotides used for siRNA transfection and stable and transient transfection of plasmids were listed in **Table 2-2**.

Table 2-2. List of transient transfection reagents, oligonucleotides, and plasmids.

siRNAs and Transfection Reagents		
Product Name	**Company, Country**	**Catalogue Number**
All-Star Negative Control siRNA	Qiagen, Germany	SI03650318
Hs_CHRNA5_5 FlexiTube siRNA	Qiagen, Germany	SI03051111
Hs_TP53_7 FlexiTube siRNA	Qiagen, Germany	SI02623747
HiPerfect Transfection Reagent	Qiagen, Germany	301705
Plasmids and Transfection & Transduction Reagents		
Product Name	**Company, Country**	**Catalogue Number**
pCMV-Neo-Bam	Addgene, USA	#16440
pCMV-Neo-Bam-TP53 WT	Addgene, USA	#16434
pCMV-Neo-Bam-TP53 R175H	Addgene, USA	#16436
pCMV-Neo-Bam-TP53 R248W	Addgene, USA	#16437
pCMV-Neo-Bam-TP53 R273H	Addgene, USA	#16439
pBabe-puro *	Addgene, USA	#1764
pCMV-VSV-G *	Addgene, USA	#8454
Gag/Pol *	Addgene, USA	#14887
Lipofectamine™ 2000 Transfection	Thermo Fisher Scientific,	11668027

Reagent	USA	
Lipofectamine™ 3000 Transfection Reagent	Thermo Fisher Scientific, USA	L3000008
Opti-MEM™ I Reduced Serum Medium	Thermo Fisher Scientific, USA	31985062
Polybrene Infection / Transfection Reagent	EMD Millipore, USA	TR-1003-G
Amicon® Ultra-15 Centrifugal Filter Unit	EMD Millipore, USA	UFC9010

The plasmids that were marked (*) were kind gifts from Asst. Prof. Onur Çizmecioğlu.

2.1.1.3. RNA & Protein Isolation Kits and Chemicals

The kits, chemicals, and reagents explicitly used for RNA and/or protein isolation and quantification were listed in **Table 2-3** with companies and catalogue numbers, as categorised according to the type of oligonucleotide.

Table 2-3. List of reagents and kits used for isolating RNA and protein and measuring RNA and protein expression levels.

RNA Isolation and Quantification Assays		
Product Name	**Company, Country**	**Catalogue Number**
AccuGENE™ Molecular Biology Water	Lonza, Switzerland	BE51200
QIAzol Lysis Reagent	Qiagen, Germany	79306
RNeasy Mini Kit	Qiagen, Germany	74104
Chloroform	Sigma-Aldrich, Germany	24216
2-Propanol	Sigma-Aldrich, Germany	24137
Ethanol	Sigma-Aldrich, Germany	32221
Sodium Acetate	Carlo Erba Reagents, Italy	366207
RevertAid First Strand cDNA Synthesis Kit	Thermo Fisher Scientific, USA	K1622
LightCycler® 480 SYBR Green I Master	Roche, Switzerland	4887352001

LightCycler® 480 Multiwell Plate 96, White	Roche, Switzerland	4729692001
Protein Isolation and Quantification Assays		
Product Name	**Company, Country**	**Catalogue Number**
Nonidet™ P 40 (NP-40) Substitute	Sigma-Aldrich, Germany	74385
Sodium Chloride (NaCl)	Isolab, Turkey	969.033.100
Trizma® Base	Sigma-Aldrich, Germany	T1503
Dodecyl Sulfate Sodium Salt (SDS)	EMD Millipore, USA	822050
cOmplete, EDTA-Free Protease Inhibitor Cocktail	Roche, Switzerland	11873580001
PhosSTOP Easypack Phosphatase Inhibitor Coctail Tablets	Roche, Switzerland	4906845001
Pierce™ BCA Protein Assay Kit	Thermo Fisher Scientific, USA	23227
2-mercaptoethanol	Sigma-Aldrich, Germany	M3148
4x Laemmli Sample Buffer	Bio-Rad, USA	1610747
Ammonium Persulfate (APS)	Carlo Erba Reagents, Italy	420627
N, N, N', N'- Tetramethyl ethylenediamine (TEMED)	EMD Millipore, USA	110732
TGX Stain-Free™ FastCast™ Acrylamide Kit, 10%	Bio-Rad, USA	1610183
PageRuler Prestained Protein Ladder	Thermo Fisher Scientific, USA	26616
PVDF Western Blotting Membranes	Roche, Switzerland	03010040001
Methanol	Sigma-Aldrich, Germany	24229
Ponceau S Solution	Sigma-Aldrich, Germany	P-7170
Albumin Bovine Modified Cohn Fraction V, pH 7.0	Serva, Germany	SE1194301
6-Aminocaproic Acid	Sigma-Aldrich, Germany	A2504
Tween® 20	Serva, Germany	39796.51
Amersham ECL Prime Western Blotting Detection Reagent	Cytiva, USA	RPN2232
Glycine	BioShop, Canada	GLN001

2.1.1.4. Bacteria Culture, Cloning and Plasmid Isolation Kits and Reagents

The reagents used for bacteria culture preparation, cloning and plasmid isolation were given in **Table 2-4** with the information of the companies and catalogue numbers.

Table 2-4. Reagents and kits used for bacteria culture, cloning and plasmid isolation.

Bacteria Culture, Cloning and Plasmid Isolation		
Product Name	**Company, Country**	**Catalogue Number**
NaCl	Isolab, Turkey	969.033.100
Bio-Tryptone	BioShop, Canada	TRP402
Yeast Extract	BioShop, Canada	YEX401
Agar	Sigma-Aldrich, Germany	05039
Ampicillin Sodium Salt	Sigma-Aldrich, Germany	A9518
Glycerol, 85%	Isolab, Turkey	927.023
NEB® Stable Competent E. coli (High Efficiency) *	NEB, USA	C3040I
EcoRI-HF®	NEB, USA	R3101
BamHI-HF®	NEB, USA	R3136
NcoI-HF®	NEB, USA	R3193
Shrimp Alkaline Phosphatase (rSAP)	NEB, USA	M0371
T4 DNA Ligase	NEB, USA	M0202
Trizma® Base	Sigma-Aldrich, Germany	T1503
EDTA Disodium Salt	AppliChem, Germany	A2937
Glacial Acetic Acid	Sigma-Aldrich, Germany	27225
Agarose, Biomax	Prona, Spain	HS-8000
Ethidium Bromide (EtBr)	Thermo Fisher Scientific, USA	17898
Monarch® DNA Gel Extraction Kit	NEB, USA	T1020
PureLink™ Rnase A (20 mg/mL)	Thermo Fisher Scientific, USA	12091021

GeneRuler 1 kb DNA Ladder with 6x TriTrack DNA Loading Dye	Thermo Fisher Scientific, USA	SM0311
PureLink™ HiPure Plasmid Midiprep Kit	Thermo Fisher Scientific, USA	K210004
NucleoBond Xtra Midi Plus kit for Transfection-Grade Plasmid DNA	Macherey-Nagel, Germany	740412

The competent cells were marked (*) were a kind gift from Asst. Onur Çizmecioğlu.

2.1.2. qPCR Primers

The sequences of forward and reverse primer pairs used for qPCR experiments were listed in **Table 2-5,** with each pair's amplicon product size.

Table 2-5. List of primers used in qPCR experiments.

Gene ID	Primer Sequences
CHRNA5	**F:** 5'- AGATGGAACCCTGATGACTATGGT -3' **R:** 5'- AAACGTCCATCTGCATTATCAAAC -3'
MDM2	**F:** 5’- TCTTGGCCTGGGTTACATGG -3’ **R:** 5’- CTCCACTGACCAAACACGGA -3’
PDLIM7	**F:** 5’- ATGTGCCCCTCTCCATTTCC -3’ **R:** 5’- GATGTGTGTGAGGCTACCCG -3’
CDH18	**F:** 5’- CACCACAGCTCCATCAAGGT -3’ **R:** 5’- TGGAGTGCAGCTTTCCAACA -3’
CCND1	**F:** 5’- CTGCGAAGTGGAAACCATCC -3’ **R:** 5'- GCACTTCTGTTCCTCGCAGA -3'
CDKN1A	**F:** 5’- GTCACTGTCTTGTACCCTTGTG -3’ **R:** 5’- CGGCGTTTGGAGTGGTAGAA -3’
TP53	**F:** 5'- CCTCCTCAGCATCTTATCCGAGT -3' **R:** 5’- GTAGTGGATGGTGGTACAGTCAG -3’
MEG3	**F:** 5’- CTGAATCACCAAAGGCACGC -3’ **R:** 5’- GTGGGAAGGGACTGACCTGT -3’
DLK1	**F:** 5’- GTACTCGGGAAAGGACTGCC -3’ **R:** 5'- CTCGCAGAAATTGCCTGAGA -3'
PRSS23	**F:** 5'- CAACGACTCCACTTCAGCCA -3'

	R: 5’- ATTGCCTGGTCGGTCATTGT -3’
RASGRP1 (Shu et al., 2021)	**F:** 5’- TGGAAACCTGTGTCGAAGTAAC -3’ **R:** 5’- ACTCCTCCATAGTGTCTGTCAAG -3’
TGFRB2 (Xu et al., 2020)	**F:** 5'- ACTGCCCATCCACTGAGACAT -3' **R:** 5’- CCATACAGCCACACAGACTTCC -3’
METTL7A	**F:** 5’- GGGTGACCTGTATTGACCCC -3’ **R:** 5’- TGAAATAGAAAGCCCCTCCCG -3’
MAP1B	**F:** 5’- GTTGGAAGGAAAGGCTCAGT -3’ **R:** 5’- CTTGCTGTTTCTCATGGGTC -3’
MKI67	**F:** 5'- GTGTCAAGAGGTGTGCAGAA -3' **R:** 5'- GCCTTACTTACAGAATTCAC -3'
VIM	**F:** 5'- CGTCACCTTCGTGAATACCA -3' **R:** 5'- CCAGAGGGAGTGAATCCAGA -3'
CXCL12	**F:** 5'- GCCAACGTCAAGCATCTCAAA -3' **R:** 5'- TTCTTCAGCCGGGCTACAAT -3'
FAS	**F:** 5'- AATAAACTGCACCCGGACCC -3' **R:** 5'- AGAAGACAAAGCCACCCCAA -3'
CDC6	**F:** 5'- AGTCAGATGTCAAAAGCCAGACT -3' **R:** 5'- TTGGCTCAAGGTCATCCTGTTA -3'
STON2	**F:** 5'- GGCTGACTCAACTGACAATTCC -3' **R:** 5'- AAACGAGCAGAGGTCACTGG -3'
FOSL2	**F:** 5'- GGCCCAGTGTGCAAGATTAGCC -3' **R:** 5'- TTTCACCACTACAGCGCCCACC -3'
TPT1	**F:** 5'- GATCGCGGACGGGTTGT -3' **R:** 5'- TTCAGCGGAGGCATTTCC -3'

2.1.3. Antibody List

The primary and secondary antibodies used for the western blot experiment were listed in **Table 2-6** with the information of companies, catalogue numbers and working dilutions of each antibody.

Table 2-6. List of antibodies used in Western Blot.

Product Name	Company	Catalogue Number	Dilution
CHRNA5	Abcam	ab259859	1:2000

p53	Santa Cruz	sc-126	1:1000
p21 **	BD Biosciences	554228	1:1000
CCND1 **	Cell Signalling	2922S	1:1000
PLK1 **	Invitrogen	PA5-28023	1:1000
IRE1a **	Cell Signalling	3294S	1:1000
Beta-Actin **	MP Biomedicals	691001	1:5000
GAPDH **	Santa Cruz	sc-47724	1:5000
Anti-rabbit IgG, HRP-linked	Cell Signalling	#7074	1:10000
Anti-mouse IgG, HRP-linked	Cell Signalling	#7076	1:10000

The antibodies were marked (**) were kind gifts from Prof. Dr Özgür Şahin.

2.1.4. Prepared Solutions and Recipes

The list of prepared solutions and buffers and their recipes were indicated in **Table 2-7**; solutions and buffers were categorised according to the experimental process they used.

Table 2-7. List of prepared buffers and solutions used in this thesis.

Western Blot	
Solutions and Buffers	**Components**
TBS (10x)	24 g of Trizma® Base and 88 g of NaCl dissolved in 900 ml of ddH_2O. After adjusting pH to 7.6 with HCl, the volume was completed to 1 litre using ddH_2O
TBS-T (Tween 20) (0.2%) (1x)	100 ml of 10X TBS and 2 ml of Tween20 into 900 ml of ddH_2O
PI (25x)	2 tablets of cOmplete, EDTA-Free were dissolved in 840 µl ddH_2O
PhosStop(20x)	2 tablets of PhosSTOP Easypack Phosphatase Inhibitor Cocktail Tablets were dissolved in 1 ml ddH_2O
RIPA Buffer (1 ml)	75 µl of 2M NaCl, 10 µl of NP-40, 50 µl of 1M Tris-HCl, pH: 8.0, 10 µl of 10% SDS, 40 µl of 25X PI, 40 µl of 20X PhosSTOP and the volume was completed to 1 ml with ddH_2O
10% APS	0.5 g of Ammonium persulfate (APS) dissolved in 5 ml of ddH_2O

SDS Loading Dye (4x)	100 µl of 2-mercaptoethanol added into 900 µl of 4x Laemmli Sample Buffer
Running buffer (10x)	30.3 g Trizma® Base, 144 g of Glycine, 10.08 g of SDS dissolved in ddH_2O up to 1 litre
Anode I Buffer	18.15 g of Trizma® Base and 100 ml of 100% Methanol prepared into ddH_2O as 500 ml of the final volume
Anode II Buffer	1.5 g of Trizma® Base and 100 ml of 100% Methanol prepared into ddH_2O as 500 ml of the final volume
Cathode Buffer	2.62 g of 6-aminocaproic acid and 100 ml of 100% Methanol prepared into ddH_2O as 500 ml of the final volume
Blocking solution (5%)	5 g of BSA or milk powder dissolved into 100 ml of 1x TBS-T (0.2%)
Mild Stripping Buffer	1.5 g of Glycine, 0.1 g of SDS, 1 ml of Tween 20 dissolved in 50 ml of ddH_2O, adjusted to 2.2 pH with HCl, and completed up to 100 ml with ddH_2O
MTT Cell Viability Assay	
Solution/Buffer	**Components**
MTT (12 mM)	5 mg of MTT dissolved into 1 ml of 1xPBS
SDS-HCl Solution (0.01 M)	1 g of SDS and 8 µl of HCl dissolved in 10 ml of ddH_2O
Mini Prep	
Solution/Buffer	**Components**
TENS Lysis Buffer	0.5 ml of 1 M Tri-HCl (pH: 7.5), 0.1 ml of 0.5M EDTA, 1 ml of 5M NaOH and 2.5 ml of 10% SDS dissolved in ddH_2O as 50 ml of the final volume
3M Potassium Acetate, pH: 7.5	29.5 g of Potassium Acetate dissolved in 80 ml of ddH_2O, then adjusted to 7.5 pH with glacial acetic acid, and completed to 100 ml with ddH_2O
DNA & RNA Isolation	
Solution/Buffer	**Components**
TAE Buffer (50x)	121 g of Trizma® Base, 50 ml of 0.5M EDTA and 28.55 ml of glacial acetic acid dissolved in 300 ml of ddH_2O; adjusted to 8.5 pH via glacial acetic acid if required, and then completed to 500 ml with ddH_2O
3 M Sodium Acetate, pH: 5.2	24.61 g of Sodium Acetate (anhydrous) in 80 ml ddH_2O, then adjusted to 5.2 pH by adding glacial acetic acid, then completed to 100 ml with ddH_2O
Agarose Gel (1%)	1 g of agarose into 100 ml of 1x TAE Buffer and the solution was boiled in a microwave until it became clear. After cooling down, 5 µl of EtBr added

Bacteria Culture	
Solution/Buffer	**Components**
Luria-Bertani (LB) Broth	5 g of Tryptone, 5 g of NaCl and 2.5 g of Yeast Extract dissolved in 500 ml of dH_2O and autoclaved
LB Agar	5 g of Tryptone, 5 g of NaCl, 2.5 g of Yeast Extract and 7.5 g of agar dissolved in 500 ml of dH_2O and autoclaved; if required, ampicillin was added at 100 µg/ml concentration
Ampicillin (1000x)	500 mg of Ampicillin Sodium Salt dissolved in 5 ml ddH_2O, filtered with a 0.22 µm filter
50% Glycerol	88.2 ml of 85% Glycerol diluted with ddH_2O up to 150 ml, then autoclaved for sterilisation

2.1.5. Laboratory Equipment

The laboratory equipment that was used to conduct experiments was listed in **Table 2-8**; the company of each equipment was specified.

Table 2-8. List of equipment used.

Instrument Name	Company, Country
NanoDrop ND-1000	Thermo Fisher Scientific, USA
PCR Thermal Cycler 2720	Applied Biosystems, USA
LightCycler® 96 Instrument	Roche, Switzerland
Synergy HT Microplate Reader	Biotek, USA
Amersham™ Imager 600	GE Healthcare Life Sciences, USA
DIC Microscope, DMi8	Leica, Germany
Biological Safety Cabinet	NuAire, USA
Air-Jacketed Automatic CO_2 Incubator	NuAire, USA

2.2. Methods

2.2.1. Bacteria Culture

This study mainly used bacteria cultures to produce overexpression plasmids to generate a transient or stable expression of TP53 wild-type and missense mutants by transforming competent cells.

2.2.1.1. LB Broth & LB Agar Plate Preparation and Bacteria Growth

For the growth of the bacteria culture, LB Broth media were prepared. NaCl (Isolab, 969.033.100), yeast extract (BioShop, YEX401) and Tryptone (BioShop, TRP402) were mixed into ddH_2O as described in **Table 2-7** and autoclaved for sterilisation. If required, ampicillin (Sigma-Aldrich, #A9518) was added as 100 µg/ml of final concentration after the media were cooled down. It was stored at four °C for up to 4 weeks if it contained ampicillin; otherwise, it might be stored for more than 2 months.

LB agar plates were prepared with and without 100 µg/ml of ampicillin for colony selection and competent cell preparation, respectively. As mentioned in **Table 2-7**, NaCl, Tryptone, yeast extract and additionally agar (Sigma-Aldrich, #05039) were autoclaved with ddH_2O. When the solution was cooled down, ampicillin was added if required. LB agar solution was distributed into Petri dishes in a sterile environment and left near the flame until it hardened and cooled. Plates were sealed with parafilm and stored upside down at 4°C for up to 4 weeks.

2.2.1.2. Cell Culture Grade Plasmid Isolation of TP53 Expressing Plasmids

Stab agar cultures of pCMV-Neo-Bam (Addgene, #16440), pCMV-Neo-Bam TP53 WT (Addgene, #16434), pCMV-Neo-Bam TP53 R175H (Addgene, #16436), pCMV-Neo-Bam TP53 R248W (Addgene, # 16437), pCMV-Neo-Bam TP53 R273H (Addgene, #16439) plasmids ordered from Addgene were streaked to LB agar with ampicillin plate. After the

overnight incubation at 37°C, a single colony was selected for each plasmid, and each selected colony was grown into 8 ml LB Broth with ampicillin media for 8 hours at 37°C into a shaker with 220 rpm as a starter culture. Starter culture was diluted with a 1:1000 ratio into 100 ml LB Broth with ampicillin and left for overnight culture in a shaker at 37°C with 220 rpm.

100 ml overnight cultured bacteria were transferred into 50 ml falcons and centrifuged at 4000 g for 15 minutes at 4°C. NucleoBond Xtra Midi Plus kit for Transfection-Grade Plasmid DNA (MN, #740412) was used to isolate plasmids. According to the manufacturer's manual, plasmids were eluted into the TRIS Buffer; purity and concentration of the plasmids were measured with NanoDrop and stored at -20°C. In the following experiments, i.e., sequencing and transfection, plasmids were precipitated and dissolved into nuclease-free water.

According to Cold Spring Harbor (CSH) Protocols, DNA precipitation was performed to precipitate plasmids from the TRIS buffer. (Green & Sambrook, 2016) One-third of the plasmids in the TRIS buffer were separated for precipitation. 3M sodium acetate was added by adjusting the final concentration to 0.3M and left for overnight incubation at -20°C. Exactly twice the volumes of ice-cold ethanol were introduced and maintained on ice for 20 minutes. Plasmids were centrifuged at 13000 rpm for 10 minutes at 4°C. After the centrifugation step, the supernatant was discarded carefully and then obtained pellet was washed with ice-cold 70% ethanol. The samples were centrifuged again for 5 minutes at 4 °C at 13000 rpm. As a final step, the pellet was resuspended into nuclease-free water, and plasmids measured with NanoDrop for concentration and purity were kept at -20°C.

2.2.1.3. Cloning of Plasmids for Stable Transfection

Since the ordered plasmids expressing wild-type and mutant TP53 gene were only mammalian expression type plasmids and unsuitable for viral transfection protocol, the backbone was

changed by cloning. For cloning, the new backbone was determined as pBabe-puro (Addgene, #1764), which has mammalian expression and retroviral type plasmid features. Insert of the pCMV-Neo-Bam plasmids were excised at their cloning site according to the manufacturer's protocol, and ligation was performed with the new backbone and extracted insert for viral transfection.

2.2.1.3.1. Excision of Inserts

According to cloning information, insert of mutant TP53 expression plasmids were excised at their cloning side. BamHI-HF (NEB, #R3136) enzyme was used for pCMV-Neo-Bam TP53 WT and pCMV-Neo-Bam TP53 R248W, with 1.8 kb fragment yielding, while EcoRI-HF (NEB, R3101) enzyme was used for both pCMV-Neo-Bam TP53 R175H and R273H plasmids with 1.3 kb yielding. For restriction enzyme reaction of each type of plasmid, two reaction solutions were prepared: one for excision of the new backbone (pBabe-puro) and one for excision of the plasmid with insert. 3 µg DNA (pBabe-puro or mutant TP53 gene expressed plasmid), 5 µl rCutSmart, 1 µl restriction enzyme, either EcoRI or BamHI according to plasmid type, and the volume was completed to 50 µl with nuclease-free water on ice. The mixture was incubated at 37°C for 3 hours. After 3-hour digestion, 2 µl of rSAP (Shrimp Alkaline Phosphatase) (NEB, M0731) was added to dephosphorylate the 5' and 3’-ends of the plasmid of the new backbone; mixtures were incubated for 30 minutes at 37°C. At the end of the incubation, to inactivate restriction enzymes, another incubation step was applied for 20 minutes at 65°C.

2.2.1.3.2. Gel Extraction and Ligation

At the end of excision, restricted products were loaded into 1% agarose gel with EtBr to verify the enzyme restriction. GeneRuler 1 kb was used as a ladder, and restricted plasmids and non-restricted plasmids, as restriction enzyme control, were loaded with 6x TriTrack DNA loading

dye (Thermo Fisher Scientific, SM0311). The agarose gel was run for 1 hour at 100 volts. After gel imaging under the UV light, the bands of insert and backbone were cut from agarose gel. By using Monarch® DNA Gel Extraction Kit, agarose was melted, and DNA fragments were isolated from the agarose by following the manufacturer's manual.

In the following step, the required amount of backbone and insert plasmids for ligation were calculated by considering the length of insert DNA, the length of vector DNA and the mass of vector DNA by using the NEBioCalculator Online Tool (https://nebiocalculator.neb.com) (**Eq. 1**).

Equation 1. The formula of NEBioCalculator Tool, Ligation Calculator, to find the required mass insert for DNA ligation with T4 DNA ligase.

$$Required\ Mass\ Insert(g) = \frac{Insert\ Molar}{Vector\ Molar} \times Mass\ of\ Vector\ (g) \times \frac{Insert\ Length}{Vector\ Length}$$

According to Ligation Calculator, the required insert DNA mass was determined with the 1:3 ratio to the molar of vector DNA (backbone), pBabe-puro (5.1 kb) and the insert, and the determined mass of plasmids used for ligation with T4 DNA Ligase (NEB, M0202) as provided on **Table 2-9**.

Table 2-9. The amount of plasmids used for ligation was determined by using NEBioCalculator.

Restricted Insert Type	Amount of Insert	Amount of Vector
TP53 WT (1.8 kb)	95.29 ng	90 ng
TP53 R175H (1.3 kb)	68.82 ng	90 ng
TP53 R248W (1.8 kb)	95.29 ng	90 ng
TP53 R273H (1.3 kb)	68.82 ng	90 ng

Ligation reaction for the defined amount of insert and vector was prepared as 20 µl of the final volume; therefore, 2 µl of T4 DNA Ligate Buffer (10x) and 1µl of T4 DNA Ligase were added, and the volume was fulfilled with nuclease-free water up to 20 µl, then incubated at room temperature overnight and run on the 1% agarose gel to check whether ligation was achieved or not. Restriction products were used as controls.

2.2.1.3.3. Transformation

NEB® Stable Competent *E. coli* competent cells (NEB, C3040I) were used for plasmid transformation of ligation products that express TP53 wild-type or missense mutants and viral packaging and envelope genes expressing plasmids separately, pCMV-VSV-G (Addgene, #8454) and Gag/Pol (Addgene, #14887), respectively.

Competent cells stored at -80°C were incubated for approximately 5 minutes on ice to be thawed. 5 µl of ligation product and control were added to cells, mixed gently without pipetting, and incubated on ice for 30 minutes. Tubes were incubated at 42°C for 30 seconds, and tubes were placed on ice to cool down for approximately 10 minutes. 800 µl of LB Broth were added, and competent cells were incubated at 37°C for 1 hour in a shaker with 220 rpm. Following the incubation, tubes were centrifuged for 5 minutes at 1500 rpm, approximately 750 µl of supernatant were discarded, and the pellet was dissolved with the remaining LB Broth. Competent cells were streaked into LB agar plates with ampicillin and left in 37°C-incubator for overnight. At least 10 colonies were selected, and each was grown into 5 ml of LB Broth media with ampicillin at 37°C for overnight on a shaker with 220 rpm for plasmid isolation.

The same procedure was followed for transforming viral packaging and envelope plasmids to clone the plasmids for viral transfection protocol.

0.5 ml of overnight incubated bacteria cultures were used to make glycerol stocks to store the transformed bacteria for long-term stable storage and plasmids isolation according to colony screening results. Glycerol was diluted to 50% with dH_2O and autoclaved for sterilisation. 500 µl of 50% glycerol was gently added to 500 µl of overnight culture in tubes under aseptic conditions, and the final concentration of glycerol was adjusted to 25%. Glycerol stocks were snap frozen with liquid nitrogen, then stored at -80°C for long-term storage.

2.2.1.3.4. Plasmid Isolation with Mini-Prep without Kit Protocol

After overnight growth of each colony, 1.5 ml of bacteria culture was transferred into tubes and spun down for 5 minutes. Supernatants were discarded entirely, and the pellet was resuspended with 100 µl of TE buffer with 10 µl/ml RNase A. 300 µl of TENS Buffer was added. Samples were vortexed for ~5 seconds until they became sticky. To stop the reaction, 150 µl of 3M Potassium Acetate (KoAc) were added, vortexed for 5 seconds and then, centrifuged at 5000 rpm for 10 minutes. The supernatant of samples was transferred into fresh tubes carefully, mixed with 900 µl of pre-cooled 100% ethanol and centrifuged at 13000 rpm for 5 minutes at 4°C to precipitate plasmids. The supernatant was replaced with 70% ethanol and centrifuged. After the supernatant was removed, pellets were left to air-dry for approximately 30 minutes. When thoroughly dried, they were resuspended into 40-50 µl of nuclease-free water, depending on the pellet size. After measuring of concentration and purity of samples on NanoDrop, plasmids were used for colony screening and stored at -20°C.

2.2.1.3.5. Colony Screening and Selection

Since the 5' and 3' cloning sites of each TP53 expressing plasmid were the same, conforming to the direction of the insert had to be controlled in addition to controlling for ligation. Therefore, a specific restriction enzyme was selected using Benchling: Cloud-based platform (https://www.benchling.com/). Two main criteria were considered during the selection; (1) the

enzyme could cut the target plasmids in the insert, and the backbone, and (2) the enzyme cutting could give cut products with different and distinguishable sizes on agarose gel when ligation was not achieved or was achieved for both insert direction. After all possible enzymes listed by their cut sites and product sizes, NcoI-HI (NEB, R3193) was selected for colony screening and *in silico* restriction cut results were obtained for each ligation product with both forward and reverse the direction of the inserts into the backbone from Bechling.

1000 ng plasmid from each colony was used for a restriction enzyme reaction. 0.5 µl NcoI-HF enzyme, 3 µl rCutSmart buffer and nuclease-free water to fulfil the final volume up to 30 µl were used with plasmids to prepare the restriction enzyme reaction. The restriction solutions were incubated at 37°C for up to 3 hours. To inactivate enzyme functionality, solutions were also incubated at 80°C for 20 minutes. Digestion products were run on 1% agarose gel, as positive control pCMV-Neo-Bam plasmids were used for each type of insert since the pattern of these plasmids with NcoI-HF enzyme cut was known.

2.2.1.3.6. Cell Culture Grade Plasmid Isolation of Cloned Plasmids and Viral Packaging and Envelope Genes Expressing Plasmids with Midi-Prep Kit

According to the colony screening procedure, glycerol stocks of the selected colony were thawed into ice, streaked into LB agar plates containing ampicillin, and incubated overnight at 37°C. A single colony was selected from overnight incubated plates and grown into 8 ml LB Broth with ampicillin as a starter culture for 8 hours at 37°C in a shaker with 220 rpm. Starter culture was diluted 1:1000 into 50 ml of LB Broth medium containing ampicillin for high copy number plasmids. The volume of LB Broth medium was increased to 100 ml for low-copy number plasmids with the same dilution rate. The culture was grown overnight at 37°C and 220 rpm. Incubated cultures were transferred into 50 ml falcons, and plasmids were isolated according to the manufacturer's instructions of PureLink™ HiPure Plasmid DNA Purification

Kits (Thermo Fisher Scientific, K2100). After the elution and precipitation step, pellets were resuspended into 40 µl of nuclease-free water; their purity and concentrations were obtained by NanoDrop and then stored at -20°C for long-term storage.

Plasmids were cut with BamHI or NcoI enzyme and run on 1% agarose gel to confirm whether these samples contained any additional DNA contamination.

2.2.2. Cell Culture Maintenance & Handling

2.2.2.1. Thawing Procedure

For the thawing procedure, frozen cell lines were taken from main cell stocks, which are kept in liquid nitrogen tanks, into 2 ml-cryovials, and each vial was thawed via the water bath at 37°C until at least half of the tube was melted. The remaining frozen sample was melted by adding warmed complete DMEM, supplemented with 10% FBS, 2% L-Glutamine, 1% sodium pyruvate, 1% non-essential amino acids and without penicillin-streptomycin, up to 5 ml. After mixing DMEM with cells, the mixture was taken into 15 ml falcons and centrifuged at 1500 rpm for 5 minutes. The supernatant was removed, and the remaining pellet was resolved into 3-4 ml of new complete DMEM with a 5 ml final volume and transferred into the T25 flask. After overnight incubation at the incubator at 37°C with 5% CO_2, flasks were examined under the microscope and maintained at the incubator for the following procedures.

2.2.2.2. Passaging of Mammalian Cell Culture

When the confluency of the cell lines reached 80-90%, old media was removed, dish/flask was washed with 1xPBS, and 0.5 or 1 ml of 1xTrypsin-EDTA was added into T25 and T75 flasks or 10 cm dishes, respectively. Following the 3-5 minutes of incubation, media was added to twice the volume of trypsin to stop the activity of trypsin, and detached cells were collected into falcons. Precipitated cells centrifugated at 1500 rpm for 5 minutes were dissolved into

fresh complete DMEM with 1% penicillin/streptomycin. Resuspension was divided into a new flask, with the dilution determined according to the growth rate of each cell line.

2.2.2.3. Cell Seeding

According to the type of cell line and multi-well plate, the required numbers of cells per well for main transfection procedures were indicated in **Table 2-10**. After cells were detached from the flask/plate surface with 1xTrypsin-EDTA, they were counted via a haemocytometer at least three times and seeded into multi-well plates.

Table 2-10. The number of cells seeded for *in vitro* studies for each type of cell line.

Cell Line	96-well	24-well	12-well	6-well
MCF7	2,000	50,000	100,000	200,000
MDA-MB-231	2,000	-	100,000	200,000
HEK293	-	-	-	200,000

2.2.2.4. Freezing Cells

To preserve the main stock of the mammalian cell lines, cells were frozen in their early passages and stored in nitrogen tanks. Cell lines collected with 1xTrypsin-EDTA were centrifuged at 1500 rpm for 5 minutes, and the pellet was resuspended with freezing media prepared as 90% FBS and 10% DMSO. Resuspension was split into 2 ml-cryovials as approximately 1 million cells per vial. Cryovials were placed into Nalgene® Mr Frosty to provide the 1°C/minute cooling rate and stored overnight at -80°C. After the overnight incubation, cryovials were placed in liquid nitrogen tanks for long-term storage.

2.2.3. MTT Analysis for Cell Viability and Toxicity Detection of Overexpression Plasmids with or without siRNA

The required number of cells were seeded per well in 96-well plates as described in **Table 2-10**. The day after cell seeding, old media was removed, and transfection was performed with Lipofectamine 2000 or HiPerfect according to the type of oligonucleotide. After 72-hour treatment, the MTT experiment was applied according to the manufacturer's instructions. 5 mg of MTT (3-(4,5-Dimethylthiazol-2-yl)-2,5-Diphenyltetrazolium Bromide) was dissolved entirely into 1 ml of 1xPBS and filtered by using 0.22 µm filter. It was mixed with 10 ml of complete DMEM phenol red-free since phenol red might interfere with the absorbance values of the reads. Old media was replaced with the phenol red-free DMEM and MTT mixture as 110 µl per well. As a result, it became 100 µl of DMEM and 10 µl of MTT per well. After 4-hour incubation of MTT in the incubator, freshly prepared 10 ml of 0.01 M HCl with 1 gram of SDS solution added as 100 µl to each well and left for 16-18-hour incubation in the incubator. The absorbance values of the MTT experiment were obtained using the Microplate Spectrometer at 570 nm wavelength. Experiments were performed as 5 replicates for each group.

2.2.4. Transient Transfection of TP53 Overexpression Plasmids

Transient transfection for overexpression of TP53 wild-type and mutant gene expression was performed in the MCF7 cell line using Lipofectamine 2000 transfection reagent (Thermo Fisher Scientific, 11668). In a previous study, optimal plasmid transfection amounts were determined by Bircan Çoban as 1 µg of plasmid and 2 µl of Lipofectamine 2000 by using pEGFP vector. Two different aspects were tried to find the optimal amount of TP53 overexpression plasmid. Firstly, different concentrations of plasmids were determined as 250 ng/ml, 500 ng/ml, and 1000 ng/ml. Since a high toxicity effect was observed on MTT results,

concentrations were changed to the amount of plasmids proportional to the seeded cell number. The amount of the plasmids were used as 500 ng, 1000 ng, and 2000 ng for 200,000 seeded cells per well in a 6-well plate. It was comparatively decreased by considering cell number with other components, i.e., Opti-MEM I and Lipofectamine 2000 reagents.

A transfection procedure was performed the day after 200,000 cells-seeding per well on 6 wells. As the first step, old media was replenished with 1.5 ml of fresh complete DMEM without penicillin/streptomycin. The required amount of plasmid was mixed with 250 µl of Opti-MEM I medium (Thermo Fisher Scientific, 31985062) in a tube, and 2 µl of Lipofectamine 2000 was diluted in 250 µl of Opti-MEM I in another tube for each well, then incubated for 5 minutes at room temperature. The diluted DNA mixture was added into Lipofectamine 2000 mixture drop by drop and slowly to allow the DNA-lipid complex formation and left for 20-minute incubation. DNA-lipid mixture was added to cells as 500 µl per well and incubated for 72 hours. At the end of the treatment, the effects of the transfection were checked by MTT assay, western blot and/or qPCR experiments, and 1000 ng plasmid was decided as an optimal dosage for transient transfection protocol.

2.2.5. Transfection of siRNA and Mimics

MCF7 and MDA-MB-231 cell lines were used for siRNA or miRNA mimic transfection by using HiPerfect (Qiagen, 301704) in this study. To downregulate CHRNA5 and wild-type and mutant TP53 gene expression, siRNA CHRNA5 (siCHRNA5) (Qiagen, SI03051111) and siRNA TP53 (siTP53) (Qiagen, SI02623747) were used with All-Star Negative Control siRNA (Qiagen, SI03650318). Syn-hsa-miR-495-3p miScript miRNA Mimic was used for the mimic transfection on the MCF7 cell line.

Cells were seeded according to **Table 2-10**. On the following cell seeding day, transfection mixtures for oligonucleotides were prepared as described in **Table 2-11**.

Table 2-11. siRNA/miRNA Mimic transfection conditions per well according to types of cell culture multi-well plates.

Type of Plate	Cell Number	Volume of HiPerfect	For 10 nM siRNA	For 10 nM miRNA Mimics
6-well	200,000	6 µl	1 µl	1 µl
12-well	100,000	3 µl	0.5 µl	0.5 µl
96-well	2,000	0.6 µl	0.1 µl	0.1 µl

When combination treatments were applied, an equal amount of negative control scrambled siRNA, scRNA or siControl, were added to individual treatment groups; therefore, scRNA was used to equalise the total concentration of oligonucleotide molecules for every group in the experimental setup. For each group required volume of oligonucleotides was mixed in tubes, and HiPerfect transfection reagent was added and mixed through pipetting. After a brief vortexing step, tubes were spun down and incubated for 10 minutes to allow the transfection complex formation at room temperature under the hood. Meanwhile, old media was changed with fresh complete DMEM, then incubated transfection complex was added drop by drop, and the plate was gently swirled to provide uniform distribution of transfection mixture into wells. Cells were incubated for 72 hours, and effects of the transfection were checked by MTT assay, western blot and/or qPCR experiments at the end of the treatment.

2.2.6. siRNA Dual Transfection with Lipofectamine 2000 on MCF7 Cell Line

To observe the effect of TP53 mutant overexpression with CHRNA5 downregulation through RNAi, the dual transfection procedure was applied using Lipofectamine 2000 according to the

manufacturer's protocol. MCF7 cells were seeded in a 96-well plate as described numbers, and the day after the cell seeding, a transfection procedure was applied. scRNA and siRNA CHRNA5 were used for RNAi treatment, pCMV-Neo-Bam, (Empty vector, EV), pCMV-Neo-Bam TP53 WT, pCMV-Neo-Bam TP53 R175H, pCMV-Neo-Bam TP53 R248W and pCMV-Neo-Bam TP53 R273H plasmids were used for overexpression treatment; also, each overexpression group was combined with RNAi reagents. While siRNA concentration was kept constant, two different plasmid amounts were used, 5 ng and 10 ng per well. In this experimental setup, EV and scRNA transfected groups were used as a negative control. The total amount of siRNA and plasmids were equalled by adding scRNA and EV to individual treatment groups.

Following the manufacturer's protocol, previously determined amounts of RNAi and TP53 wild-type and mutant gene-expressing plasmids were given to MCF7 cells. MCF7 cells were seeded in a 96-well plate as 2000 cells per well. The next day, similar to the transient transfection protocol in section 2.2.4, for each well, RNAi and plasmids were diluted into 50 µl of Opti-MEM I in a tube, and 0.2 µl of Lipofectamine 2000 was diluted in another tube, then incubated for 5 minutes. DNA-RNAi complex was added drop by drop to Lipofectamine 2000 dilution mixture and incubated for 20 minutes at room temperature. Then, the DNA &RNAi-lipid complex was distributed to cells and left for 72-hour of treatment. The MTT protocol was applied to verify the effects of the treatment at the end of the treatment.

2.2.7. Generation of Stable Expression MCF7 Cell Line by Retrovirus

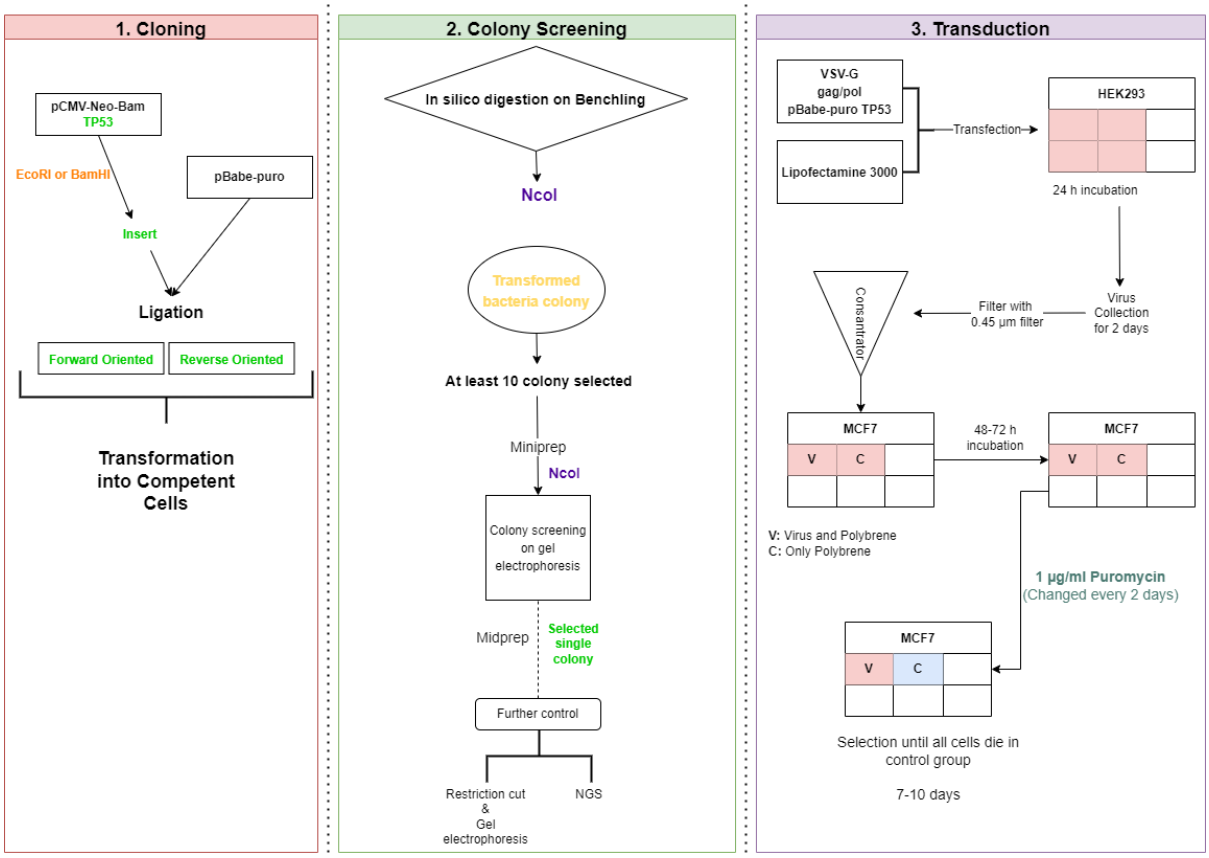

Figure 2-1. Workflow of stable MCF7 cell line generation. Generated on diagrams.net.

Since the low efficiency of the siRNA dual transfection experiment, it was decided to generate stable TP53 WT, TP53 R175H, TP53 R248W or TP53 R273H gene expressing MCF7 cell line to investigate the relationship between CHRNA5 and TP53. Among the other methods, retroviral transfection was considered the most promising approach. Accordingly, retroviruses encapsulated in the interested overexpression plasmid were produced in the HEK293 packaging cell line; these viruses were concentrated and used for transduction on the target breast cancer cell line, MCF7 (***Figure 2-1***).

2.2.7.1. Kill Curve Generation with Selection Antibiotic & Crystal Violet Staining

To determine the dosage of the puromycin as a positive selection marker for the transduced MCF7 cell line, the dosage range was identified as between 0 - 3 µg/ml of puromycin, according to both manufacturer directions and literature. MCF7 cells were seeded as 50,000 cells per well into a 24-well plate with 0.5 ml complete DMEM with penicillin/streptomycin. After 24-hour incubation, cells were treated with puromycin as 2 replicates for each dosage. Cells were observed for 10 days, and media with puromycin were changed every two days. At the end of the 10 days, cells were fixed with 4% PFA (paraformaldehyde), and 0.5% crystal violet stain was used to stain the remaining cells in wells.

4% PFA was prepared as a fixative reagent. 20g f PFA powder was added to 400 ml of heated 1xPBS to approximately 60°C while stirring under the ventilated chemical hood. The pH of the solution was slowly raised by adding 1N NaOH dropwise to dissolve the PFA powder completely. When the solution became clear, it was cooled down, pH was adjusted to 6.9-7, and the solution was stored at -20°C as aliquots.

0.5 % crystal violet stain was freshly prepared as 0.5% crystal violet powder and 25% methanol into ddH_2O. 10% acetic acid into ddH_2O was used as a destaining solution of crystal violet staining.

At the end of the 10-day selection, old media were discarded, and wells were washed with 1x PBS. Under the ventilated chemical hood, 500 µl of 4% PFA was added to wells on a shaker and incubated for 20 minutes at room temperature. 4%PFA solution in each well was discarded, wells were washed with 1x PBS 3 times, and 0.5% of crystal violet stain was added as 500 µl

per well and incubated for 15 minutes at room temperature. The stain was discarded, an excessive amount of crystal violet stain was washed with ddH_2O, and the plate was left for air-dry overnight at room temperature in the dark. After the incubation, a plate image was taken by scanning, and 250 µl of staining solution was added to each well and incubated for 15 minutes. Destained solutions from each well was transformed into 96-well plates, 1:100 diluted into 100 µl of ddH_2O, as triplicates and the reads were obtained at 590 nm wavelength by using the microplate reader.

2.2.7.2. Transfection on HEK293 Cell Line & Virus Collection

HEK293 cells were seeded into a 6-well plate as 200,000 cells per well, and 4 wells were used for virus collection of each type of stable line. The day after cell seeding, the old medium was replenished with 1.75 ml of fresh complete DMEM. Plasmids containing envelope gene (VSV-G) and packaging genes (viral Gag/Pol) were co-transfected with LTR containing TP53 wild-type or mutant genes gene expressing plasmids (pBabe-puro TP53 WT or R175H or R248W or R273H) through Lipofectamine 3000 transfection reagent (Thermo Fisher Scientific, L3000008). In total, 2.5 µg of TP53 wild-type or mutant gene expressing pBabe-puro, pCMV-VSV-G and Gag/Pol and pBabe-puro plasmids were diluted for each well according to a 2:1:1 ratio in Opti-MEM I, then 5 µl of P3000 reagent was added; the volume was completed to 125 µl with Opti-MEM I. Accordingly, 1.25 µg of pBabe-puro TP53 WT or mutant, 0.625 µg of pCMV-VSV-G and 0.625 µg of Gag/Pol plasmids were used per well. In another tube, 3.75 µl of Lipofectamine 3000 transfection reagent was diluted in 125 µl of Opti-MEM I for each well. The DNA-lipid complex was mixed with Lipofectamine 3000 dilution drop by drop, incubated for 10-15 minutes under the cell culture hood, and 250 µl of solution per well was distributed to wells gently.

24 hours after the treatment, the medium was changed to 1.5 ml of new complete DMEM and incubated for 24 more hours in the incubator. Media was collected twice over 24 hours periods into 50 ml falcon, wrapped with aluminium foil and kept at 4°C. After each collection, the media was changed to 1.5 ml fresh media. Collected media from 4 wells was filtered with a 0.45µm filter to eliminate any remaining HEK293 cells in the media and concentrated with Amicon® Ultra-15 centrifugal filter unit by centrifuging at 5000 rpm for 20 minutes at 4°C up to 1 week.

2.2.7.3. Transduction on MCF7 Cell Line

MCF7 cells were seeded as 50.000 cells per well into a 6-well plate for transduction with Polybrene infection/transfection reagent (EMD Millipore, TR-1003-G). One well was used for transduction, and another well was used as a control, containing only polybrene into DMEM. The day after cell seeding, 2 ml of media was replenished, and approximately 200 µl of concentrated media was added into the transduction well. 2 µl of polybrene was added into both control and transduction groups as 10 µg/ml final concentration and incubated for 24 hours. 24 hours later, the media was replaced with new complete media, and cells were incubated into fresh media for 48 hours.

At the end of the incubation, 1 µg/ml puromycin was used for selection of control and treatment wells, and it was changed every 2 days until all endogenous cells died in the control group. When all the control group cells died, the transduction group was passaged into a T25 flask to grow into complete DMEM with 1µg/ml puromycin.

2.2.8. Total Protein Extraction and Quantification

2.2.8.1. Total Protein Extraction

RIPA lysis buffered prepared as described in **Table 2-7** freshly. For protein isolation, dead cells were collected with media and first 1xPBS-wash. Collected dead cells were centrifuged at 5000 rpm for 5 minutes, and cell pellets were dissolved into RIPA buffer. Cells were rewashed with cold 1x PBS, then scraped with freshly prepared RIPA lysis buffer, and collected into 1.5 ml tubes. Every group's collected dead cells were combined with its scraped cells, and these were incubated on ice with vortexing every 5 minutes for 30 minutes. Cell lysates were centrifuged at 13000 rpm for 15 minutes, and then supernatants, which contains proteins, were transferred into new tubes. Collected proteins were stored at -80°C against degradation for long-term storage.

2.2.8.2. BCA Analysis and Protein Quantification

Quantification of isolated protein concentrations were performed by using Pierce™ BCA Protein Assay Kit (Thermo Fisher Scientific, 23227) according to the kit's protocol with triplicates of each experimental group. A standard curve was plotted as a linear regression graph according to "$y = ax + b$" equation, where y refers to absorbance values, and x refers to the concentration of each sample. In addition to the main formula, concentrations of each sample were found by multiplying with 12.5, which is a dilution factor of the samples.

According to BCA results, 10 µg protein from each sample was transferred into tubes, and a 1:4 total volume of 4x Laemmli sample buffer was added (Bio-Rad, 1610747). Each sample's final volume and concentrations were equalised by adding RIPA lysis buffer. Samples were denatured at 95°C for 5 minutes and stored at -20°C if required.

2.2.8.3. SDS-Page and Western Blot & Mild Stripping Protocol

10% SDS page was prepared by using TGX Stain-Free™ FastCast™ Acrylamide Kit (Bio-Rad, 1610183) according to the manufacturer's protocol. Samples were loaded as 10 µg unless otherwise stated, and 2 µl of PageRuler prestained protein ladder (Thermo Fisher Scientific, 26616) was loaded into the gel. It was placed in a running buffer, described in **Table 2-7**, at 80 volts; after the loaded samples passed from the stacking gel to the resolver gel, the voltage was increased to 120 volts. After the running step, proteins were transferred from the gel to PVDF (polyvinylidene difluoride) western blotting membranes (Roche, 03010040001) by semi-dry transfer method for 55 minutes at 25 volts and up to 1.3 amps. Also, transfer buffers used during this procedure were listed in **Table 2-7**.

Following the transfer, the membrane was stained with Ponceau S solution (Sigma-Aldrich, P-7170) on a shaker for 5 minutes and rinsed with dH_2O to remove the excessive Ponceau S solution. The membrane was blocked by using 5% BSA in 0.2% TBS-T for 60 minutes at room temperature and left for overnight incubation at 4°C on a rotator into the primary antibody solution. Primary antibodies utilised in this study were given in **Table 2-6** including working dilutions. The next day, incubated membrane was washed three times with 1x TBS-T for 10 minutes and incubated with 1:5000 diluted secondary antibodies for 60 minutes in room temperature. When the incubation period finished, it was washed 3 times with 1x TBS-T for 10 minutes. Protein detection was perfomed by using Amersham ECL Prime Western Blotting Detection Reagent (Cytiva, RPN2232) on Amersham Imager 600.

To detect more than one protein having similar sizes in one membrane, a mild stripping protocol was performed to remove previously visualised antibodies. Freshly prepared mild stripping buffer was used according to **Table 2-7**. The membrane was incubated twice with

mild stripping buffer for 10 minutes at room temperature on a shaker. It was washed twice with 1x TBS for 5 minutes and with 1x TBS-T 2 times; each wash step took 10 minutes. After the washing steps, the membrane was blocked and incubated with primary, then secondary antibodies, as described above.

GAPDH (Glyceraldehyde 3-phosphate dehydrogenase) or beta-Actin proteins were used as loading control proteins to normalise the level of the proteins to check whether the amount of the loaded proteins was the same in the gel.

2.2.8.4. ImageJ Analysis of Western Blot Results

To represent the quantification of the western blot results, densitometry of bands was measured using ImageJ (version 1.53a) programme. The image taken by Amersham Imager 600 was uploaded to ImageJ, and the image type was turned to an 8-bit scale. After, the bands belonging to a specific primary antibody were linearised horizontally. The line of the bands was selected by a rectangular, area of the bands was plotted, and the percentage for these areas was calculated. These percentages were used for relative expression analysis of protein expressions.

Percentages from densitometry measurement were transformed to the logarithm of the values to base 2 and normalised to each sample's GAPDH value through subtraction. Next, the values were normalised to the mean of the biological replicates of the control group, and obtained values were used for statistical analysis; results were represented as relative expressions.

2.2.9. Total RNA Isolation and Quantification

2.2.9.1. Total RNA Isolation

For total RNA isolation, pellets were collected by detaching with 1x Trypsin-EDTA and washed twice with ice-cold 1x PBS. Collected cells were centrifuged at 1500 rpm for 5 minutes between each step. After snap-freezing with liquid nitrogen, cell pellets could be kept at -80°C.

Total RNA isolation of MCF7 cells treated with 10 nM siCHRNA5 and/or 10 nM siTP53 was performed on ice with RNeasy Mini Kit (Qiagen, 74104) by following the kit's protocol. RNA was eluted into 40 µ of nuclease-free water at the elution step. After the concentration and purity measurements with NanoDrop, samples were stored at -80°C.

Differently from the kit protocol, total RNA isolation of optimisation experiments, siRNA and/or overexpression plasmid transfected samples were performed using QIAzol Lysis Reagent (Qiagen, 79306). Cell pellets were thawed and dissolved with 0.7 ml of QIAzol on ice. After the homogenisation, 140 µl of chloroform was added, tubes were mixed by pipetting and inverting several times, and left for 5-minute incubation at room temperature. Tubes were centrifuged at 13000 rpm for 17 minutes at 4°C, and the mixture became separated into three distinct phases, pink-coloured, white-cloudy and colourless aqueous, from bottom to top. The upper aqueous phase was taken cautiously by not contaminating the cloudy interphase and mixed with 500 µl of 100% filtered isopropanol by inverting the tubes five times. Tubes were incubated for 10 minutes at room temperature, then centrifuged at 13000 rpm for 12 minutes at 4°C. After discarding the supernatant, 1 ml of 75% ethanol, filtered with a 0.22 µm filter, was added, and tubes were centrifuged for 8 minutes at 8000 rpm at 4°C. After discarding the supernatant, 1 ml of 100% filtered ethanol was added, and samples were centrifuged at 8000 rpm for 8 minutes at 4°C. Tubes were left to air-dry under the ventilating chemical hood at an

upside-down position. Dried samples were resuspended into 30-40 µl of nuclease-free water, and concentrations and the purity of the sample were measured using NanoDrop. RNA samples could be stored at -80°C.

2.2.9.2. cDNA Synthesis

For the cDNA synthesis of isolated total mRNA or RNA, RevertAid First Strand cDNA Synthesis Kit (Thermo Fisher Scientific, K1622) was used with 800 ng of RNA for each sample, according to the manufacturer's protocol. 800 ng of RNA volume was completed to 11 µl with nuclease-free water, and 1 µl of Oligo $(dT)_{18}$ primer was added. 4 µl of 5x Reaction Buffer, 1 µl of RiboLock RNase Inhibitor (RI), 2 µl of 10 mM dNTP Mix and 1µl of RevertAid M-MuLV RT (RT) were mixed in this order for each sample. After gently mixing and brief centrifuging, samples were incubated at 42°C for 60 minutes, and then the reaction ceased by incubating at 70°C for 5 minutes. To perform qPCR experiments, 1:20 diluted cDNA samples were used, and the main stocks of cDNAs were stored at -80°C.

2.2.9.3. qPCR Primer Design

Gene-specific forward and reverse primers, used to check gene expression levels, were designed by using the Primer-BLAST Tool of the National Center for Biotechnology Information (NCBI) (Ye et al., 2012). Primer parameters were changed to 1°C for Max melting temperature (T_m) difference, 60°C for optimal T_m, and maximum product size was limited to 200 bp. In addition to these criteria, GC content (ideally around 50-60%) and mismatch scores were checked. All primers with at least one predicted product were eliminated due to non-specific binding.

After primers were designed, these were controlled by using the Oligo Analyzer Tool of IDT (Integrated DNA Technologies) (https://eu.idtdna.com/pages/tools/oligoanalyzer) for self- or

heterodimerisation or hairpin structure generation. ΔG score of each designed primer pair was checked whether it was ≥ -5.0 kcal.mol^{-1}. Lastly, primers were examined using the In-Silico PCR Tool of the University of California Santa Cruz (UCSC) Genomics Institute (https://genome.ucsc.edu/cgi-bin/hgPcr). GRCh38/hg38 human genome assembly was used.

2.2.9.4. qPCR Experiment & Analysis

Gene expression analysis on mRNA level was observed using a qPCR experiment with LightCycler® 96 Instrument. LightCycler® 480 SYBR Green I Master (Roche, 4887352001) was used to prepare the qPCR reaction. The qPCR reaction mixture was prepared as a final volume of 8 µl per well; according to this, 5 µl of LightCycler® 480 SYBR Green I Master, 1 µl of the forward primer (10 µM), 1 µl of the reverse primer (10 µM) and 1 µl of nuclease-free water were mixed. 1:10 primer dilutions were used for the master mix. After the master mix was distributed to wells as 8 µl per well, 2 µl of 1:20 diluted cDNA was added to each well, and the final volume became 10 µl per well; then, the plate was sealed. If primers were diluted at a 1:10 ratio instead of 1:20, nuclease-free water in the master mix was increased to 2 µl per well, and cDNA was added as 1 µl to keep both final volume and the concentrations constant. The qPCR plate was centrifuged at 1500 rpm for 2 minutes, and the experiment was started on LightCycler® 96 Instrument with optimal annealing temperature of each primer pair. The experimental steps, conditions, and the number of cycles of each step were described in **Table 2-12**. qPCR experiment was planned as two technical replicates of two biological replicates for each sample. To control any oligonucleotide contamination, the negative control group did not contain any cDNA but nuclease-free water. TPT1 (Tumor Protein, Translationally Controlled 1) gene was used for housekeeping gene normalisation as a reference gene.

Table 2-12. Reaction conditions of qPCR to detect gene expression levels.

Step	Hold Temperatures (°C)	Time	Number of Cycle
Pre-Incubation	95	5 min	1
Amplification	95	10 sec	45-50
	58-60	20 sec	
	72	20 sec	
Melting Curve	95	5 sec	1
	55	1 min	
	95	Acquisition per 5°C	
Cooling	40	30 sec	1

qPCR measurements were obtained by using "Abs Quan (Absolute Quantification) analysis as C_T (Cycle threshold) or Cq (Quantification cycle) by using LightCycler® 96 System programme. Melting curves and melting peaks graphs were used to detect any contamination.

Relative expression levels of the genes were calculated according to the $\Delta\Delta C_T$ method or Livak method. (Livak & Schmittgen, 2001) According to this, mean C_T values of technical replicates of sample groups were subtracted from mean C_T values of technical replicates of the control group and $-\Delta C_T$ values were obtained. $2^{-\Delta C_T}$ values were used for normalisation with the TPT1 gene, the housekeeping gene, by subtraction. As a result, $2^{-\Delta\Delta C_T}$ values were transformed to logarithmic values to base 2 and used for statistical analysis.

2.2.10. Statistical Analysis

All presented statistical analyses were performed using GraphPad Prism 9.0 programme in this study. Western blot results with two sample groups were analysed with Student's t-test. Experiments comparing multiple sample groups, qPCR, western blot and MTT, and One-way or Two-Way ANOVA analysis were used, followed by Tukey multiple comparison method.

Chapter 3

3. Results

3.1. Confirmation of Downregulation of DLK1 and MEG3 Expression in siRNA CHRNA5 Transfected MCF7 Cell Line

In previous studies from our lab, the downregulation of CHRNA5 expression at both mRNA and protein levels was achieved by treatments of three different siRNAs targeting CHRNA5 (siCHRNA5) (Koker et al., 2018). To demonstrate that the cDNAs obtained in previous experiments were still a high quality, I have remeasured the level of CHRNA5 mRNA in 10nM scrambled siRNA, and siRNA CHRNA5 (si1 or siCHRNA5) treated MCF7 cells and confirmed around 3-fold (log_2FC) reduction in expression (**Figure *3-1*A**). Based on the GSE89333 dataset that we performed (Cingir-Koker et al., 2018), it was shown that several genes in the DLK1-DIO3 imprinted region were downregulated when treated with siRNA CHRNA5 in MCF7 cells (**Table *3-1***). DLK1 and MEG3 were significantly reduced and hence these genes were selected for further study. In the present thesis, I have confirmed by qPCR that DLK1 (**Figure *3-1*B**) and MEG3 expression (**Figure *3-1*C**) were downregulated in response to siCHRNA5 treatment.

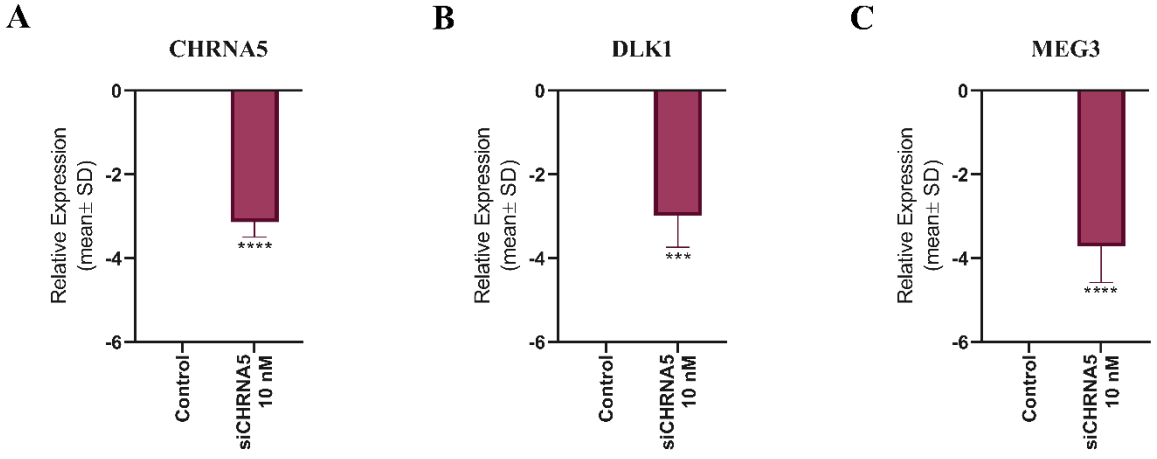

Figure 3-1. qPCR analysis of relative mRNA expression levels of CHRNA5 and DLK1 genes using MCF7 cell line treated with 10 nM siRNA CHRNA5 (siCHRNA5) or control scrambled siRNA for 3 days. CHRNA5 (A), DLK1 (B), and MEG3 (C) gene expressions upon siCHRNA5 treatments. Data were represented in a log2FC format, and error bars were determined according to Mean ΔΔCT±SD (n=5). TPT1 gene is used as a loading control. The student's t-test was applied to analyse the data. (*: p-value ≤ 0.05, **: p-value ≤ 0.01 and ****: p-value ≤ 0.0001)

3.2. Effects of 14q32.31 miRNA Mimic Treatments on the DLK1 and MEG3 Expression Levels

Previously Sahika Cingir-Koker (Bilkent University PhD Thesis, 2019), Said Tiryaki (Bilkent University MS Thesis, 2020) and Ayse G. Keskus (Bilkent University PhD Thesis, 2021) have performed mRNA microarray experiments with MCF7 cells treated with 14q32.31 miRNAs, which are miR-376c-3p, miR-409-3p and miR-495-3p mimics, in the presence of siRNA CHRNA5 or control siRNA followed by independent sets of experiments of the similar designs for validation purposes. 14q32.31 miRNAs are located in the same imprinted region where DLK1 and MEG3 are found and expressed from the same maternal allele in which MEG3 is transcribed (Rocha et al., 2008). Accordingly, my hypothesis to test was that DLK1 and MEG3

might be increased in expression in the presence of either of these mimics. I first extracted the DLK1 and MEG3 microarray expression values (**Table *3-1***).

Table 3-1. Gene expression values as log_2FC values of DLK1 and MEG3 genes for the miR-495-3p and/or siCHRNA5 treated MCF7 cells.

Gene Symbol	Log_2FC	p-Val	adj p-val	siCHRNA5	miR-495	siCHRNA5+ miR-495	siCHRNA5	miR-376a	siCHRNA5 + miR-376a	siCHRNA5	miR-409	siCHRNA5+ miR-409
DLK1	-2.14555	4.92E-07	0.000325	-0.227	0.256	-0.483	-2.056	0.097	-2.152	-3.26795	-1.31988	-1.94807
MEG3	-0.28858	0.041626	0.133368	NA	NA	NA	-0.466	0.359	-0.825	-0.30295	-0.13474	-0.16821

Accordingly, DLK1 was significantly highly downregulated, while MEG3 was mildly downregulated by CHRNA5 siRNA treatment. On the other hand, in the presence of miR-495-3p, DLK1 became stable or negligibly upregulated, although when miR-495-3p mimic combined with CHRNA5 siRNA, the downregulation in the DLK1 levels observed by CHRNA5 siRNA alone was reverted entirely. This rescue/reversion was not seen in the presence of mimic 376a. Interestingly mimic of miR-409 alone resulted in a further decrease in the DLK1 levels, and when combined with CHRNA5 siRNA, the reduction in the DLK1 levels observed in response to CHRNA5 depletion became more in magnitude and significant. In order to test these interesting findings, I performed qPCR analyses in cDNA panels previously used by Ayse G. Keskus, Sahika Cingir Koker in their thesis (**Figure *3-2***).

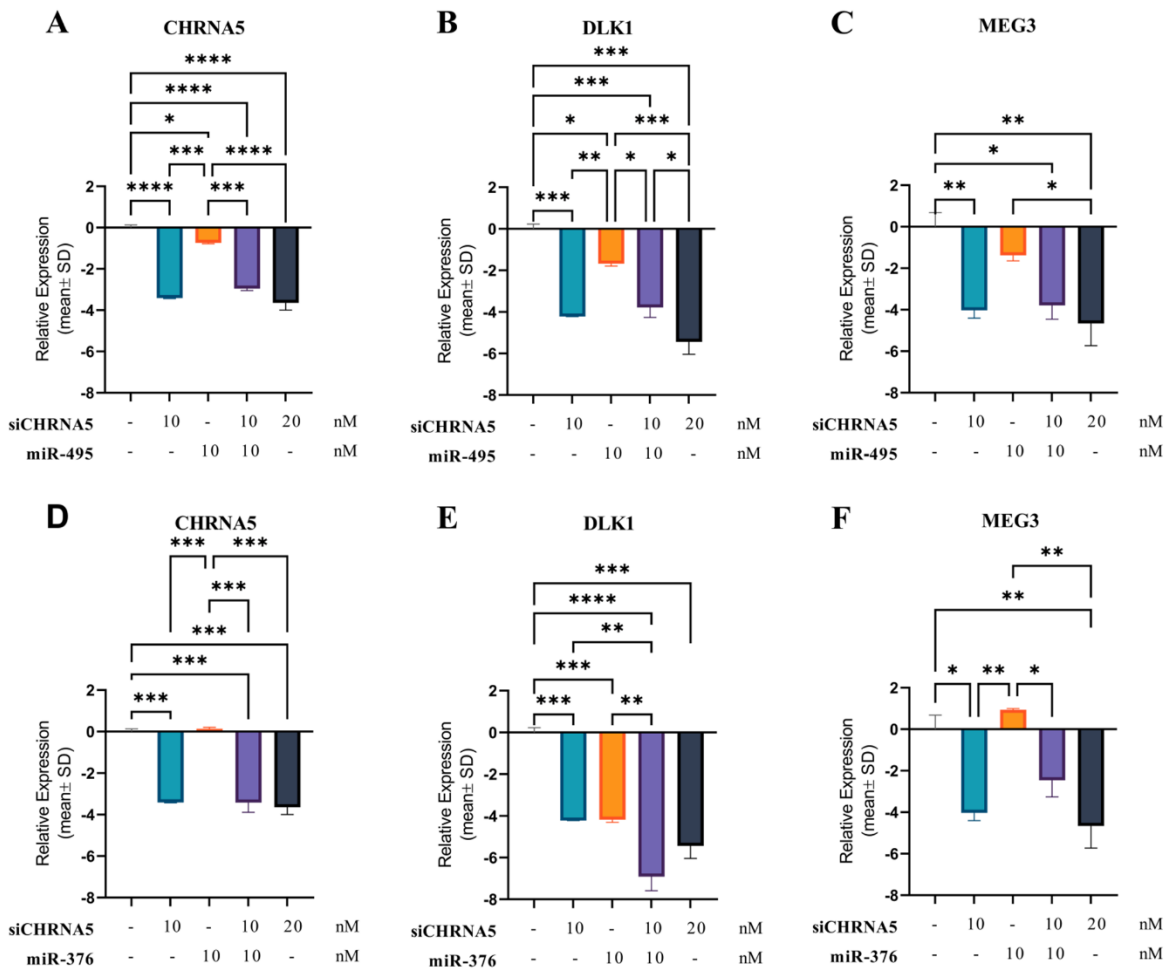

Figure 3-2. Effects of 14q32.31 miRNAs on DLK1 and MEG3 gene expressions. log_2FC values for CHRNA5 (A), DLK1 (B) and MEG3 (C) in the presence of miR-495 in the presence of siRNA CHRNA5 or control siRNA. log_2FC values for CHRNA5 (D), DLK1 (E) and MEG3 (F) in the presence of miR-376 with siRNA CHRNA5 or control siRNA. (*: p-value ≤ 0.05, **: p-value ≤ 0.01 and ****: p-value ≤ 0.0001)

According to qPCR experiments on siCHRNA5 and miR-495 treated MCF7 cell line, the effect of 10 nM CHRNA5 depletion is seen on CHRNA5 expression level (**Figure *3-2*A)**, and miR-495-3p alone has also significantly decreased DLK1 (**Figure *3-2*B**) and non-significantly decreased MEG3 (**Figure *3-2*C**) around 1.5-2 fold. The combination of siCHRNA5 and miR-495-3p treatment shows a similar decreasing trend with the siCHRNA5 10 nM group on DLK1 and MEG3.

In addition to miR-495 & siCHRNA5 combinations, a decrease in CHRNA5 could not be observed on miR-376 only samples (**Figure *3-2*D**).

The experiment shown in **Figure *3-2*** is a full set of experiment including combinatorial dosage of miR-376 and miR-495. Since the difference between miR-495 or miR-376 only samples and miR-495 & miR-376 combinatorial sample were not significant for CHRNA5 and MEG3 expression, and to ease the depiction of the data, data analysis of the whole experiment was shown in ***Appendix Figure 1*A & C**. On the other hand, DLK1 expression on miR-495 & miR-376 samples were significantly decreased than in miR-495-only samples (***Appendix Figure 1*B**).

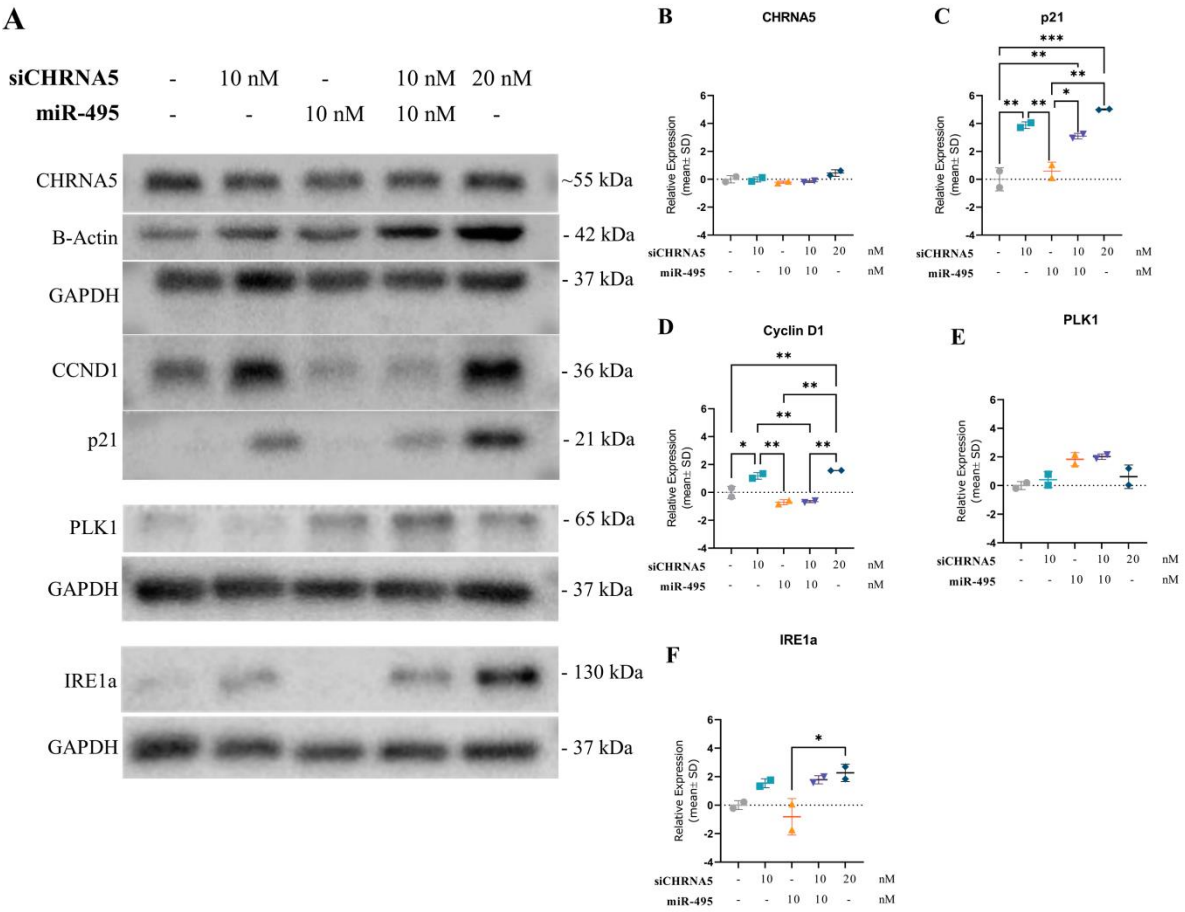

Figure 3-3. Western blot analysis of selected proteins on MCF7 cell line siCHRNA5 and miR-495 for 3 days. Effects of siCHRNA5 and miR-495 on protein level (A) and densitometry analysis of CHRNA5 (B), p21 (C), Cyclin D1 (D), PLK1 (E) and IRE1a (F) expression levels. GAPDH was used as a loading control. One-way ANOVA analysis was used with Tukey multiple comparison analysis. (*: p-value ≤ 0.05, **: p-value ≤ 0.01 and ****: p-value ≤ 0.0001)

Effects of CHRNA5 depletion and miR-495 induction were also checked on protein level, and transfection of siCHRNA5 and miR-495 was performed by Sahika Cingir-Koker. Even though depletion of CHRNA5 was observed on the RNA level, the same effect could not be observed on the protein expression level when normalized with GAPDH (***Figure 3-3*B**), despite the downstream effect of p21 and Cyclin D1 expression levels, which increases with CHRNA5 depletion (**Figure *3-3*C**). Significantly increased Cyclin D1 protein expression level with CHRNA5 depletion might indicate the effects of CHRNA5 on primary ESR1 targets

(Shehwana et al., 2021) and induction of cell metastasis and invasion (Fusté et al., 2016) (**Figure *3-3*D**). According to a previous study performed by Ayse G. Keskus (Bilkent University, PhD Thesis, 2021), the effect of siCHRNA5 was also confirmed with PLK1 expression levels, and IRE1a expression (**Figure *3-3***E&**F**) levels were observed for future aspects of the project.

Although we have shown a significant decrease in mRNA level, CHRNA5 protein level upon exposure to siCHRNA5 could not be observed when normalized to GAPDH loading control; hence another commonly used reference gene, beta-Actin, was considered as a potential loading control (**Figure *3-4***).

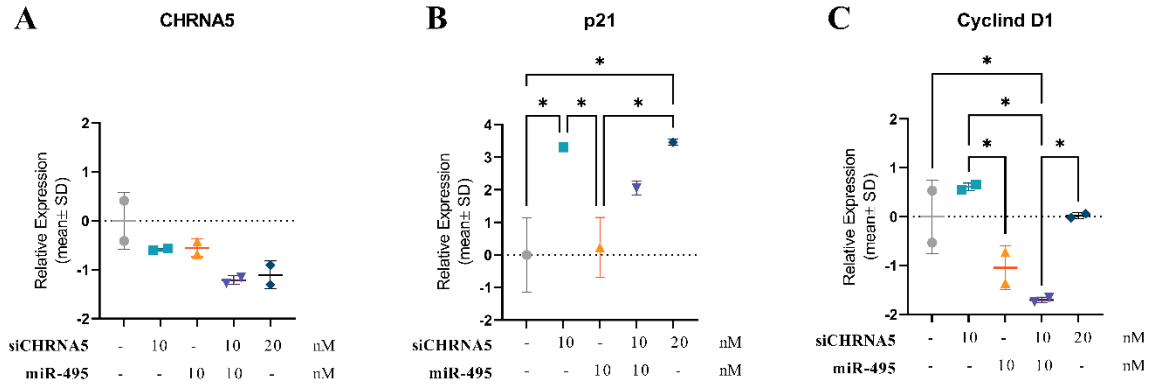

Figure 3-4. Western blot analysis of selected proteins on MCF7 cell line siCHRNA5 and miR-495 for 3 days. Effects of siCHRNA5 and miR-495 on protein level and densitometry analysis of CHRNA5 (A), p21 (B) and Cyclin D1(C) expression levels. Beta-Actin was used as a loading control. One-way ANOVA analysis was used with Tukey multiple comparison analysis. (*: p-value ≤ 0.05, **: p-value ≤ 0.01 and ****: p-value ≤ 0.0001)

Even if CHRNA5 expression levels decreased upon siCHRNA5 treatment, the change was not significant when multiple tests corrected due to high variability in the control group. However similar expression pattern could be significantly observed in both Cyclin D1 and p21 protein expression (**Figure *3-3***). Statistical result of CHRNA5 expression level was given in **Appendix**

Figure *2*. I have also confirmed other highly modulated genes from the miRNA microarray study (**Figure *3-5***).

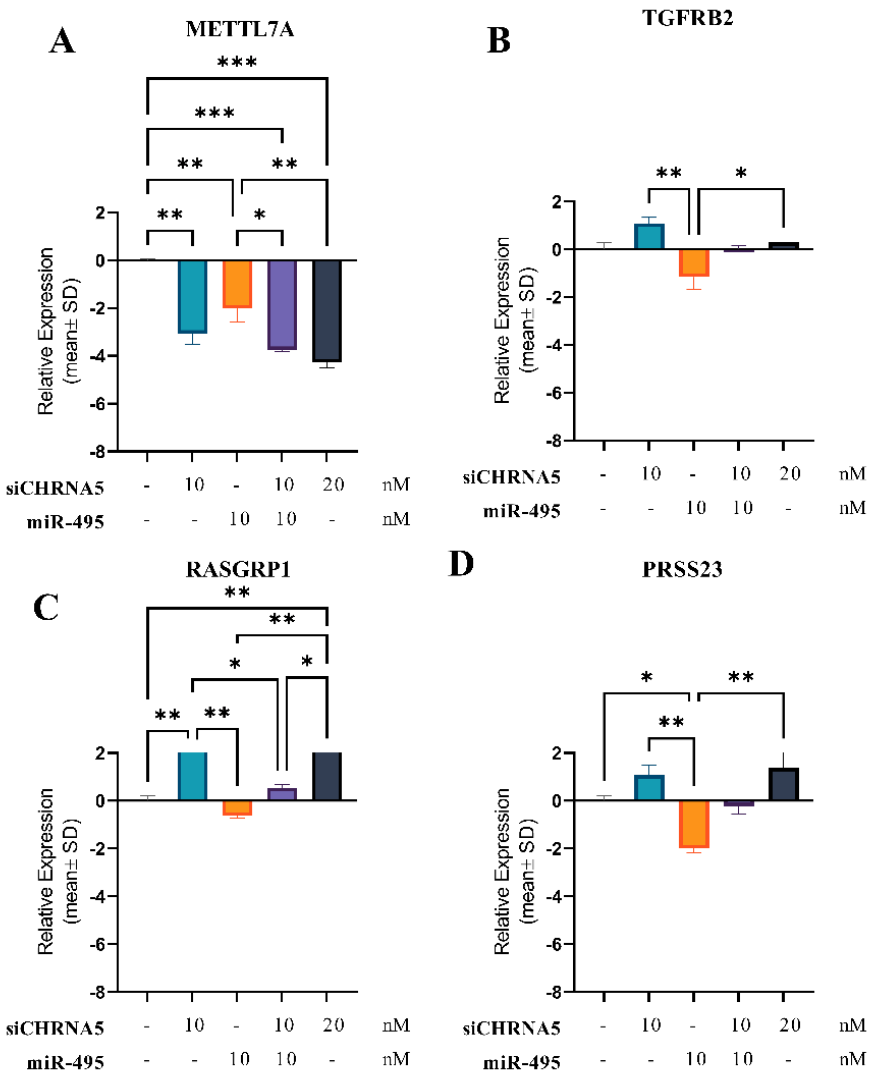

Figure 3-5. Effects of 14q32.31 miRNAs on selected gene expressions. log_2FC values for METTL7A (A), TGFRB2 (B), RASGRP1 (C) and PRSS23 (D) in the presence of miR-495 with siRNA CHRNA5 or control siRNA. log_2FC values for CHRNA5 (D), DLK1 (E) and MEG3 (F) in the presence of miR-376 with siRNA CHRNA5 or control siRNA. (*: p-value ≤ 0.05, **: p-value ≤ 0.01 and ****: p-value ≤ 0.0001)

3.3. Effects of TP53 Downregulation via siRNA TP53 on DLK1 and MEG3 Expression in the Presence or Absence of CHRNA5

Previously, Ayse G. Keskus (Bilkent University, PhD Thesis, 2021) has shown that CHRNA5 depletion exhibits effects in TP53-dependent and TP53-independent manners by using an RNAseq experiment she performed in MCF7 cells. According to limma analysis results obtained by Ayse G. Keskus, I have extracted the $\log_2$FC and significance values between siRNA CHRNA5 (siCHRNA5) and control siRNA (scRNA) treated TP53 intact cells; siRNA TP53 (siTP53) and control siRNA treated MCF7 cells, and siRNA TP53 and siRNA CHRNA5 and control siRNA treated MCF7 cells (

Table 3-2). Accordingly, a decrease in DLK1 expression was relatively TP53 independent, while MEG3 expression was significantly downregulated in the absence/reduction of siTP53. When siRNA CHRNA5 was given in the presence of siRNA against TP53, there was less yet still significant downregulation of DLK1 that might suggest partial independence. On the other hand, while in the absence of TP53, siRNA CHRNA5 reduced the MEG3 levels effectively to the same degree when compared with intact TP53 levels, but the effect was not additive, suggesting that siRNA CHRNA5 and siRNA TP53 worked independently and the effects of siRNA CHRNA5 was inhibitory on MEG3 levels regardless of TP53 status.

Table 3-2. The log_2FC expression values of DLK1 and MEG3 in the siRNA CHRNA5, siRNA TP53 and combination treatments in MCF7 cells in comparison with the control siRNA group from RNAseq results.

Gene Symbol	siCHRNA5 log_2FC	siCHRNA5 adj. p-val.	siTP53 log_2FC	siTP53 adj. p-val.	siCHRNA5 – siTP53 log_2FC	siCHRNA5 – siTP53 adj. p-val.
DLK1	-3.19847	2.47E-09	-0.79807	0.20307	-2.57879	8.11E-07
MEG3	-3.77442	0.000627	-2.51192	0.026135	-3.65393	0.000666

Accordingly, I wanted to confirm these findings from RNAseq data using an independent experiment with the same groups and performed RNA isolation, cDNA synthesis of the same groups and a qPCR run with DLK1 and MEG3 genes. Before performing these, I wanted to double-check if I had successfully downregulated CHRNA5 and TP53 expression levels and if the expected changes in the targets of TP53 and known CHRNA5 regulated transcripts were observed. I found that CHRNA5 and TP53 expression were downregulated significantly by the siRNA treatments (**Figure *3-6*A & B**). MAP1B, a significantly upregulated gene as shown in Cingir-Koker et al. 2018 for CHRNA5 downregulation regardless of the cell line, was also upregulated by the siRNA CHRNA5 in the new experiment while CDKN1A was upregulated by CHRNA5 and expectedly downregulated by treatment with siRNA against TP53 as it is one of the primary targets of TP53 (**Figure *3-6*C & D**).

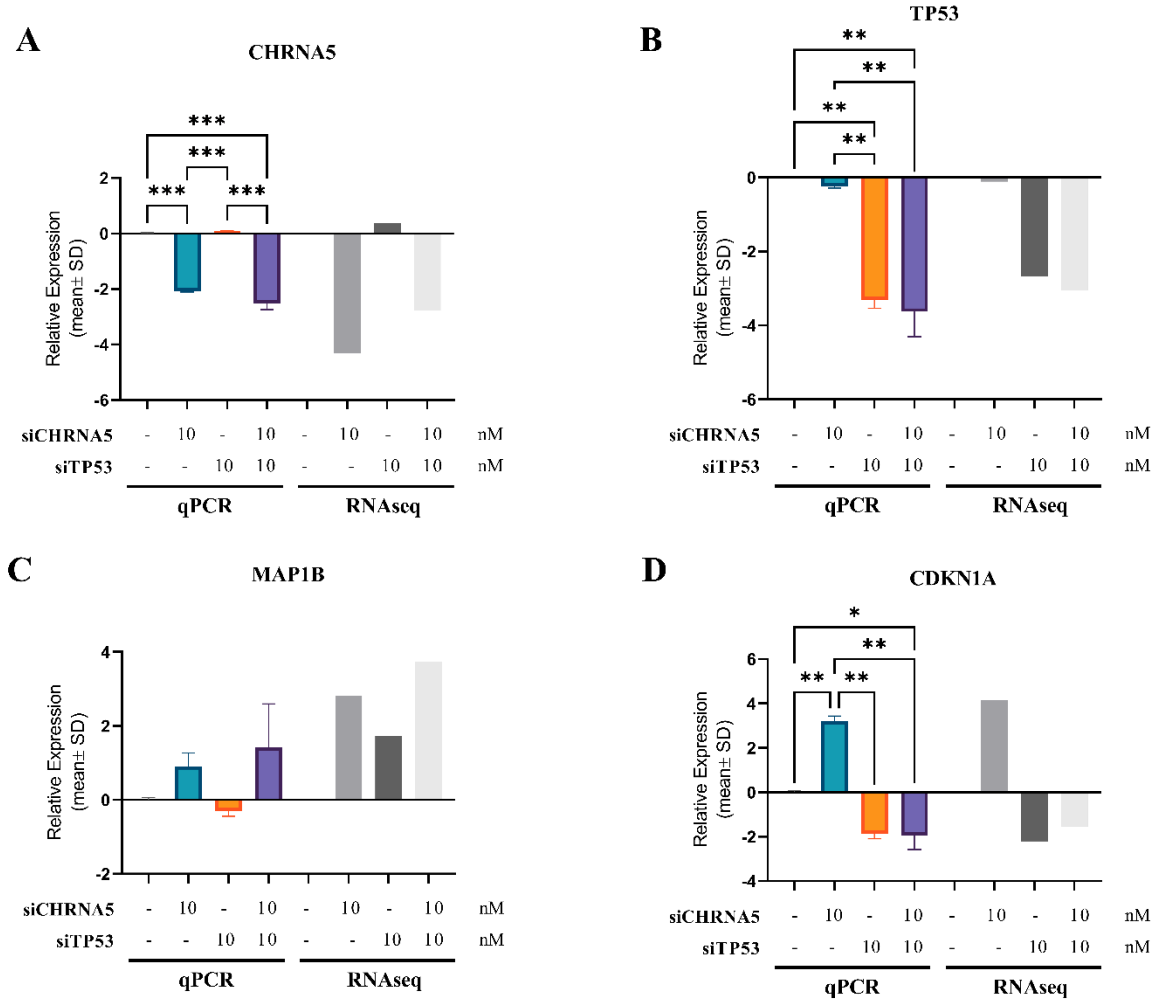

Figure 3-6. The levels of TP53 (A) and CHRNA5 (B) along with CDKN1A (p21) (C) and MAP1B (D) in the presence of TP53 siRNA, CHRNA5 siRNA, or both TP53 and CHRNA5 siRNAs. Data were represented in a $\log_2$FC format, normalized to control, and error bars were determined according to Mean ΔΔCT±SD. TPT1 gene is used as a loading control. One-way ANOVA analysis was used with Tukey multiple comparison analysis. (*: p-value ≤ 0.05, **: p-value ≤ 0.01 and ****: p-value ≤ 0.0001)

Next, I tested DLK1 and MEG3 mRNA expression in the presence of siCHRNA5, siTP53, or both siRNAs and showed that DLK1 was significantly downregulated, as expected by siCHRNA5 alone. Similarly, in the RNAseq data, siTP53 did not modulate the expression of DLK1, while in the absence of TP53, siCHRNA5 could not downregulate DLK1 as

significantly as it did when it was given alone (**Figure *3-7*A**). On the other hand, siCHRNA5, siTP53 or both siRNAs could not lead to the significant down-regulation of MEG3 expression. although siCHRNA5 managed to decrease MEG3 expression level by around 2-fold, and the presence of combinatorial siRNAs decreased the expression of MEG3 by approximately 1.5-fold (**Figure *3-7*B**).

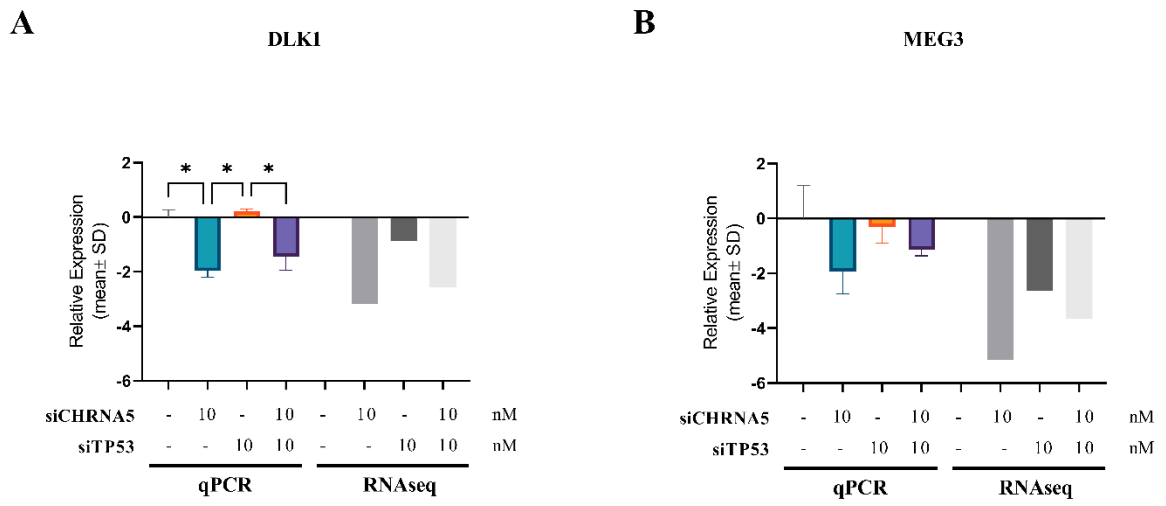

Figure 3-7. The levels of DLK1 and MEG3 in the presence of TP53 siRNA, CHRNA5 siRNA, or both TP53 and CHRNA5 siRNAs. Data were represented in a $\log_2$FC format, normalized to control, and error bars were determined according to Mean ΔΔCT±SD. TPT1 gene is used as a loading control. One-way ANOVA analysis was used with Tukey multiple comparison analysis. (*: p-value ≤ 0.05, **: p-value ≤ 0.01 and ****: p-value ≤ 0.0001)

3.4. Effects of TP53 Downregulation via siRNA TP53 on MDM2, CDH18 and PDLIM7 Expression in the Presence or Absence of CHRNA5

I then analysed the RNAseq data for TP53 regulators such as MDM2 and its associated markers CDH18 and PDLIM7 (Klein et al., 2018) and found that MDM2 was downregulated only in the combinatorial treatment (**Table *3-3***).

Table 3-3. According to RNAseq data, the expression level changes (log2FC) of TP53 regulators, MDM2, PDLIM7, and CDH18. (Ayse G. Keskus, Bilkent University PhD Thesis). Bold indicates significance.

Gene Symbol	siCHRNA5 log_2FC	siCHRNA5 adj. p-val.	siTP53 log_2FC	siTP53 adj. p-val.	siCHRNA5 – siTP53 log_2FC	siCHRNA5 – siTP53 adj. p-val.
CDH18	0.294686757	0.748074834	-1.824979897	0.116206713	**-4.154728019**	0.024958523
PDLIM7	0.230306549	0.595125067	-0.328657791	0.424864307	-0.527376151	0.175845159
MDM2	-0.258154947	0.1962633	0.019133614	0.931575472	**-1.460713853**	0.000305894

My aim was then to confirm by qPCR whether MDM2, an inhibitor of TP53, was downregulated to prevent further loss of TP53 in the presence of siCHRNA5 and to see whether there was synergism between CHRNA5 and TP53 siRNAs to regulate TP53 levels as feedback. I found again that MDM2 was significantly downregulated only in the combinatorial treatment of siCHRNA5 and siTP53 (**Figure *3-8*A**). Similar patterns were seen for PDLIM7 and CDH18; however, the downregulation in the combinatorial treatment was more significant for these two when compared with MDM2, which was highly variable (**Figure *3-8*B & C**).

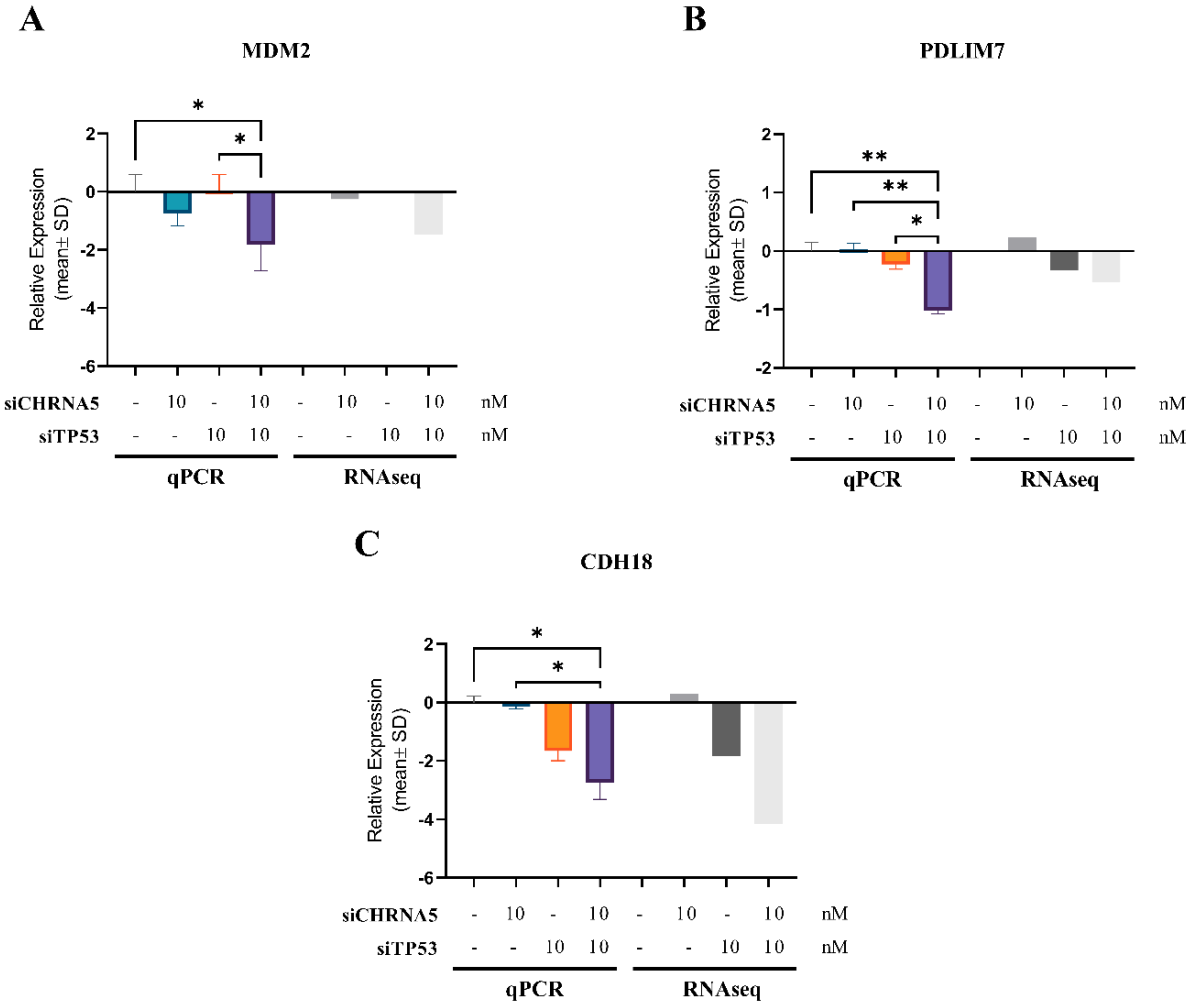

Figure 3-8. The levels of MDM2 (A), PDLIM7 (B) and CDH18 (C) in the presence of TP53 siRNA, CHRNA5 siRNA, or both TP53 and CHRNA5 siRNAs. Data were represented in a log2FC format, normalized to control, and error bars were determined according to Mean ΔΔCT±SD. TPT1 gene is used as a loading control. One-way ANOVA analysis was used with Tukey multiple comparison analysis. (*: p-value ≤ 0.05, **: p-value ≤ 0.01 and ****: p-value ≤ 0.0001)

3.5. Effects of TransientTP53 Overexpression on MCF7 Cell Line

Since previously shown that siCHRNA5 induced TP53 signalling (Cingir Koker, et al., 2018) and decreased the TP53 inhibitor MDM2 expression level with its associated genes, CDH18 and PDLIM7, there might be a common effect of siCHRNA5 depletion and TP53 expression.

Hence, I have evaluated whether TP53 wild-type or mutant overexpression would also affect DLK1 and MEG3 gene expression. For this reason, I first amplified and purified pCMV-Neo-Bam plasmids, which included insert of TP53 WT, TP53 R175H, TP53 R248W or TP53 R273H (Baker et al., 1990), obtained from Addgene (**Appendix Figure *3***), and after the NGS results and confirming the mutation status of each plasmids, I tested them in different concentrations concerning their effects on cell proliferation. I have used MCF7 TP53 and MDA-MB-231 cancer cell lines for the optimizations, which have endogenously wild-type TP53 and mutant TP53 R280K expression status, respectively. (The TP53 Database | ISB-CGC, 2022)

3.5.1. Optimisation Studies for Transient Overexpression of TP53 Wild-Type and Mutant Plasmids

3.5.1.1. Selection of a TNBC cell line in TP53 siRNA and overexpression studies

To complement the overexpression studies with additional cell lines, I have tried to silence TP53 levels in MDA-MB-231, yet the maximum dose studied (50 nM) only reduced half of the TP53 mRNA (**Figure *3-9***). I have decided to continue overexpressing TP53 wild-type and mutant plasmids in the MCF7 cell line and MDA-MB-231 without the initial downregulation of TP53.

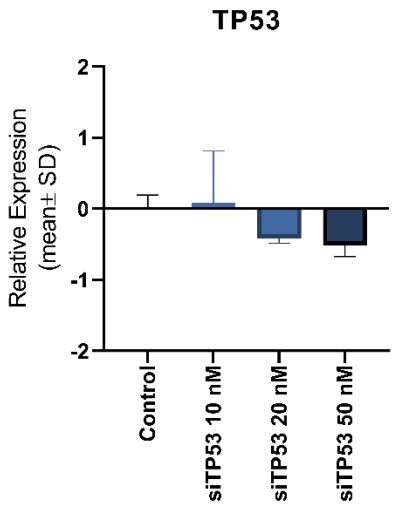

Figure 3-9. Quantitative Real-Time PCR analysis of relative mRNA expression level of TP53 genes on MDA-231 cell line treated with or without 10, 20 and 50 nM siRNA TP53 (siTP53) for 3 days. Data is represented in a $\log_2$FC format, and error bars are determined according to Mean ΔΔCT±SD. (*: p-value ≤ 0.05, **: p-value ≤ 0.01 and ****: p-value ≤ 0.0001)

3.5.1.2. Amplification, purification, and sequencing of the WT and mutant TP53 vectors

After receiving pCMV-Neo-Bam TP53 WT, TP53 R175H, TP53 R248W and TP53 R273H plasmids, they were transformed and purified as described in **Materials & Methods**. Next-generation sequencing was used to confirm the mutation status and sequences of the plasmids. According to sequencing results, I compared the consensus sequences with expected sequences (**Appendix Figure *4-5***) and amino acid sequence of the wild-type TP53 insert with the TP53 R175H, R248W and R273H insert sequences to verify the mutation status (**Appendix Figure *9***).

3.5.1.3. Effects of transient transfection of TP53 WT and mutant overexpression vectors on cell viability in breast cancer cell lines

I have exposed MDA-MB-231 and MCF7 cells to different TP53 overexpression vectors over 3 different time points and in different concentrations to optimize the transient transfection.

Exposure to different vectors was found to be dose dependent. 1000 ng/ml at 72h was significantly toxic for all TP53 vectors, including WT; hence it was found to be not useful. On the other hand, TP53 wild-type overexpression in the presence of a TP53 mutant allele in MDA-MD-231 cells was inhibitory of cell proliferation at all time points and 500 ng/ml doses. At 72h, at which the downstream effects of WT overexpression could be more stabilized, only WT but not the mutants seemed to exhibit cell proliferation inhibitory effects. However, high variability prevented significance attainment (**Figure *3-10***).

In a wildtype TP53 cell line MCF7, I optimized the amount of the TP53 overexpression plasmids in a transient transfection setup using an MTT assay applied on MCF7 treated with 250, 500 and 1000 ng/ml plasmids. Since the transfection efficiency was identified as 1000 ng on 200.000 cells of MCF7 in a 6-well plate (Bircan Çoban, Bilkent MSc Thesis, 2016), the concentrations were determined proportionally to the volume of the media.

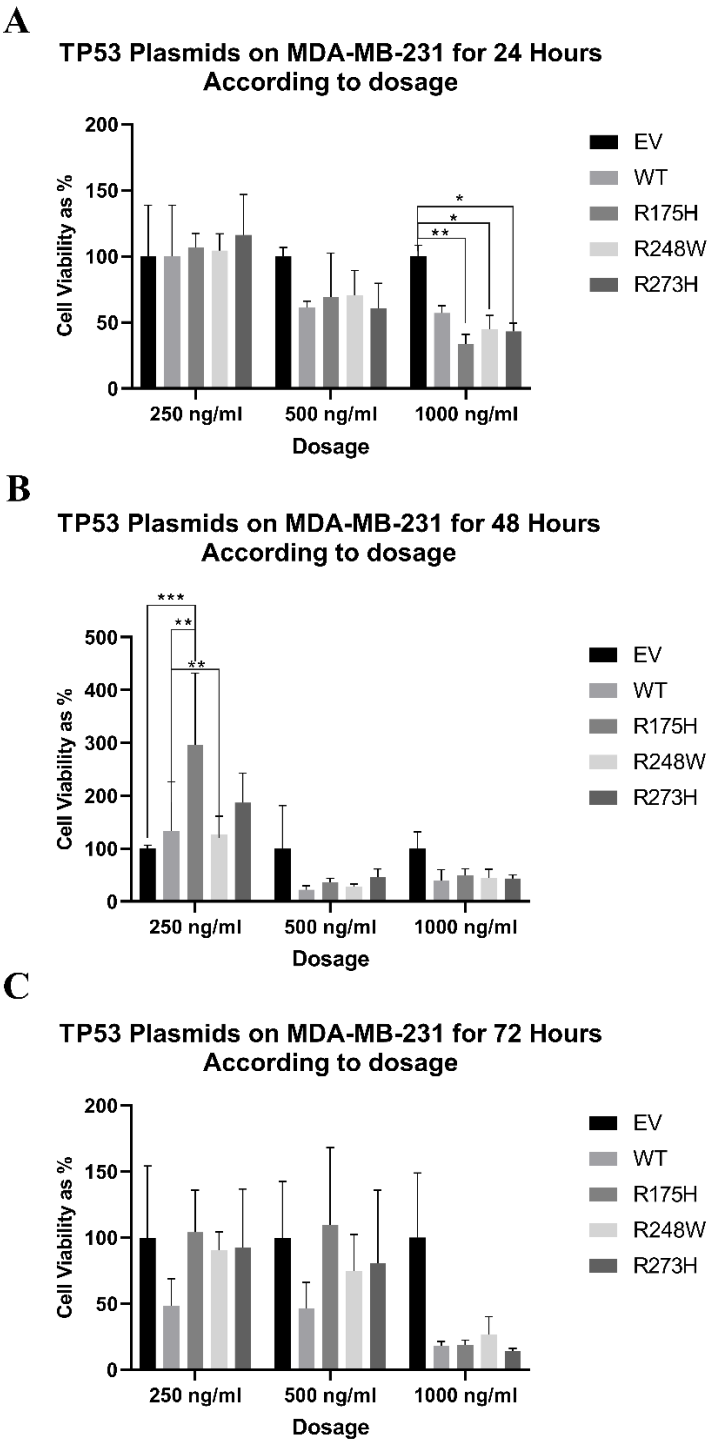

Figure 3-10. Relative cell viability assay on MDA-MB-231 cell line treated with WT and mutant TP53 overexpressed vectors at 250, 500 and 1000 ng/ml concentrations over 24h, 48h, and 72h. Two-way ANOVA analysis was used according to dosage and plasmid type factors with Tukey multiple comparisons. Data is represented in percentage format, and error bars are determined according to Mean±SD values. (*: p-value ≤ 0.05, **: p-value ≤ 0.01 and ****: p-value ≤ 0.0001)

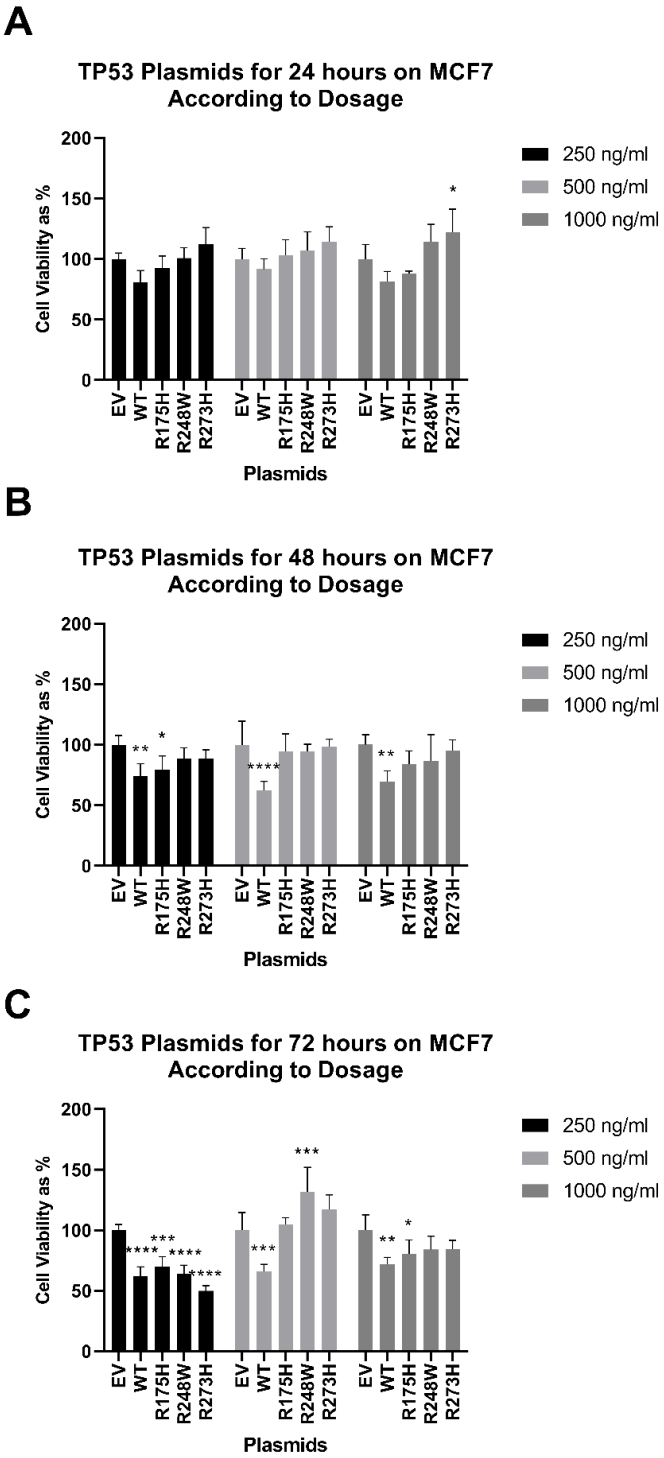

Figure 3-11. Relative cell viability assay on MCF7 cell line treated with WT and mutant TP53 overexpressed vectors at 250, 500 and 1000 ng/ml concentrations at 24 hours (A), 48 hours (B) and 72 hours (C). Each treatment was compared with the belonging control group. Two-way ANOVA analysis was used according to dosage and plasmid type factors with Tukey multiple comparisons. Data is represented in percentage format, and error bars are determined according to Mean±SD values. (*: p-value ≤ 0.05, **: p-value ≤ 0.01 and ****: p-value ≤ 0.0001)

In **Figure *3-11***, WT TP53 overexpression reduced viability in MCF7 cells in all doses at 48h. At 72-hour, the cytotoxicity was apparent at low doses in all transfections, while WT was more cytotoxic in others. However, cell numbers were low, and the experiment was repeated with other dose regimes using 5, 10, and 20 ng plasmid per well as proportional to the cell number instead of the amount of the plasmids over the volume of media ratio. According to the MTT assay, from 48-hour of transient transfection, the effect of the mutant TP53 overexpression could be seen significantly, and the most optimal effect was observed for 10 ng plasmids. The overexpression of wild-type TP53 resulted in inhibition of cell viability at 5 and 10ng levels at 48 and 72 hours, while R248 and R273 were consistently proliferative at 10 and 20ng doses (**Figure *3-12***).

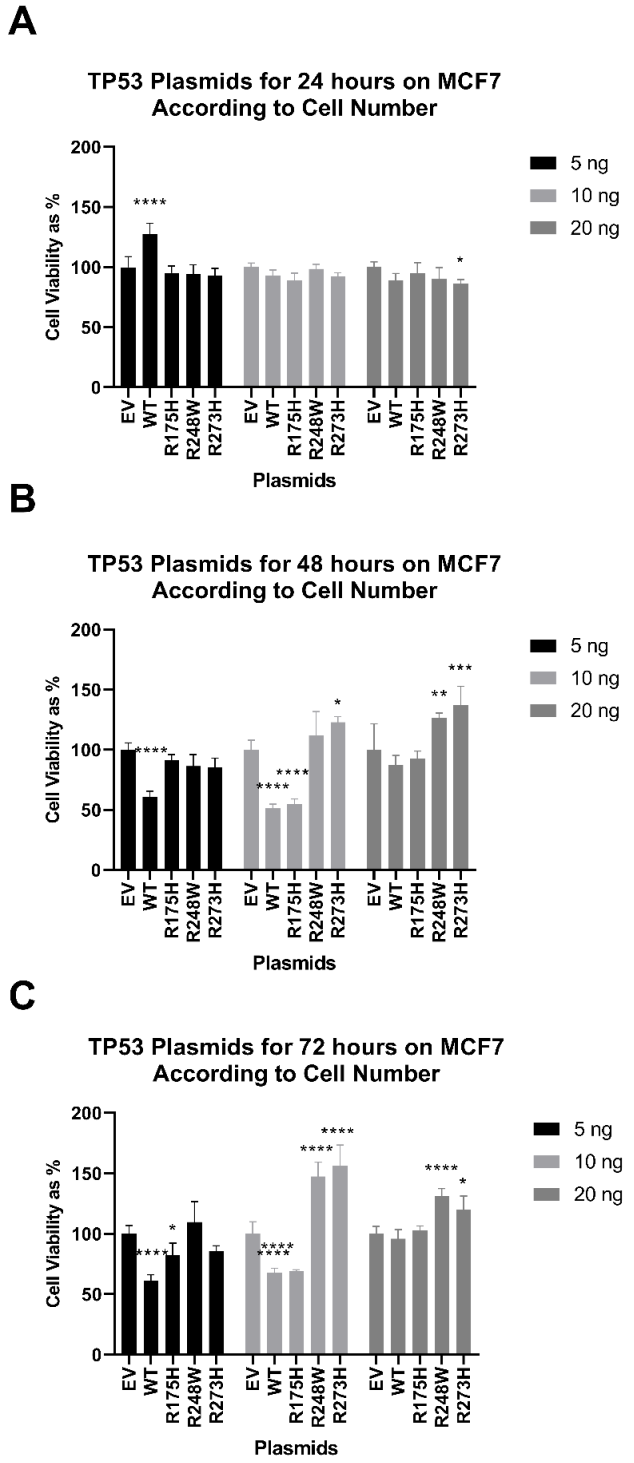

Figure 3-12. Relative cell viability assay on MCF7 cell line treated with WT and mutant TP53 overexpressed vectors at 5, 10 and 20 ng plasmids for 2000 cells per well at 24 hours (A), 48 hours (B) and 72 hours (C). Two-way ANOVA analysis was used according to dosage and plasmid type factors with Tukey multiple comparisons. Data is represented in percentage format, and error bars are determined according to Mean±SD values. (*: p-value ≤ 0.05, **: p-value ≤ 0.01 and ****: p-value ≤ 0.0001)

After the dosage optimization of TP53 overexpression vectors on the 96-well plate, to confirm the effects on cell viability, I also performed a transient transfection experiment on a 12-well plate to see the effects of plasmids with 500 ng plasmids for 100.000 cells per well for qPCR measurements of proliferative cell mRNAs. This was achieved using an experimental setup in which the mRNA level of WT or mutant TP53 was induced more than 7-fold compared to the control (EV) group (**Figure *3-13*A**). CHRNA5 levels were reduced only in the R273 mutants (**Figure *3-13*B**). I also tested several other mRNAs as markers of proliferation, i.e., MKI67, and mesenchymal phenotype, i.e., VIM (**Figure *3-13*C & D**). All the overexpression vectors reduced MKI67 levels suggesting they reduced cell proliferation to a certain extent. Mesenchymal marker increased in only the R248W transfection group suggesting the cell proliferation might have slowed down during the EMT transition.

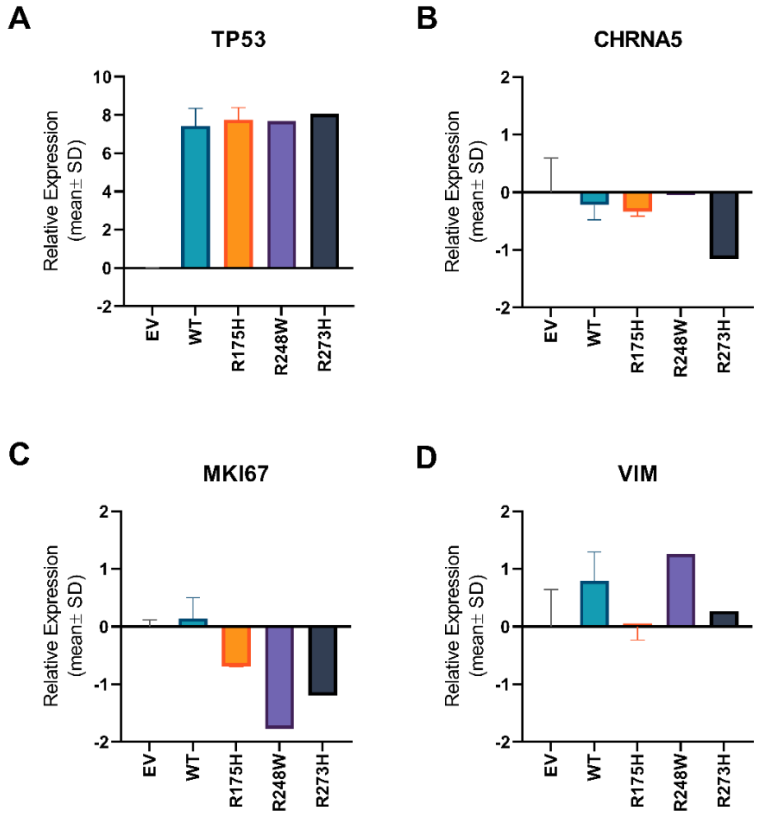

Figure 3-13. Quantitative Real-Time PCR analysis of relative mRNA expression levels of TP53, CHRNA5, MKI67, VIM, DLK1, and MEG3 genes on the MCF7 cells treated with or

without WT and mutant TP53 overexpression plasmids for 3 days. Data is represented as Mean ΔΔCT±SD. Except for R248W and R273H samples, the experiment was conducted as 2 replicates.

3.5.1.4. Effects of dual transient transfection of TP53 WT and mutant overexpression vectors on cell viability in the presence or absence of CHRNA5 siRNA

To address the interaction between overexpression of TP53 levels and CHRNA5 depletion, I performed optimization experiments using siCHRNA5 with or without each type of TP53 overexpression vector as a dual transfection procedure. Since the optimal CHRNA5 depletion effect of siRNA CHRNA5 was observed at 72 hours in previous experiments, I observed the effect of dual transfection at 48 hours and 72 hours on cell viability.

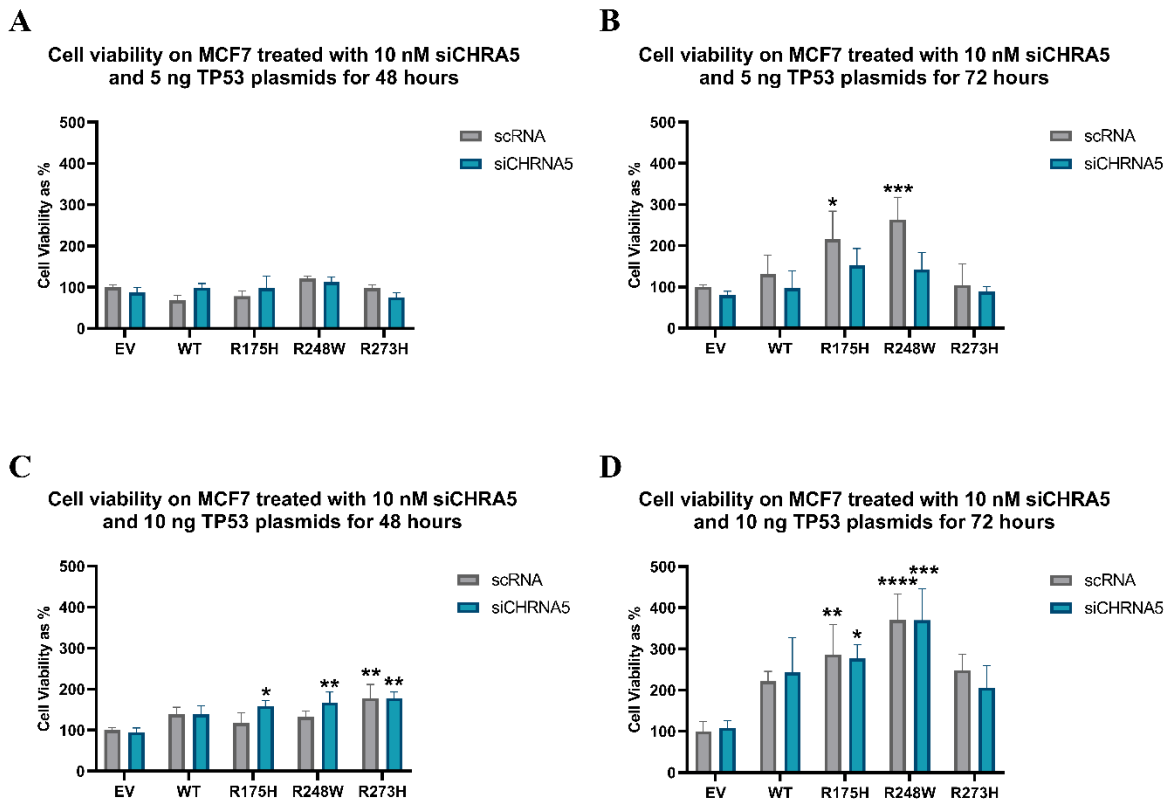

Figure 3-14. Relative cell viability assay on MCF7 cell line treated with siRNA CHRNA5 and scRNA combining with empty vector (EV), TP53 wild-type (WT) TP53 R175H (R175), TP53 R248W (R248W) or TP53 R273H mutant (R273H) overexpression plasmids as a dual transfection method for two different time periods. 5 ng TP53 wild-type and mutant overexpression transfection were applied for 48 hours (A) and 72 hours (B), 10 ng TP53 wild-type and mutant overexpression transfection was applied for 48 hours (C), and 72 hours (D) with 10 nM scRNA or siCHRNA5. (*: p-value ≤ 0.05, **: p-value ≤ 0.01 and ****: p-value ≤ 0.0001)

To induce CHRNA5 depletion with WT or mutant TP53 expression on the MCF7 cell line, a dual transfection method was applied using Lipofectamine 2000. Even the effect of TP53 overexpression vectors could be seen more in the 72-hour treatment group since the expected effect of siCHRNA5 of the control group (EV) on cell viability could not be observed significantly; the experiment was not counted as successful. In addition, WT overexpression at 10 ng exhibited unexpected increases in cell viability along with the mutant vectors. Therefore,

the dual transfection protocol was decided to change into siRNA CHRNA5 transfection on MCF7 cell line overexpressing wild type and mutant TP53 stably (**Figure *3-14***).

3.6. Obtaining WT and Mutant TP53 Stably Overexpressing MCF7 Cells

In order to observe the TP53 dependency with CHRNA5 depletion, stable cell lines were obtained. To achieve this, MCF7 was chosen as a cell line known to express TP53 WT endogenously, and viral transfection experiments were performed. Since the original backbone of the plasmids is not eligible to produce the viral particles, TP53 gene vectors were extracted from the ordered plasmids and cloned into the pBabe-puro plasmid, which has a retroviral characteristic (Morgenstern & Land, 1990).

3.6.1. Cloning TP53 overexpressing vectors into the retroviral backbone

According to the protocol of the manufacturer, the vectors were cut with EcoRI and BamHI restriction enzymes, and after purification, they were cloned into the pBabe-puro backbone. Since both sides of the vectors were cut with the same enzyme, colony screening was performed to confirm the direction of the cloning. NcoI enzyme was selected as ligated plasmids would have the NcoI restriction site both in the vector and outside of the vector; it would give different patterns on the gel electrophoresis according to the direction of the insert. The pattern of each plasmid according to the direction of their insert was visualized using Benchling *in silico* cloning and digest tools for each plasmid (**Figure *3-15***).

Ladder	GeneRuler 1 kb Plus
1	pBABE-puro - NcoI
2	pBabe-puro-TP53-WT_BamHI - NcoI
3	pBabe-puro_TP53-WT_BamHI_Reverse - NcoI
4	pBabe-puro_TP53-R175H_EcoRI - NcoI
5	pBabe-puro_TP53-R175H_EcoRI_Reverse - NcoI
6	pBabe-puro_TP53-R248W_BamHI - NcoI
7	pBabe-puro_TP53-R248W_BamHI_Reverse - NcoI
8	pBabe-puro_TP53-R273H_EcoRI - NcoI
9	pBabe-puro_TP53-R273H_EcoRI_Reverse - NcoI

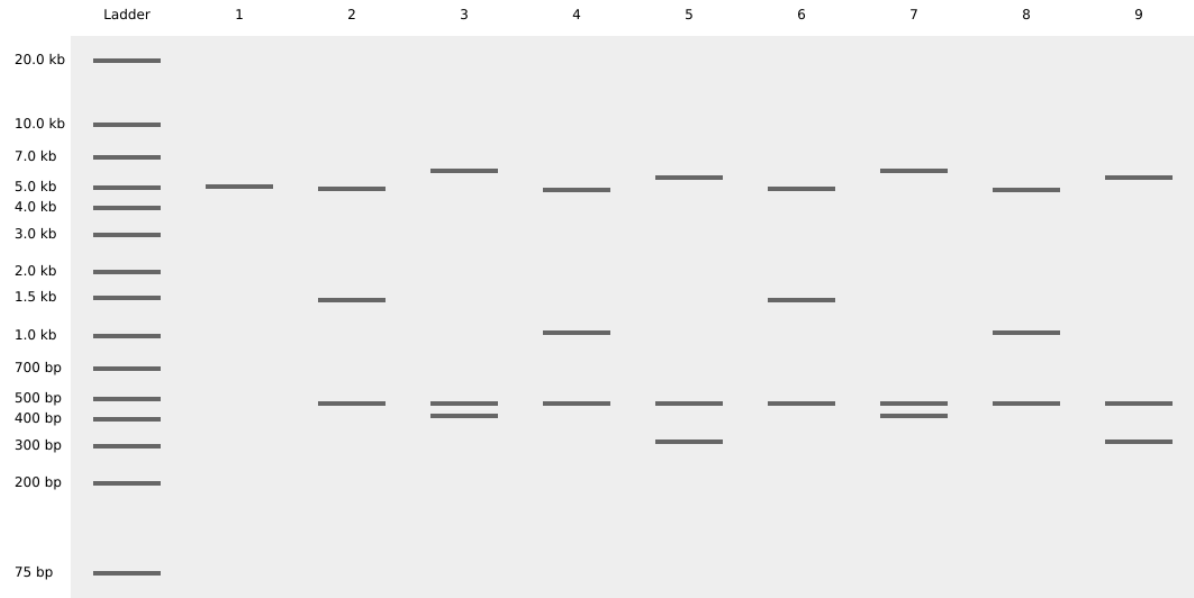

Figure 3-15. *In silico* colony selection experiment design was generated using Benchling for each plasmid. Each sample is named according to the type of plasmid, type of cloning cites cut enzyme and ligation possibility, as a reverse or forward. (Benchling [Biology Software]. (2022). Retrieved from https://benchling.com.)

According to the Benchling results used as a reference, cloned plasmids were digested using the NcoI restriction enzyme and plasmids were run on the gel electrophoresis. For pBabe-puro TP53 WT, colony 2 gave the band around 1500 bp due to NcoI digestion (**Figure *3-16***). To control the enzyme activity, pCMV-Neo-Bam-TP53 WT was used as a positive control.

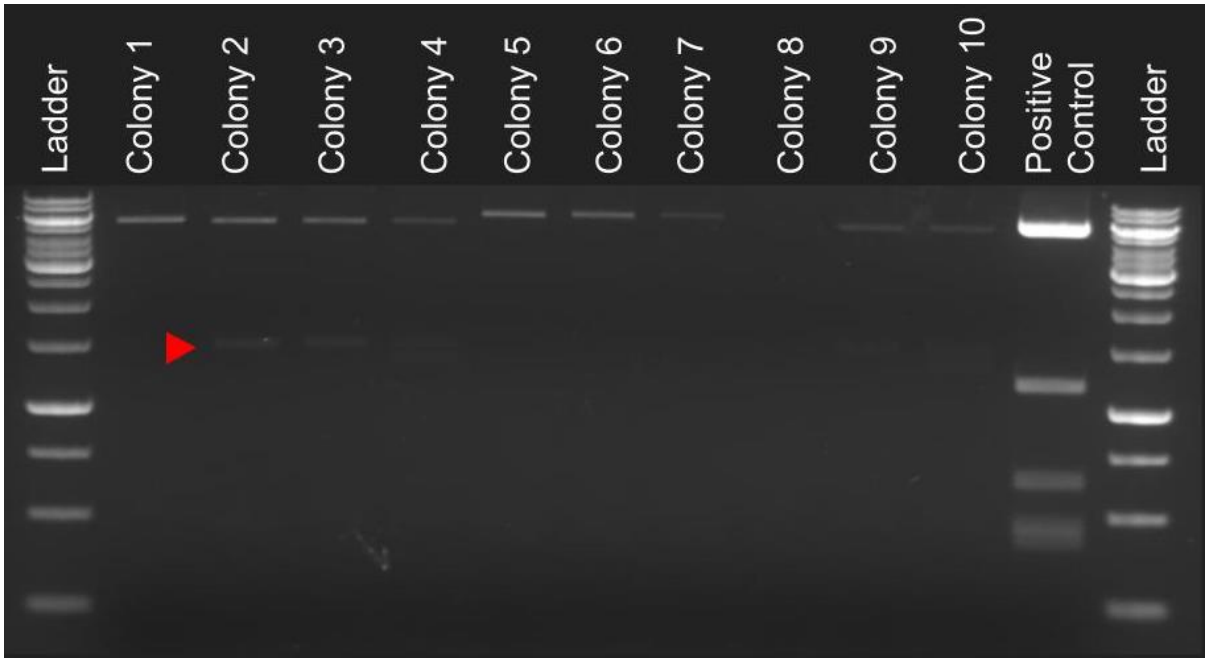

Figure 3-16. pBabe-puro-TP53 WT plasmid screening by NcoI restriction enzyme. Colony 3 was selected, indicated by a red arrow.

For pBabe-TP53 R175H plasmid, colony 3 gave the band around 1000 bp due to NcoI digestion. (**Figure *3-17***) In order to control the enzyme cut, pCMV-Neo-Bam-TP53 R175H was used as a positive control.

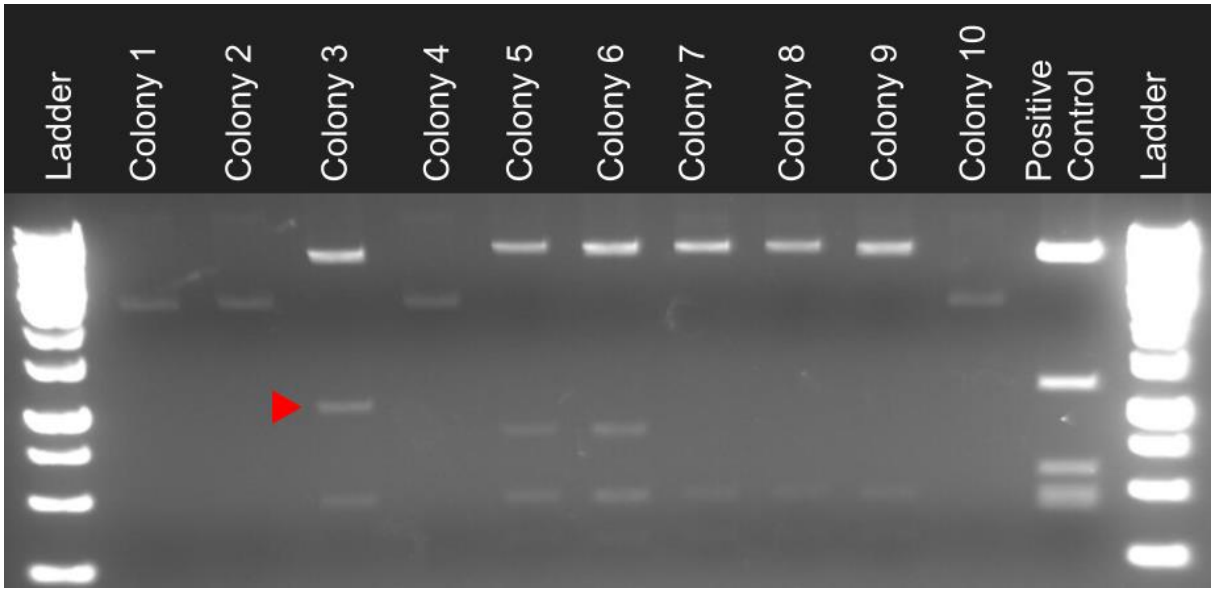

Figure 3-17. pBabe-puro-TP53 R175H plasmid screening by NcoI restriction enzyme. Colony 3 was selected, indicated by a red arrow.

For the pBabe-TP53 R248W plasmids, the colonies with a band around 1.5 kb were identified as clones with the correct orientation. These patterns can be seen in colonies 3, 6, 7 and 10 (**Figure 3-18**). Colony 7 was selected as a pBabe-TP53 R248W plasmid.

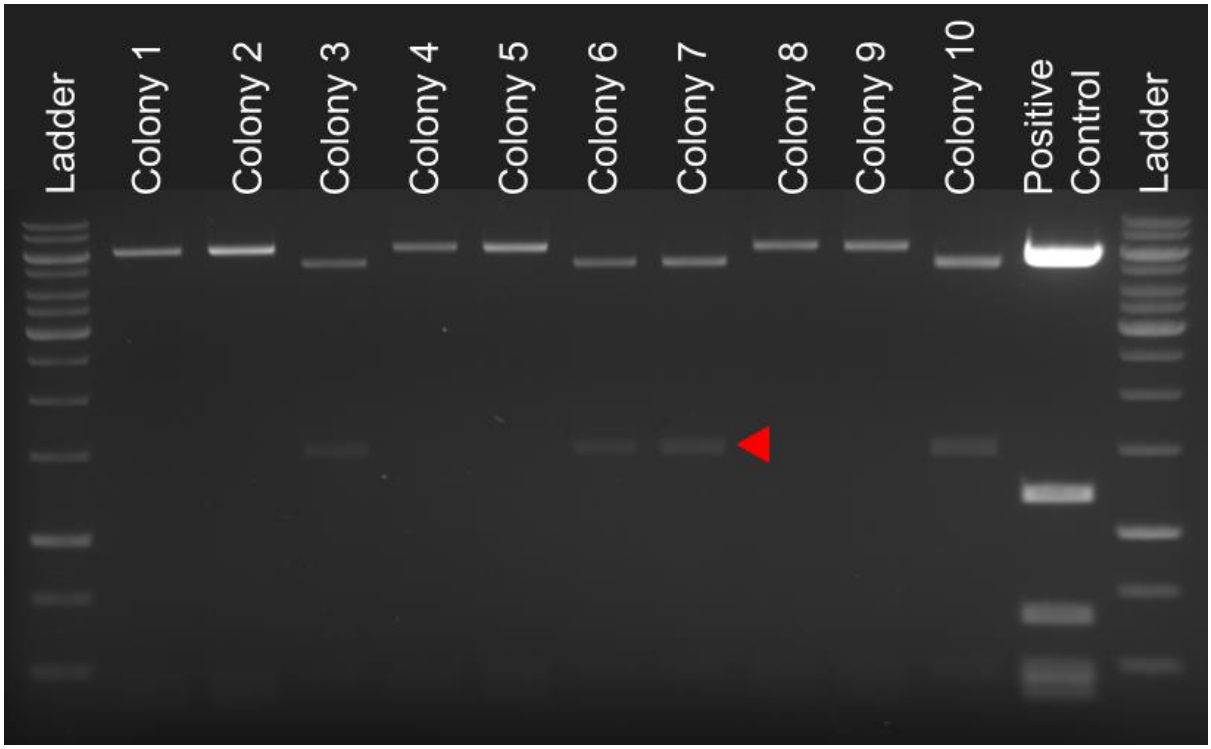

Figure 3-18. pBabe-puro-TP53 R248W plasmid screening by NcoI restriction enzyme. Colony 7 was selected, indicated by a red arrow.

The identifying marker was used to determine the correct direction of TP53 R273H insert into the pBabe-puro plasmid, having two bands at 500 bp and 1000 bp. Therefore, colonies 3, 4, 5, 6, 7 and 8 were identified as potential plasmids that contained the correctly directed insert. Since the clearest bands were observed on colony 7, I selected colony 7 as pBabe-T53 R273H plasmid (**Figure *3-19***).

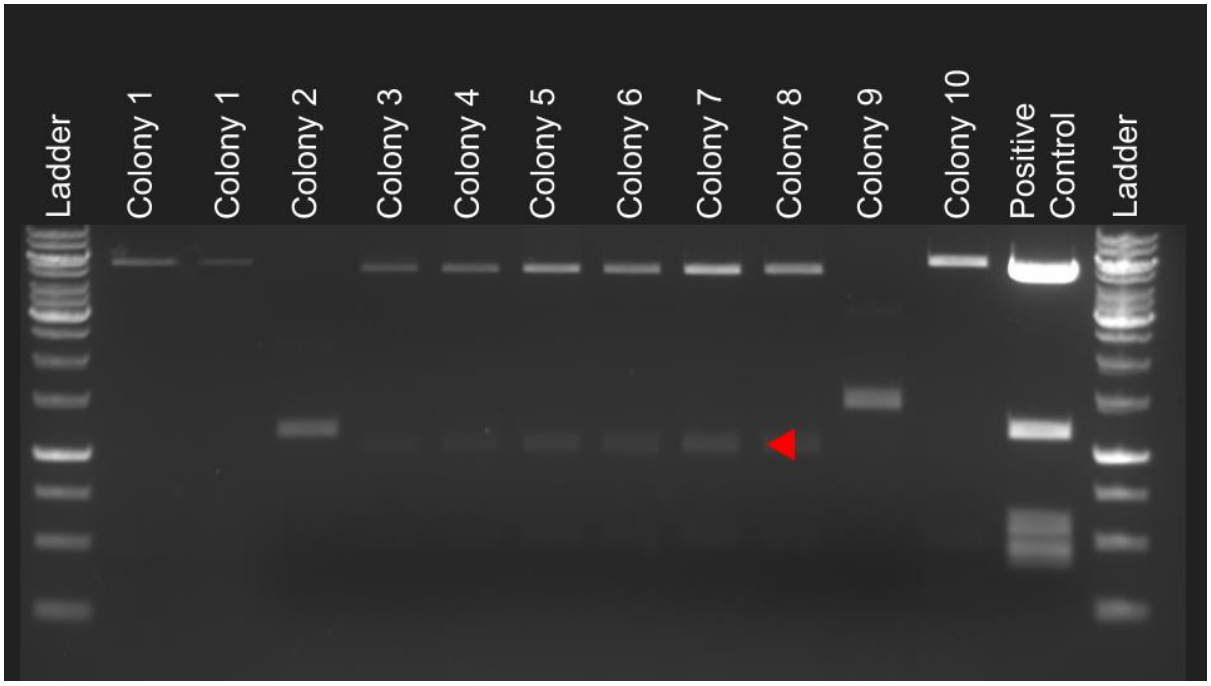

Figure 3-19. pBabe-puro-TP53 R273H plasmid screening by NcoI restriction enzyme. Colony 7 was selected, indicated with a red arrow.

3.6.2. Determining the Optimal Positive Selection Dosage of Puromycin by Kill Curve on MCF7 Cell Line

Since the selection antibiotic of pBabe-puro in cell culture grade is puromycin, a kill curve was performed, and three different antibiotic dosages were determined.

MCF7 cells were exposed to different dosages of puromycin for 10 days, and three different dosages were tested; a low dose of 0.2 µg/ml, which could not kill the cells even after the 10-day period, and 0.4-0.75 µg/ml since these achieved to kill the 100% of the cells at the end of the 10 days, optimal dose as 1 µg/ml since at which visual toxicity was obtained after 5-7 days of antibiotic selection. More than 2 µg/ml and higher doses were classified as high doses since the effect of the excessive toxicity were observed within the 2-3 days of the section.

At the end of the antibiotic selection, the 12-well plate was stained using crystal violet to indicate the cell viability results of the antibiotic selection assay (**Figure *3-20***).

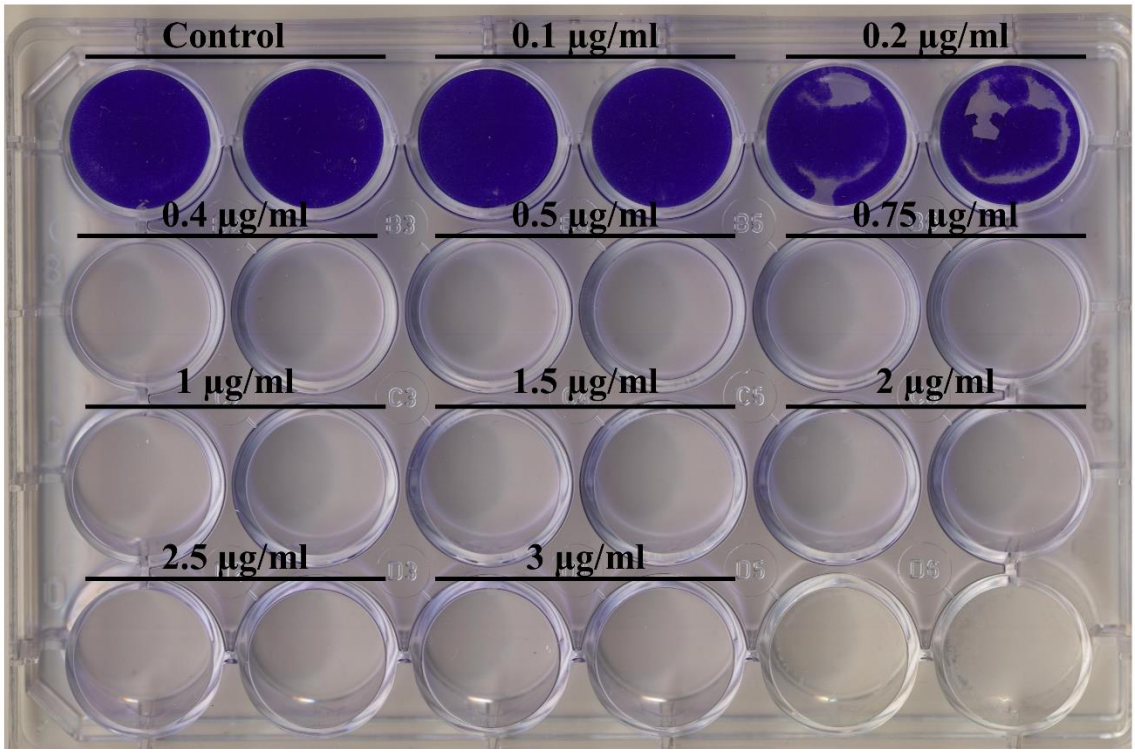

Figure 3-20. Crystal violet staining of 10-day kill curve generation on MCF7 of puromycin antibiotic.

3.6.3. Conformation of Stable TP53 Overexpressing on MCF7 Cell Line at the mRNA and Protein Levels

Stable MCF7 cell lines were generated according to methods mentioned in section **2.2.7.** Even if these cell lines were selected by using puromycin, to confirm whether the TP53 expression status was successfully increased or not, I investigated the TP53 expression levels on protein and RNA levels.

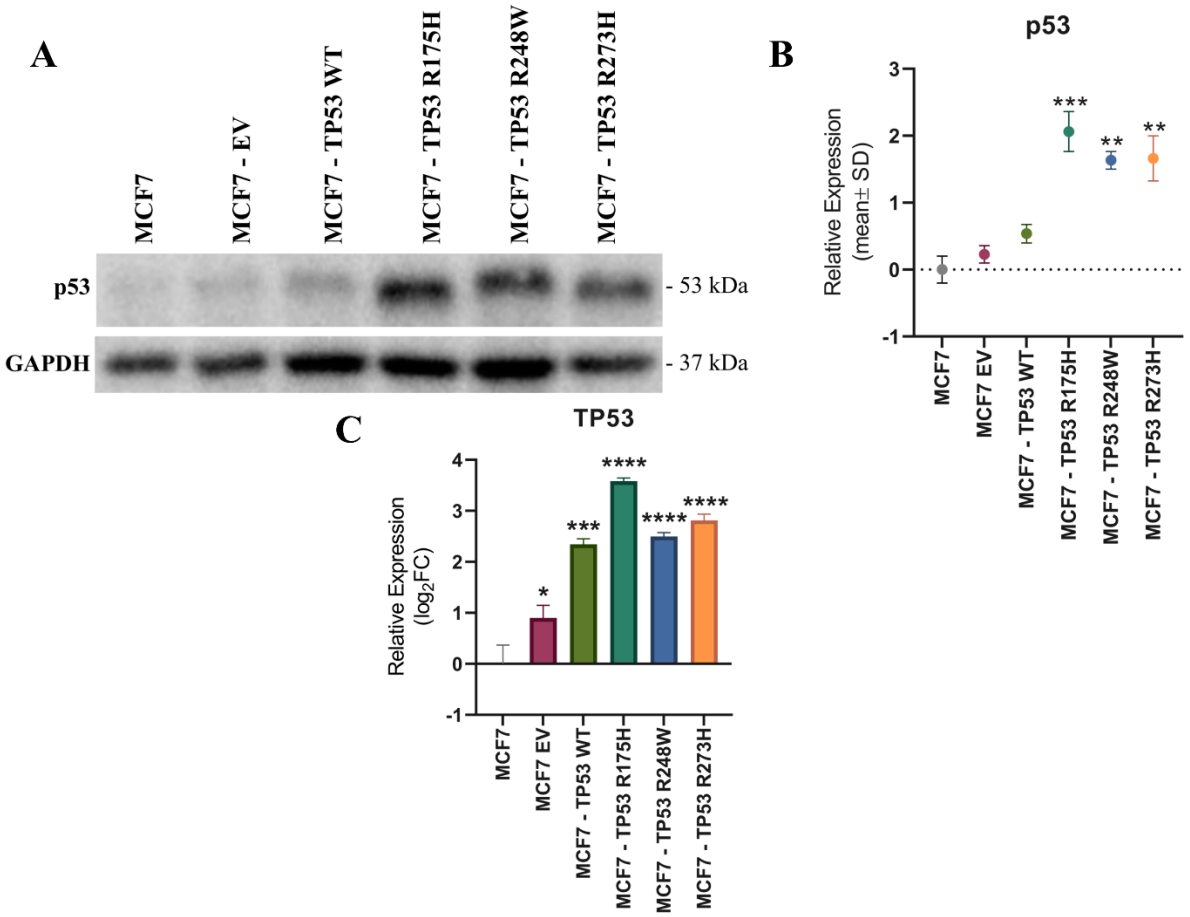

Figure 3-21. Conformation of the TP53 expression levels of stable MCF7 cell lines at protein (A-B) and RNA (C) levels. (*: p-value ≤ 0.05, **: p-value ≤ 0.01 and ****: p-value ≤ 0.0001)

As depicted in **Figure *3-21*A**, increased p53 expression levels were observed in all of the TP53 transduced lines. According to the gel analysis of western blot results, all mutant p53 expressions on protein level (**Figure *3-21*B**) and TP53 expressions on RNA increased significantly (**Figure *3-21*C**). Since p53 is degraded continuously via the canonical pathways, this might explain why the expression level of p53 wild-type did not increase significantly. Additionally, significantly increased wild-type TP53 expression on RNA supported that the generation of MCF7 - TP53 WT cell line was achieved.

3.6.4. MTT Analysis on MCF7 the Stable Cell Lines

After confirming TP53 stable expression, the effect of overexpression on MCF7 cell lines was observed by MTT cell viability assay to obtain approximate values to compare them if siCHRNA5 treatment would be applied. Since we found that siCHRNA5 treatment decreased the cell viability up to 50% from the previous experiment while comparing the different cell lines in terms of viability, these values could be used as a piece of background information. Furthermore, it showed whether TP53 wild-type or mutant stable overexpression would be fatal for the cells on its own or not.

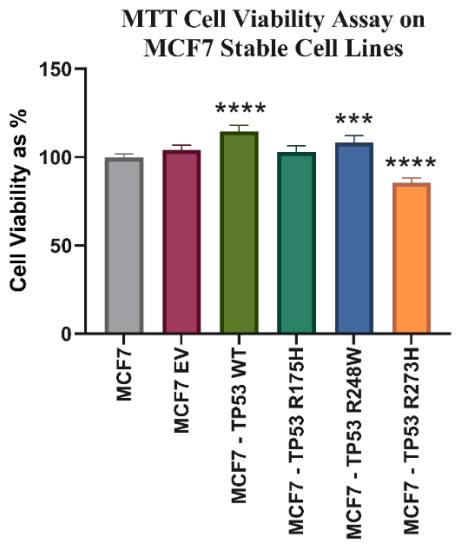

Figure 3-22. Cell viability analysis of TP53 stable overexpressed MCF7 cell lines compared to the EV transduced MCF7 cell line. One-way ANOVA analysis was used with Tukey multiple comparison analysis. Data are represented in percentage format, and error bars are determined according to the Mean±SD values. (*: p-value ≤ 0.05, **: p-value ≤ 0.01 and ****: p-value ≤ 0.0001)

Although the difference in cell viability between MCF7 cell lines and TP53 stably overexpressed MCF7 cell lines was not dramatically changed, significant increases were observed in the MCF7 - TP53 WT and MCF7- TP53 R248W cell lines and a significant decrease was observed in the MCF7 - TP53 R273H cell line (**Figure *3-22***).

3.6.5. Relation Between TP53 Wild-Type and Mutant Stable Overexpression and CHRNA5 Expression

Since selected TP53 mutants in this study are known dominant negative mutants over wild-type TP53, and we previously showed that CHRNA5 depletion could involve TP53 expression, I examined CHRNA5 expression levels of these cell lines. This might give an answer to whether TP53 expression or function could affect CHRNA5 or not. As shown in **Figure *3-23***, CHRNA5 expression levels on TP53 stable overexpressed MCF7 cell lines did not change significantly, even though a slightly increasing trend could be observed in all.

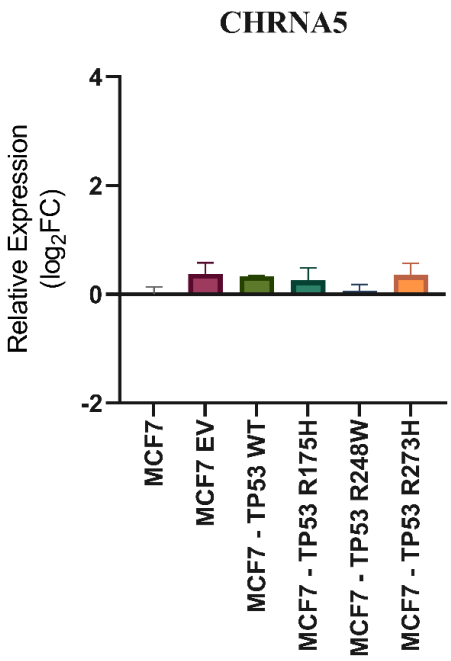

Figure 3-23. CHRNA5 expression level on TP53 table overexpressed MCF7 cell lines. One-way ANOVA analysis was used with Tukey multiple comparisons. Data is represented in

percentage format, and error bars are determined according to Mean±SD values. (*: p-value ≤ 0.05, **: p-value ≤ 0.01 and ****: p-value ≤ 0.0001)

3.6.6. DLK1 and MEG3 Expression Levels on TP53 Stable Expressed MCF7 Cell Line

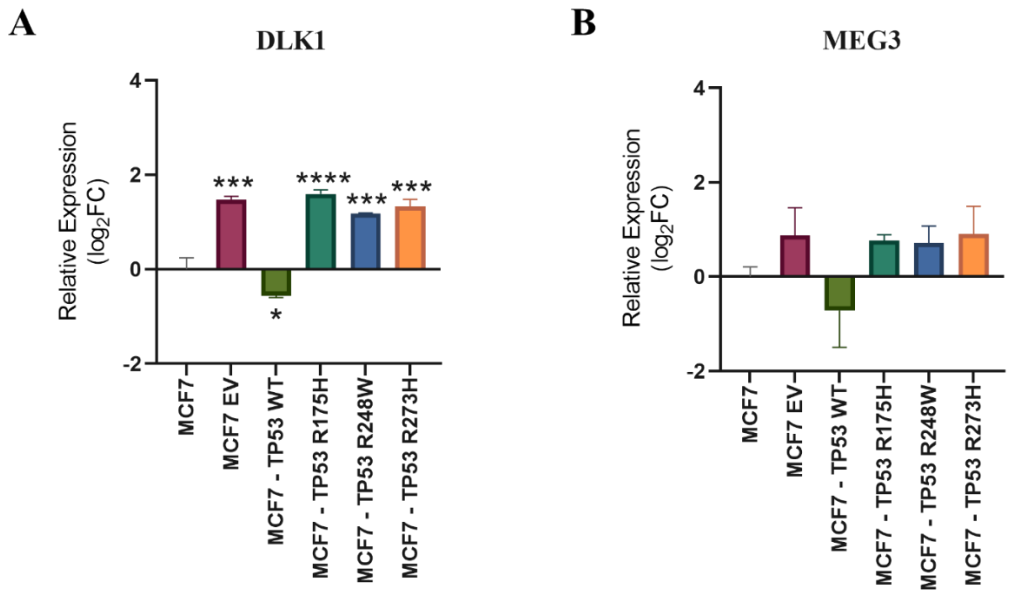

Figure 3-24. CHRNA5 expression level on TP53 table overexpressed MCF7 cell lines. One-way ANOVA analysis was used with Tukey multiple comparisons. Data is represented in percentage format, and error bars are determined according to Mean±SD values. (*: p-value ≤ 0.05, **: p-value ≤ 0.01 and ****: p-value ≤ 0.0001)

Increasing DLK1 expression level was expected with overexpression of TP53 mutant since these are DNA-binding domain mutations (**Figure *3-24*A**). As a part of the DLK1-DiO3 locus, the parallel expression pattern changes were also observed for MEG3. Even if it is not significant, decreasing the primary functionality of TP53 via the overexpression of TP53 mutants might induce DLK1 and MEG3 expression to induce Notch signalling ligands such as p21 to induce p53 in cells (**Figure *3-24*B**).

Chapter 4

4. Conclusion and Discussion

4.1. CHRNA5 Depletion Methods

In this study, CHRNA5 depletion was performed via siRNA, an RNAi method, and its success was confirmed our previous study findings, i.e., the downregulation on three isoforms of CHRNA5 with three different siRNA (Koker et al., 2018). Although it was a confirmed methodology, and I have used the most effective siRNA, not using an additional strategy might have caused some limitations in this study and should be further explored in the future.

Among these potential strategies of reduction of protein levels, the first method is called the "auxin-inducible degron (AID) system", which uses transgenic E3 ubiquitin ligase, SCF (Skp1, Cullin 1 and F-box), and TIR1 (transport inhibitor response 1) complex to target AID tagged protein of interest through auxin binding, and it leads rapid protein degradation by the proteasome (Macdonald et al., 2022). The second potential method is called "trim-away". It consists of a three-step application; exogenously induced E3 ubiquitin ligase TRIM21 binding to an antibody against the protein of interest leads to rapid degradation of the protein of interest by proteasomal degradation (Clift et al., 2017). Another protein knockdown approach is called "deGradFP", using the degradation of GFP-tag fused target protein through poly-ubiquitination of SCF complex with vhh-GFP4, which is an anti-nanobody for GFP (Caussinus & Affolter, 2016). In addition to the degradation of the protein of interest, functional inhibition of the protein could be used as a potential approach. Anchor-Away is based on functional inhibition of nuclear-localized proteins via Rapamycin-dependent treatment, and it is reversible.

Rapamycin creates a complex between anchor protein fused with FKBP12 and FKBP12-rapamycin-binding-domain of FRAP (FRB) fused target protein. Due to the displacement of the target protein from its physiological place, its function is inhibited (Bosch et al., 2020; Samwer et al., 2017). All of these methods provide an advantage over reducing the mRNA levels first to reduce the protein since it might be possible that mRNA could not be effectively reduced or feeds back before protein can be reduced. Future studies should explore these different options of knocking down or knocking out of the CHRNA5 protein levels.

4.2. Depletion of CHRNA5 Decreases both DLK1 and MEG3 Expression Levels on RNA Level

In the previous studies performed in our lab, the effects of CHRNA5 depletion in the breast cancer MCF7 cell line were determined as the induction of G_1 cell cycle arrest and apoptosis, decreasing DDR and increased drug sensitivity by CHEK1 inhibition in addition to downregulation of 14q32.31 miRNAs (Koker et al., 2018).

Herein, I aimed to investigate the effect of CHRNA5 depletion on the expressions of DLK1 and MEG3, found in the 14q32.31 region, which is located within the DLK-DIO3 region. DLK1 downregulation through CHRNA5 depletion was mentioned in the PhD Thesis of Ayse G. Keskus. (Bilkent University PhD Thesis, 2021). As a further step from her work, I also checked the expression level of the MEG3 gene, which is also located in the 14q32 region. I was able to verify significant downregulation of DLK1 and MEG3 through CHRNA5 depletion and miR-495 treatment samples. Even if the downregulation of these genes was also observed in the combination group, we could not be sure that these down-regulation effects are solely led by miRNA expression since CHRNA5 depletion might lead to decreased miR-495 and miR-376 levels,(Köker, 2018; Tiryaki, 2019) and these miRNAs expression may cause

CHRNA5 downregulation. Therefore, CHRNA5 overexpression study should be implied to verify the reason of this effect. Furthermore, even if DLK1 downregulation was seen also with miR-495 expression, this effect was not additive or antagonized by each when compared with the effect on combination groups. On the other hand, miR-376 led to downregulation only in DLK1 expression level and it was nearly the same with siCHRNA5 sample group; this might indicate that miR-376 could target DLK1 gene, which warrants further study. Due to this possibility, investigating the general downregulation effects of MEG3-DLK1 was considered more appropriate with the miR-495 miRNAs.

Considering our previous results, and since MEG3 expression regulates p53 expression, it could be said that the p53 stabilisation observed on the protein level might not the result from MEG3 regulation. Especially in siCHRNA5 downregulation, we saw a highly downregulated expression pattern of both DLK1 and MEG3, which was shown to be related to carcinoma tissues and cell lines (Greife et al., 2014). Also, especially the downregulation of MEG3 lncRNA was found to induce cell proliferation, and might be related to poor prognosis, and even inhibition of mitochondria-mediated apoptosis pathway (Sun et al., 2014; W.-W. Zhang et al., 2019). These findings show that CHRNA5 depletion might cause poor prognostic and cell proliferative changes which are contradict the previous study. CHRNA depletion may have different effects in the presence of different gene interactions, e.g., presence of mir-495 mimic, and other possible interactions and should be studied further.

Oppositely, expression of DLK1 is mainly associated with tumour growth, poor survival and prognosis, cell invasion and metastases in most cancer types (C.-C. Huang et al., 2019; Jin et al., 2008; Takagi et al., 2021) despite its complete opposite effects. Therefore, specifically in luminal A breast cancer, its downregulation by CHRNA5 depletion can be associated with

reduced chemoresistance and malignancy potentiation as these outcomes remain unclear. Since DLK1 inhibits Notch signalling (M.-L. Nueda et al., 2006), depletion of DLK1 might be the result of NOTCH1 activation, which could cause p53 activation, induction of growth arrest and apoptosis (Duan et al., 2006; Henning et al., 2008; Purow et al., 2008; Qi et al., 2003). Therefore, investigating downstream elements of the Notch signalling pathway could be vital for further studies.

Since the effect of CHRNA5 depletion on the DLK1-MEG3 locus is cumulative with other elements such as decreasing miRNA expressions and reduced DNA damage response, there could be another mechanism which affects the cellular pathways more dominantly than the DLK1-MEG3 downregulation. To verify this possibility, overexpression of DLK1 and/or MEG3 could be used so it could be found whether the expression of these proteins variously affects the outcomes of the CHRNA5 depletion.

4.3. Combination of Both TP53 and CHRNA5 Depletion Leads to Significant Downregulation of MDM2 Regulatory Mechanism

Our findings indicated that MDM2 levels significantly decreased only in the presence of siRNAs against CHRNA5 and against TP53 in combination but not when given alone. This synergy is novel and may have implications since MDM2 downregulation is implicated in SAGA (Kovatcheva et al., 2015). Indeed, CHRNA5 siRNA has been shown to induce p53 activity, CDKN1A mRNA and p21 protein levels, so in its absence, we expect TP53 signalling to be significantly induced, which has been confirmed in our previous study (Cingir-Koker et al., 2018; Shehwana et al., 2021) and also in this thesis. When CHRNA5 siRNA was combined

with TP53 siRNA, CDKN1A decreased expectedly so did other TP53 targets by RNAseq (Ayse G. Keskus, PhD Thesis, Bilkent University, 2021). However, this combination also reduced MDM2 levels, which may not be due to autoregulatory feedback but potentially activation or feedback of the SAGA pathway, leading to MDM2 auto-ubiquitination; this hypothesis awaits confirmation by first confirming MDM2 protein levels whether they are also downregulated as in the case of mRNA shown herein and along with PDLIM7 levels being downregulated and CDH18 upregulated and/or not changed and still sequestering PDLIM7 in the cytoplasmic foci (Klein et al., 2018). Moreover, other proteins that are involved in the regulation of MDM2 mRNA and protein levels should be studied to understand genes other than PDLIM7 and CDH18 could be involved in the modulation of MDM2 levels when siRNAs for CHRNA5 and TP53 combined. The synergism observed for MDM2 downregulation in the presence of these two siRNAs needs to be also tested for phenotypical and molecular consequences, such as induction of senescence or acquired resistance to senescence. Accordingly, senescence markers should be studied, such as using beta-Gal activity or performing bioinformatics analysis of our RNAseq dataset (Ayse G. Keskus, PhD Thesis, Bilkent University, 2021) to mine for senescence-associated gene signature to find out whether MDM2 downregulation with siRNA CHRNA5 and siRNA TP53 combination is also associated with mRNA markers of senescence from the literature. These are planned in future studies. Moreover, whether CHRNA5-TP53 siRNA combination would still lead to reduced MDM2 levels in the WT and mutant P53 stable MCF7 cell lines can provide answers to whether dominant negative forms of TP53 mutants behave differently than null or knockdown phenotypes with or without Palbociclib treatment.

Additionally, since one of the most important outcomes in this research is the stabilisation or the induction of p53 expression, besides the doxorubicin treatment established in our previous

study (Koker et al., 2018), exposure to cycloheximide could be used to measure the half-life of p53 protein on MCF7 cells treated with CHRNA5 depletion to verify whether there is a stabilisation of p53 or not upon these treatments. Since cycloheximide inhibits the protein biosynthesis, the half-life of the stabilised p53 would be measured longer than non-phosphorylated or non-stabilised p53, which is called cycloheximide chase assay (Choi et al., 2010; Kao et al., 2015). This method also may help to understand the effects of CHRNA5 depletion on MDM2 regulation in addition to the CHRNA5 depletion effect on p53 stabilisation.

4.4. Effects of Stable Overexpression of Wild Type and Mutant TP53 on CHRNA5, DLK1 and MEG3 Expressions

To investigate the relation between CHRNA5 and TP53, we used stable overexpression models of TP53 R175H, R248W and R273H mutants, wild-type TP53 and empty backbone plasmids in MCF7. According to the findings, overexpression of neither wildtype nor mutant TP53 expression does not affect CHRNA5 expression at the mRNA level. Since we presented p53 induction on protein level through CHRNA5 depletion in our previous study (Koker et al., 2018), possible effects of TP53 overexpression were also checked. Independently of the functionality of TP53, it did not change the CHRNA5 expression at the mRNA level. On the other hand, overexpression of only the wild-type TP53 led to significant downregulation on the DLK1 expression level, and a similar pattern was seen insignificantly on the MEG3 expression level as well. This effect could be related to the transcription factor role of p53 (Monti et al., 2020). Also, both DLK1 and MEG3 expressions were induced in all groups, except the wild-type, when compared to endogenous MCF7 cells; and since the stable overexpression was performed via viral transduction, this could have caused cellular stress or might have induced an immune response (Sáez-Cirión & Manel, 2018). As the stable cells I generated came from

polyclonal cell selection, this could be considered as a common trait among the all stable MCF7 cells including those of transduced with the empty vector.

4.5. Future Perspectives

- CHRNA5 depletion causes general downregulation on the 14q32 region, including a coding and a non-coding gene in addition to 14q32.31 miRNAs. For further studies, 14q32 knockout via CRISPR/Cas 9 could be used with CHRNA5 depletion.
- Effects of CHRNA5 depletion on 14q32 might be a combinatorial effect since even if the location of miRNAs are the same, they have different targets and downstream effects. DLK1 and/or the MEG3 overexpression model might be used for further research with these miRNAs.
- Additionally, methylation assays might be helpful in investigating the effect of the 14q32 parental imprinting region to understand if methylation plays a role in mediating CHRNA5 siRNA and overexpression effects.
- The results indicated that DLK1 might be a miR-376 target, hence a luciferase reporter assay could be used to verify this finding.
- It was shown that DLK1 and MEG3 downregulation could be siTP53 independent, or partially dependent on TP53; needs further study at the protein level.
- Because DLK1 is known as a NOTCH1 inhibitor and Notch1 is a downstream target of CHRNA5 (Dang et al., 2020; González et al., 2015), DLK1 downregulation might be required to examine this effect comprehensively.
- It has been shown that MDM2 and its associated proteins were downregulated through only in the presence of both CHRNA5 and TP53 depletion; hence MDM2 auto-ubiquitinylation might be induced due to Senescence After Growth Arrest pathway

(SAGA). Therefore, senescence markers could be studied, and senescence assays such as beta-galactosidase activity could be measured.

- In order to investigate the relation of CHRNA5 depletion with p53 and p21 induction through cell cycle arrest, PI staining could be performed. To study the effects of siA5-siTP53 on CHK1 and DNA damage response, siRNAs and/or overexpression vectors which are specific for CHK1 and ATM/ATR, can be used. In this way, we can see whether CHRNA5 has an effect on the DNA repair system or not. As an alternative way, we can check the localization of ATM/ATR and p53 proteins on the cell. Previous studies showed that CHRNA5 expression is associated with DDR gene expression (Cingir-Koker et al., 2018). Therefore, we need depletion and/or overexpression of CHK1 protein and checking the ATM/ATR localization to explain these findings.
- We can use a comet assay to investigate the effects of siA5-siTP53 treatment on DNA damage. For the effects on apoptosis, we need to perform Annexin V/PI assay or similar types of procedures.
- ARF could also be studied to observe whether there are any other upstream regulations affected by CHRNA5 depletion.
- Due to experimental limitations, protein levels and MTT analysis of CHRNA5 and/or TP53 depletion set could not be performed. Examination of protein levels shows priority, especially the p53 phosphorylation levels.
- Effects of CHRNA5 depletion on stable cells expressing the different types of TP53 gene mutations should be investigated to observe the p53-dependent effects of siCHRNA5.
- Due to both cell cycle arrest effect and MDM2 down-regulation pattern, CDK4/6 inhibitor Palbociclib could be used to test synergistic effects in the presence and absence of wild- type p53.

- Besides RNAi assay, other potential methods could be used to decrease more successfully CHRNA5 protein expression levels, such as AID or Trim-Away.
- To verify the stabilisation of TP53, treatment with the cycloheximide method could be used.

5. Appendix

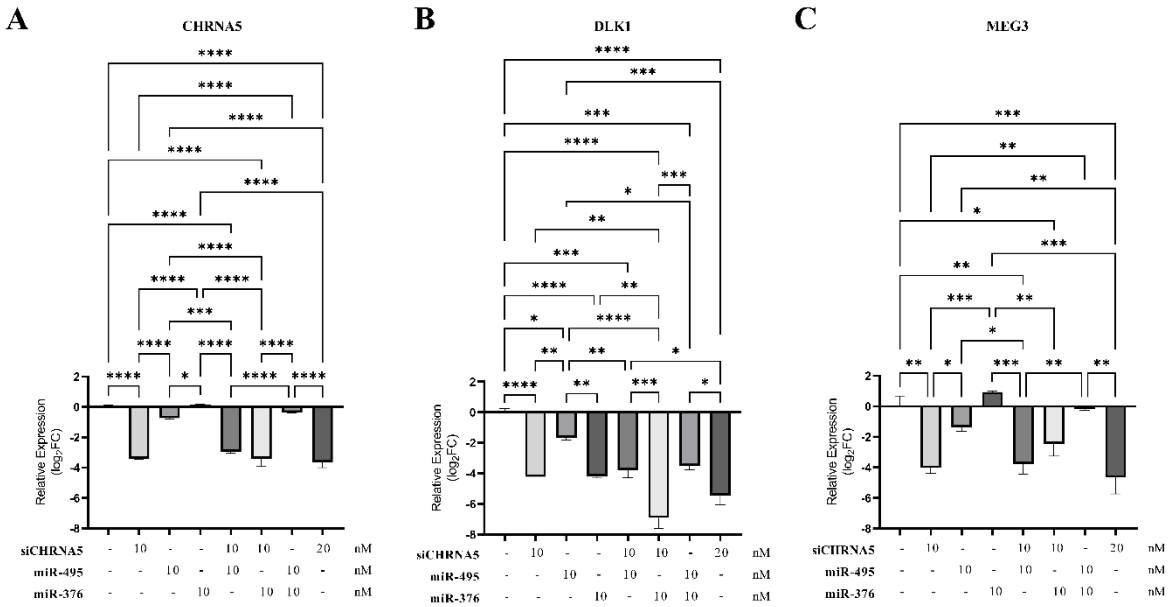

Appendix Figure 1. qPCR validation of miR-495 and miR-376 treatment on MCF7 cell line. Expression levels of CHRNA5 (A), DLK1 (B) and MEG3 (C). One-way ANOVA analysis was with Tukey multiple comparison analysis. Data is represented in percentage format, and error bars are determined according to Mean±SD values. (*: p-value ≤ 0.05, **: p-value ≤ 0.01 and ****: p-value ≤ 0.0001)

5	**Tukey's multiple comparisons test**	**Mean Diff.**	**95.00% CI of diff.**	**Below threshold?**	**Summary**	**Adjusted P Value**			
6	sc20 vs. si10	0.5855	-0.6310 to 1.802	No	ns	0.4069	A-B		
7	sc20 vs. sc+miR45	0.5519	-0.6646 to 1.768	No	ns	0.4528	A-C		
8	sc20 vs. si+miR495	1.215	-0.001969 to 2.431	No	ns	0.0503	A-D		
9	sc20 vs. si20	1.105	-0.1116 to 2.321	No	ns	0.0710	A-E		
10	si10 vs. sc+miR45	-0.03361	-1.250 to 1.183	No	ns	>0.9999	B-C		
11	si10 vs. si+miR495	0.6291	-0.5874 to 1.846	No	ns	0.3528	B-D		
12	si10 vs. si20	0.5194	-0.6971 to 1.736	No	ns	0.5003	B-E		
13	sc+miR45 vs. si+miR495	0.6627	-0.5538 to 1.879	No	ns	0.3153	C-D		
14	sc+miR45 vs. si20	0.5530	-0.6635 to 1.770	No	ns	0.4511	C-E		
15	si+miR495 vs. si20	-0.1096	-1.326 to 1.107	No	ns	0.9951	D-E		
16									
17	**Test details**	**Mean 1**	**Mean 2**	**Mean Diff.**	**SE of diff.**	**n1**	**n2**	**q**	**DF**
18	sc20 vs. si10	0.000	-0.5855	0.5855	0.3033	2	2	2.730	5
19	sc20 vs. sc+miR45	0.000	-0.5519	0.5519	0.3033	2	2	2.574	5
20	sc20 vs. si+miR495	0.000	-1.215	1.215	0.3033	2	2	5.664	5
21	sc20 vs. si20	0.000	-1.105	1.105	0.3033	2	2	5.153	5
22	si10 vs. sc+miR45	-0.5855	-0.5519	-0.03361	0.3033	2	2	0.1568	5
23	si10 vs. si+miR495	-0.5855	-1.215	0.6291	0.3033	2	2	2.934	5
24	si10 vs. si20	-0.5855	-1.105	0.5194	0.3033	2	2	2.422	5
25	sc+miR45 vs. si+miR495	-0.5519	-1.215	0.6627	0.3033	2	2	3.090	5
26	sc+miR45 vs. si20	-0.5519	-1.105	0.5530	0.3033	2	2	2.579	5
27	si+miR495 vs. si20	-1.215	-1.105	-0.1096	0.3033	2	2	0.5113	5

Appendix Figure 2. Statistical analysis of **Figure 3-4A**.

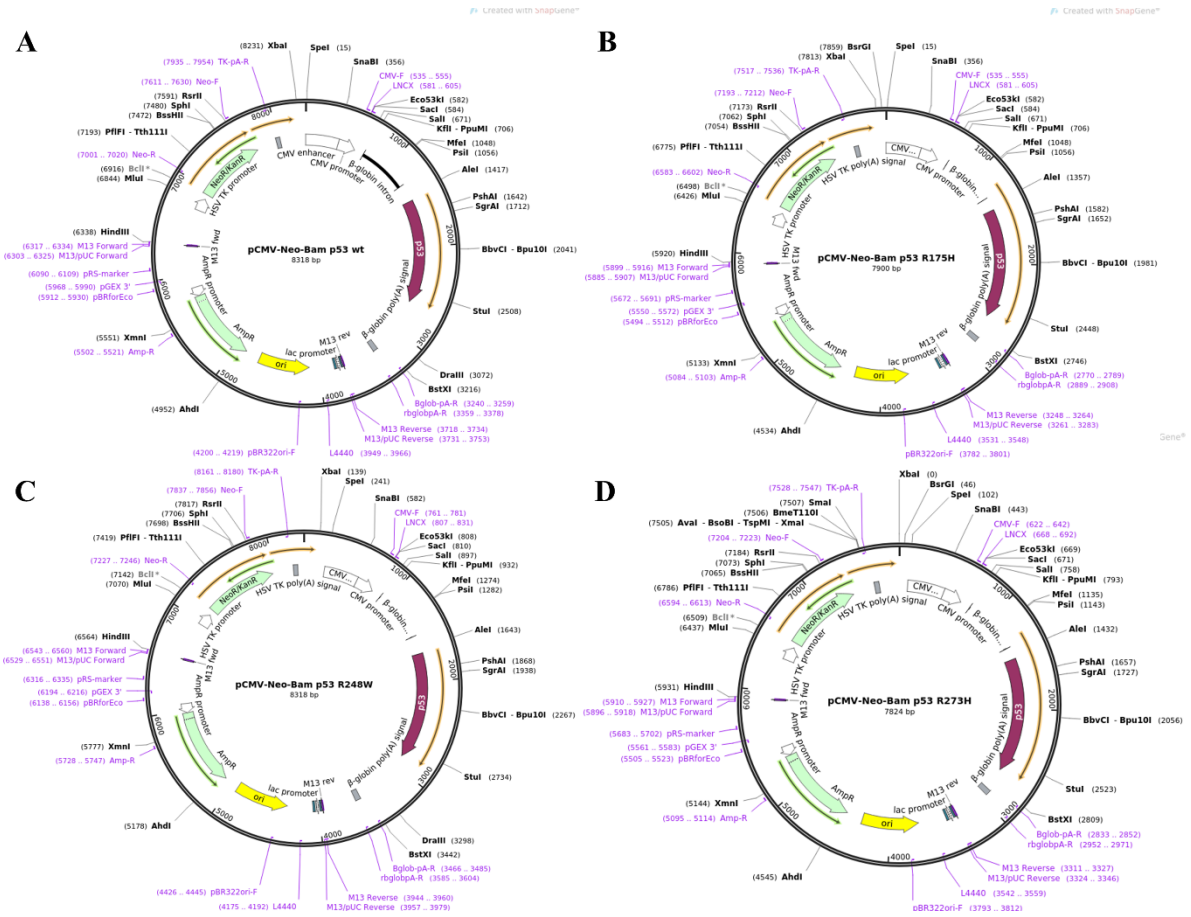

Appendix Figure 3. Plasmid map of plasmids ordered from Addgene, (A) pCMV-Neo-Bam TP53 WT, (B) pCMV-Neo-Bam TP53 R175H, (C) pCMV-Neo-Bam R248W, (D) pCMV-Neo-Bam TP53 R273H.

#PW_consensus

Sequence ID: **Query_511861** Length: **8318** Number of Matches: **1**

Range 1: 1 to 8318 Graphics ▼ Next Match ▲ P

Score	Expect	Identities	Gaps	Strand
15361 bits(8318)	0.0	8318/8318(100%)	0/8318(0%)	Plus/Plus

```
Query  1    GACATTGATTATTGACTAGTTATTAATAGTAATCAATTACGGGGTCATTAGTTCATAGCC  60
            ||||||||||||||||||||||||||||||||||||||||||||||||||||||||||||
Sbjct  1    GACATTGATTATTGACTAGTTATTAATAGTAATCAATTACGGGGTCATTAGTTCATAGCC  60

Query  61   CATATATGGAGTTCCGCGTTACATAACTTACGGTAAATGGCCCGCCTGGCTGACCGCCCA  120
            ||||||||||||||||||||||||||||||||||||||||||||||||||||||||||||
Sbjct  61   CATATATGGAGTTCCGCGTTACATAACTTACGGTAAATGGCCCGCCTGGCTGACCGCCCA  120

Query  121  ACGACCCCCGCCCATTGACGTCAATAATGACGTATGTTCCCATAGTAACGCCAATAGGGA  180
            ||||||||||||||||||||||||||||||||||||||||||||||||||||||||||||
Sbjct  121  ACGACCCCCGCCCATTGACGTCAATAATGACGTATGTTCCCATAGTAACGCCAATAGGGA  180

Query  181  CTTTCCATTGACGTCAATGGGTGGAGTATTTACGGTAAACTGCCCACTTGGCAGTACATC  240
            ||||||||||||||||||||||||||||||||||||||||||||||||||||||||||||
Sbjct  181  CTTTCCATTGACGTCAATGGGTGGAGTATTTACGGTAAACTGCCCACTTGGCAGTACATC  240

Query  241  AAGTGTATCATATGCCAAGTACGCCCCCTATTGACGTCAATGACGGTAAATGGCCCGCCT  300
            ||||||||||||||||||||||||||||||||||||||||||||||||||||||||||||
```

Appendix Figure 4. Consensus sequence similarity score of pCMV-Neo-Bam TP53 WT plasmid on BLAST tool.

Description	Scientific Name	Max Score	Total Score	Query Cover	E value	Per. Ident	Acc. Len	Accession
cellular tumor antigen p53 isoform a [Homo sapiens]	Homo sapiens	813	813	99%	0.0	100.00%	393	NP_001119584.1
cellular tumor antigen p53 isoform a [Homo sapiens]	Homo sapiens	813	813	99%	0.0	100.00%	393	NP_000537.3
P53 [Homo sapiens]	Homo sapiens	806	806	99%	0.0	99.24%	393	BAC16799.1
cellular tumor antigen p53 isoform g [Homo sapiens]	Homo sapiens	737	737	89%	0.0	100.00%	354	NP_001263690.1
cellular tumor antigen p53 isoform g [Homo sapiens]	Homo sapiens	737	737	89%	0.0	100.00%	354	NP_001263689.1
cellular tumor antigen p53 isoform g [Homo sapiens]	Homo sapiens	737	737	89%	0.0	100.00%	354	NP_001119590.1
cellular tumor antigen p53 isoform c [Homo sapiens]	Homo sapiens	689	689	86%	0.0	97.65%	346	NP_001119585.1
cellular tumor antigen p53 isoform b [Homo sapiens]	Homo sapiens	688	688	84%	0.0	100.00%	341	NP_001119586.1
cellular tumor antigen p53 isoform i [Homo sapiens]	Homo sapiens	612	612	74%	0.0	100.00%	302	NP_001263625.1
cellular tumor antigen p53 isoform h [Homo sapiens]	Homo sapiens	612	612	76%	0.0	97.35%	307	NP_001263624.1
cellular tumor antigen p53 isoform d [Homo sapiens]	Homo sapiens	549	549	66%	0.0	100.00%	261	NP_001119587.1
cellular tumor antigen p53 isoform j [Homo sapiens]	Homo sapiens	491	491	59%	3e-180	100.00%	234	NP_001263626.1
cellular tumor antigen p53 isoform e [Homo sapiens]	Homo sapiens	422	422	50%	2e-153	100.00%	209	NP_001119588.1
cellular tumor antigen p53 isoform f [Homo sapiens]	Homo sapiens	422	422	53%	2e-153	96.17%	214	NP_001119589.1
cellular tumor antigen p53 isoform k [Homo sapiens]	Homo sapiens	365	365	43%	3e-131	100.00%	182	NP_001263627.1
cellular tumor antigen p53 isoform l [Homo sapiens]	Homo sapiens	364	364	46%	6e-131	95.60%	187	NP_001263628.1

Appendix Figure 5. Comparison of TP53 variants with TP53 WT inserts of the plasmid on BLAST tool.

#P175_consensus

Sequence ID: **Query_28841** Length: **7900** Number of Matches: **5**

Range 1: 1 to 7900 Graphics ▼ Next Match ▲ Previous Match

Score	Expect	Identities	Gaps	Strand
14589 bits(7900)	0.0	7900/7900(100%)	0/7900(0%)	Plus/Plus

```
Query  1    GACATTGATTATTGACTAGTTATTAATAGTAATCAATTACGGGGTCATTAGTTCATAGCC  60
            ||||||||||||||||||||||||||||||||||||||||||||||||||||||||||||
Sbjct  1    GACATTGATTATTGACTAGTTATTAATAGTAATCAATTACGGGGTCATTAGTTCATAGCC  60

Query  61   CATATATGGAGTTCCGCGTTACATAACTTACGGTAAATGGCCCGCCTGGCTGACCGCCCA  120
            ||||||||||||||||||||||||||||||||||||||||||||||||||||||||||||
Sbjct  61   CATATATGGAGTTCCGCGTTACATAACTTACGGTAAATGGCCCGCCTGGCTGACCGCCCA  120

Query  121  ACGACCCCCGCCCATTGACGTCAATAATGACGTATGTTCCCATAGTAACGCCAATAGGGA  180
            ||||||||||||||||||||||||||||||||||||||||||||||||||||||||||||
Sbjct  121  ACGACCCCCGCCCATTGACGTCAATAATGACGTATGTTCCCATAGTAACGCCAATAGGGA  180

Query  181  CTTTCCATTGACGTCAATGGGTGGAGTATTTACGGTAAACTGCCCACTTGGCAGTACATC  240
            ||||||||||||||||||||||||||||||||||||||||||||||||||||||||||||
Sbjct  181  CTTTCCATTGACGTCAATGGGTGGAGTATTTACGGTAAACTGCCCACTTGGCAGTACATC  240

Query  241  AAGTGTATCATATGCCAAGTACGCCCCCTATTGACGTCAATGACGGTAAATGGCCCGCCT  300
            ||||||||||||||||||||||||||||||||||||||||||||||||||||||||||||
```

Appendix Figure 6. Consensus sequence similarity score of pCMV-Neo-Bam TP53 R175H plasmid on BLAST tool.

#248_consensus

Sequence ID: **Query_22753** Length: **8318** Number of Matches: **1**

Range 1: 1 to 8318 Graphics ▼ Next Match ▲ Pr

Score	Expect	Identities	Gaps	Strand
15361 bits(8318)	0.0	8318/8318(100%)	0/8318(0%)	Plus/Plus

```
Query  1    AATACGCCCGCGTTTCTTCCTTTTccccaccccaccccccAAGTTCGGGTGAAGGCCCAG  60
            ||||||||||||||||||||||||||||||||||||||||||||||||||||||||||||
Sbjct  1    AATACGCCCGCGTTTCTTCCTTTTCCCCACCCCACCCCCCAAGTTCGGGTGAAGGCCCAG  60

Query  61   GGCTCGCAGCCAACGTCGGGGCGGCAAGCCCTGCCATAGCCACGGGCCCCGTGGGTTAGG  120
            ||||||||||||||||||||||||||||||||||||||||||||||||||||||||||||
Sbjct  61   GGCTCGCAGCCAACGTCGGGGCGGCAAGCCCTGCCATAGCCACGGGCCCCGTGGGTTAGG  120

Query  121  GACGGCGGATCGCGGCCCTCTAGAGAGCTTGGCCCATTGCATACGTTGTATCCATATCAT  180
            ||||||||||||||||||||||||||||||||||||||||||||||||||||||||||||
Sbjct  121  GACGGCGGATCGCGGCCCTCTAGAGAGCTTGGCCCATTGCATACGTTGTATCCATATCAT  180

Query  181  AATATGTACATTTATATTGGCTCATGTCCAACATTACCGCCATGTTGACATTGATTATTG  240
            ||||||||||||||||||||||||||||||||||||||||||||||||||||||||||||
Sbjct  181  AATATGTACATTTATATTGGCTCATGTCCAACATTACCGCCATGTTGACATTGATTATTG  240

Query  241  ACTAGTTATTAATAGTAATCAATTACGGGGTCATTAGTTCATAGCCCATATATGGAGTTC  300
            ||||||||||||||||||||||||||||||||||||||||||||||||||||||||||||
```

Appendix Figure 7. Consensus sequence similarity score of pCMV-Neo-Bam TP53 R248W plasmid on BLAST tool.

pCMV-Neo-Bam/p53 R273H

Sequence ID: **Query_25697** Length: **7824** Number of Matches: **1**

Range 1: 1 to 7824 Graphics ▼ Next Match ▲ Previous M

Score	Expect	Identities	Gaps	Strand
14449 bits(7824)	0.0	7824/7824(100%)	0/7824(0%)	Plus/Plus

```
Query  1    CTAGAGAGCTTGGCCCATTGCATACGTTGTATCCATATCATAATATGTACATTTATATTG  60
            ||||||||||||||||||||||||||||||||||||||||||||||||||||||||||||
Sbjct  1    CTAGAGAGCTTGGCCCATTGCATACGTTGTATCCATATCATAATATGTACATTTATATTG  60

Query  61   GCTCATGTCCAACATTACCGCCATGTTGACATTGATTATTGACTAGTTATTAATAGTAAT  120
            ||||||||||||||||||||||||||||||||||||||||||||||||||||||||||||
Sbjct  61   GCTCATGTCCAACATTACCGCCATGTTGACATTGATTATTGACTAGTTATTAATAGTAAT  120

Query  121  CAATTACGGGGTCATTAGTTCATAGCCCATATATGGAGTTCCGCGTTACATAACTTACGG  180
            ||||||||||||||||||||||||||||||||||||||||||||||||||||||||||||
Sbjct  121  CAATTACGGGGTCATTAGTTCATAGCCCATATATGGAGTTCCGCGTTACATAACTTACGG  180

Query  181  TAAATGGCCCGCCTGGCTGACCGCCCAACGACCCCCGCCCATTGACGTCAATAATGACGT  240
            ||||||||||||||||||||||||||||||||||||||||||||||||||||||||||||
Sbjct  181  TAAATGGCCCGCCTGGCTGACCGCCCAACGACCCCCGCCCATTGACGTCAATAATGACGT  240

Query  241  ATGTTCCCATAGTAACGCCAATAGGGACTTTCCATTGACGTCAATGGGTGGAGTATTTAC  300
            ||||||||||||||||||||||||||||||||||||||||||||||||||||||||||||
```

Appendix Figure 8. Consensus sequence similarity score of pCMV-Neo-Bam TP53 R273H plasmid on BLAST tool.

A

p53_WT_NGS_Result (393 aa)

Sequence ID: **Query_12447** Length: **394** Number of Matches: **1**

Range 1: 1 to 394 Graphics ▼ Next Match ▲ Previ

Score	Expect	Method	Identities	Positives	Gaps
808 bits(2088)	0.0	Compositional matrix adjust.	392/394(99%)	392/394(99%)	0/394(0%)

```
Query  1    MEEPQSDPSVEPPLSQETFSDLWKLLPENNVLSPLPSQAMDDLMLSPDDIEQWFTEDPGP  60
            MEEPQSDPSVEPPLSQETFSDLWKLLPENNVLSPLPSQAMDDLMLSPDDIEQWFTEDPGP
Sbjct  1    MEEPQSDPSVEPPLSQETFSDLWKLLPENNVLSPLPSQAMDDLMLSPDDIEQWFTEDPGP  60

Query  61   DEAPRMPEAAPRVAPAPAAPTPAAPAPAPSWPLSSSVPSQKTYQGSYGFRLGFLHSGTAK  120
            DEAPRMPEAAP VAPAPAAPTPAAPAPAPSWPLSSSVPSQKTYQGSYGFRLGFLHSGTAK
Sbjct  61   DEAPRMPEAAPPVAPAPAAPTPAAPAPAPSWPLSSSVPSQKTYQGSYGFRLGFLHSGTAK  120

Query  121  SVTCTYSPALNKMFCQLAKTCPVQLWVDSTPPPGTRVRAMAIYKQSQHMTEVVRHCPHHE  180
            SVTCTYSPALNKMFCQLAKTCPVQLWVDSTPPPGTRVRAMAIYKQSQHMTEVVR CPHHE
Sbjct  121  SVTCTYSPALNKMFCQLAKTCPVQLWVDSTPPPGTRVRAMAIYKQSQHMTEVVRRCPHHE  180

Query  181  RCSDSDGLAPPQHLIRVEGNLRVEYLDDRNTFRHSVVVPYEPPEVGSDCTTIHYNYMCNS  240
            RCSDSDGLAPPQHLIRVEGNLRVEYLDDRNTFRHSVVVPYEPPEVGSDCTTIHYNYMCNS
Sbjct  181  RCSDSDGLAPPQHLIRVEGNLRVEYLDDRNTFRHSVVVPYEPPEVGSDCTTIHYNYMCNS  240

Query  241  SCMGGMNRRPILTIITLEDSSGNLLGRNSFEVRVCACPGRDRRTEEENLRKKGEPHHELP  300
            SCMGGMNRRPILTIITLEDSSGNLLGRNSFEVRVCACPGRDRRTEEENLRKKGEPHHELP
Sbjct  241  SCMGGMNRRPILTIITLEDSSGNLLGRNSFEVRVCACPGRDRRTEEENLRKKGEPHHELP  300

Query  301  PGSTKRALPNNTSSSPQPKKKPLDGEYFTLQIRGRERFEMFRELNEALELKDAQAGKEPG  360
            PGSTKRALPNNTSSSPQPKKKPLDGEYFTLQIRGRERFEMFRELNEALELKDAQAGKEPG
Sbjct  301  PGSTKRALPNNTSSSPQPKKKPLDGEYFTLQIRGRERFEMFRELNEALELKDAQAGKEPG  360

Query  361  GSRAHSSHLKSKKGQSTSRHKKLMFKTEGPDSD*  394
            GSRAHSSHLKSKKGQSTSRHKKLMFKTEGPDSD*
Sbjct  361  GSRAHSSHLKSKKGQSTSRHKKLMFKTEGPDSD*  394
```

B

p53_WT_NGS_Result (393 aa)

Sequence ID: **Query_7015** Length: **394** Number of Matches: **1**

Range 1: 1 to 394 Graphics ▼ Next Match ▲ Pre

Score	Expect	Method	Identities	Positives	Gaps
811 bits(2094)	0.0	Compositional matrix adjust.	393/394(99%)	393/394(99%)	0/394(0%)

```
Query  1    MEEPQSDPSVEPPLSQETFSDLWKLLPENNVLSPLPSQAMDDLMLSPDDIEQWFTEDPGP  60
            MEEPQSDPSVEPPLSQETFSDLWKLLPENNVLSPLPSQAMDDLMLSPDDIEQWFTEDPGP
Sbjct  1    MEEPQSDPSVEPPLSQETFSDLWKLLPENNVLSPLPSQAMDDLMLSPDDIEQWFTEDPGP  60

Query  61   DEAPRMPEAAPPVAPAPAAPTPAAPAPAPSWPLSSSVPSQKTYQGSYGFRLGFLHSGTAK  120
            DEAPRMPEAAPPVAPAPAAPTPAAPAPAPSWPLSSSVPSQKTYQGSYGFRLGFLHSGTAK
Sbjct  61   DEAPRMPEAAPPVAPAPAAPTPAAPAPAPSWPLSSSVPSQKTYQGSYGFRLGFLHSGTAK  120

Query  121  SVTCTYSPALNKMFCQLAKTCPVQLWVDSTPPPGTRVRAMAIYKQSQHMTEVVRRCPHHE  180
            SVTCTYSPALNKMFCQLAKTCPVQLWVDSTPPPGTRVRAMAIYKQSQHMTEVVRRCPHHE
Sbjct  121  SVTCTYSPALNKMFCQLAKTCPVQLWVDSTPPPGTRVRAMAIYKQSQHMTEVVRRCPHHE  180

Query  181  RCSDSDGLAPPQHLIRVEGNLRVEYLDDRNTFRHSVVVPYEPPEVGSDCTTIHYNYMCNS  240
            RCSDSDGLAPPQHLIRVEGNLRVEYLDDRNTFRHSVVVPYEPPEVGSDCTTIHYNYMCNS
Sbjct  181  RCSDSDGLAPPQHLIRVEGNLRVEYLDDRNTFRHSVVVPYEPPEVGSDCTTIHYNYMCNS  240

Query  241  SCMGGMNWRPILTIITLEDSSGNLLGRNSFEVRVCACPGRDRRTEEENLRKKGEPHHELP  300
            SCMGGMN RPILTIITLEDSSGNLLGRNSFEVRVCACPGRDRRTEEENLRKKGEPHHELP
Sbjct  241  SCMGGMNRRPILTIITLEDSSGNLLGRNSFEVRVCACPGRDRRTEEENLRKKGEPHHELP  300

Query  301  PGSTKRALPNNTSSSPQPKKKPLDGEYFTLQIRGRERFEMFRELNEALELKDAQAGKEPG  360
            PGSTKRALPNNTSSSPQPKKKPLDGEYFTLQIRGRERFEMFRELNEALELKDAQAGKEPG
Sbjct  301  PGSTKRALPNNTSSSPQPKKKPLDGEYFTLQIRGRERFEMFRELNEALELKDAQAGKEPG  360

Query  361  GSRAHSSHLKSKKGQSTSRHKKLMFKTEGPDSD*  394
            GSRAHSSHLKSKKGQSTSRHKKLMFKTEGPDSD*
Sbjct  361  GSRAHSSHLKSKKGQSTSRHKKLMFKTEGPDSD*  394
```

C

p53_WT_NGS_Result (393 aa)

Sequence ID: **Query_39193** Length: **394** Number of Matches: **1**

Range 1: 1 to 394 Graphics ▼ Next Match ▲ Pre

Score	Expect	Method	Identities	Positives	Gaps
807 bits(2084)	0.0	Compositional matrix adjust.	391/394(99%)	391/394(99%)	0/394(0%)

```
Query  1    MEEPQSDPSVEPPLSQETFSDLWKLLPENNVLSPLPSQAMDDLMLSPDDIEQWFTEDPGP  60
            MEEPQSDPSVEPPLSQETFSDLWKLLPENNVLSPLPSQAMDDLMLSPDDIEQWFTEDPGP
Sbjct  1    MEEPQSDPSVEPPLSQETFSDLWKLLPENNVLSPLPSQAMDDLMLSPDDIEQWFTEDPGP  60

Query  61   DEAPRMPEAAPRVAPAPAAPTPAAPAPAPSWPLSSSVPSQKTYQGSYGFRLGFLHSGTAK  120
            DEAPRMPEAAP VAPAPAAPTPAAPAPAPSWPLSSSVPSQKTYQGSYGFRLGFLHSGTAK
Sbjct  61   DEAPRMPEAAPPVAPAPAAPTPAAPAPAPSWPLSSSVPSQKTYQGSYGFRLGFLHSGTAK  120

Query  121  SVTCTYSPALNKMFCQLAKTCPVQLWVDSTPPPGTRVRAMAIYKQSQHMTEVVRRCPHHE  180
            SVTCTYSPALNKMFCQLAKTCPVQLWVDSTPPPGTRVRAMAIYKQSQHMTEVVRRCPHHE
Sbjct  121  SVTCTYSPALNKMFCQLAKTCPVQLWVDSTPPPGTRVRAMAIYKQSQHMTEVVRRCPHHE  180

Query  181  RCSDSDGLAPPQHLIRVEGNLRVEYLDDRNTFRHSVVVPYEPPEVGSDCTTIHYNYMCNS  240
            RCSDSDGLAPPQHLIRVEGNLRVEYLDDRNTFRHSVVVPYEPPEVGSDCTTIHYNYMCNS
Sbjct  181  RCSDSDGLAPPQHLIRVEGNLRVEYLDDRNTFRHSVVVPYEPPEVGSDCTTIHYNYMCNS  240

Query  241  SCMGGMNRRPILTIITLEDSSGNLLGRNSFEVHVCACPGRDRRTEEENLRKKGEPHHELP  300
            SCMGGMNRRPILTIITLEDSSGNLLGRNSFEV VCACPGRDRRTEEENLRKKGEPHHELP
Sbjct  241  SCMGGMNRRPILTIITLEDSSGNLLGRNSFEVRVCACPGRDRRTEEENLRKKGEPHHELP  300

Query  301  PGSTKRALSNNTSSSPQPKKKPLDGEYFTLQIRGRERFEMFRELNEALELKDAQAGKEPG  360
            PGSTKRAL NNTSSSPQPKKKPLDGEYFTLQIRGRERFEMFRELNEALELKDAQAGKEPG
Sbjct  301  PGSTKRALPNNTSSSPQPKKKPLDGEYFTLQIRGRERFEMFRELNEALELKDAQAGKEPG  360

Query  361  GSRAHSSHLKSKKGQSTSRHKKLMFKTEGPDSD*  394
            GSRAHSSHLKSKKGQSTSRHKKLMFKTEGPDSD*
Sbjct  361  GSRAHSSHLKSKKGQSTSRHKKLMFKTEGPDSD*  394
```

Appendix Figure 9. Comparison of the amino acid sequence of TP53 WT insert with TP53 R175H (A), R248W (B) and R273H (C) inserts to verify the mutation status on the BLAST tool.

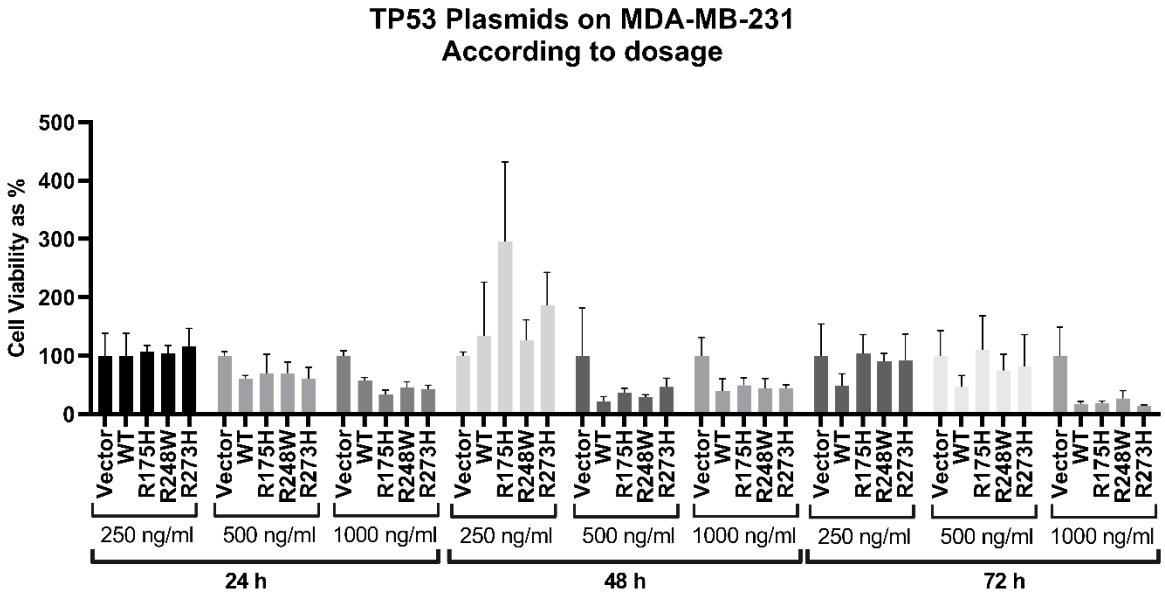

Appendix Figure 10. Whole data of relative cell viability assay on MDA-MB-231 cell line treated with WT and mutant TP53 overexpressed vectors at different concentrations over 24h, 48h, and 72h. Data is represented in percentage format, and error bars are determined according to Mean±SD values.

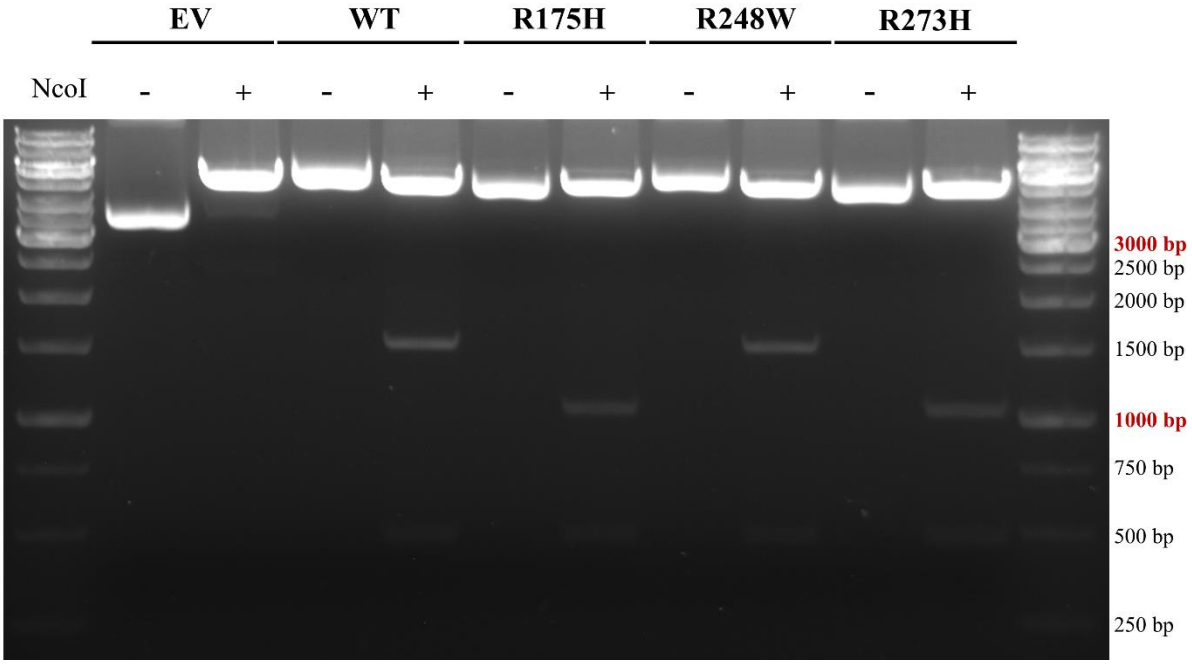

Appendix Figure 11. Gel electrophoresis result of pBabe-puro (EV) and pBabe-puro TP53 wild-type (WT), R175H mutant (R175H), R248W mutant (R248W) and R273H mutant (R273H) plasmids with NcoI restriction digestion enzyme.

6. References

Ahn, H. J., Jung, S. J., Kim, T. H., Oh, M. K., & Yoon, H.-K. (2015). Differences in Clinical Outcomes between Luminal A and B Type Breast Cancers according to the St. Gallen Consensus 2013. *Journal of Breast Cancer*, *18*(2), 149. https://doi.org/10.4048/jbc.2015.18.2.149

Appella, E., & Anderson, C. W. (2001). Post-translational modifications and activation of p53 by genotoxic stresses. *European Journal of Biochemistry*, *268*(10), 2764–2772. https://doi.org/10.1046/j.1432-1327.2001.02225.x

Baker, S. J., Markowitz, S., Fearon, E. R., Willson, J. K. V., & Vogelstein, B. (1990). Suppression of human colorectal carcinoma cell growth by wild-type p53. *Science (New York, N.Y.)*, *249*(4971), 912–915. https://doi.org/10.1126/SCIENCE.2144057

Barak, Y., Juven, T., Haffner, R., & Oren, M. (1993). mdm2 Expression is induced by wild type p53 activity. *EMBO Journal*, *12*(2), 461–468. https://doi.org/10.1002/j.1460-2075.1993.tb05678.x

Barroso-Sousa, R., & Metzger-Filho, O. (2016). Differences between invasive lobular and invasive ductal carcinoma of the breast: Results and therapeutic implications. In *Therapeutic Advances in Medical Oncology* (Vol. 8, Issue 4, pp. 261–266). SAGE Publications Inc. https://doi.org/10.1177/1758834016644156

Bosch, P. S., Pepperl, J., & Basler, K. (2020). Anchor Away – A Fast, Reliable and Reversible Technique To Inhibit Proteins in Drosophila melanogaster. *G3: Genes|Genomes|Genetics*, *10*(5), 1745. https://doi.org/10.1534/G3.120.401055

Bouaoun, L., Sonkin, D., Ardin, M., Hollstein, M., Byrnes, G., Zavadil, J., & Olivier, M. (2016). TP53 Variations in Human Cancers: New Lessons from the IARC TP53 Database and Genomics Data. *Human Mutation*, *37*(9), 865–876. https://doi.org/10.1002/humu.23035

Cancer Genome Atlas Network, T. (2012). Comprehensive molecular portraits of human breast tumours. *Nature*, *490*(7418), 61–70. https://doi.org/10.1038/nature11412

Cao, R., Wang, L., Wang, H., Xia, L., Erdjument-Bromage, H., Tempst, P., Jones, R. S., & Zhang, Y. (2002). Role of histone H3 lysine 27 methylation in Polycomb-group silencing. *Science (New York, N.Y.)*, *298*(5595), 1039–1043. https://doi.org/10.1126/SCIENCE.1076997

Caussinus, E., & Affolter, M. (2016). deGradFP: A System to Knockdown GFP-Tagged Proteins. *Methods in Molecular Biology (Clifton, N.J.)*, *1478*, 177–187. https://doi.org/10.1007/978-1-4939-6371-3_9

Cho, Y., Gorina, S., Jeffrey, P. D., & Pavletich, N. P. (1994). Crystal structure of a p53 tumor suppressor-DNA complex: understanding tumorigenic mutations. *Science (New York, N.Y.)*, *265*(5170), 346–355. https://doi.org/10.1126/SCIENCE.8023157

Choi, S. H., Wright, J. B., Gerber, S. A., & Cole, M. D. (2010). Myc protein is stabilized by suppression of a novel E3 ligase complex in cancer cells. *Genes & Development*, *24*(12), 1236. https://doi.org/10.1101/GAD.1920310

Ciriello, G., Gatza, M. L., Beck, A. H., Wilkerson, M. D., Rhie, S. K., Pastore, A., Zhang, H., McLellan, M., Yau, C., Kandoth, C., Bowlby, R., Shen, H., Hayat, S., Fieldhouse, R., Lester, S. C., Tse, G. M. K., Factor, R. E., Collins, L. C., Allison, K. H., … Perou, C. M. (2015). Comprehensive Molecular Portraits of Invasive Lobular Breast Cancer. *Cell*, *163*(2), 506–519. https://doi.org/10.1016/j.cell.2015.09.033

Clift, D., McEwan, W. A., Labzin, L. I., Konieczny, V., Mogessie, B., James, L. C., & Schuh, M. (2017). A Method for the Acute and Rapid Degradation of Endogenous Proteins. *Cell*, *171*(7), 1692-1706.e18. https://doi.org/10.1016/J.CELL.2017.10.033

Cordle, J., Johnson, S., Zi Yan Tay, J., Roversi, P., Wilkin, M. B., de Madrid, B. H., Shimizu, H., Jensen, S., Whiteman, P., Jin, B., Redfield, C., Baron, M., Lea, S. M., & Handford, P. A. (2008). A conserved face of the Jagged/Serrate DSL domain is involved in Notch trans-activation and cis-inhibition. *Nature Structural & Molecular Biology*, *15*(8), 849–857. https://doi.org/10.1038/NSMB.1457

Dai, X., Li, T., Bai, Z., Yang, Y., Liu, X., Zhan, J., & Shi, B. (2015). Breast cancer intrinsic subtype classification, clinical use and future trends. In *Am J Cancer Res* (Vol. 5, Issue 10). www.ajcr.us/

Dang, N. N., Meng, X., Qin, G., An, Y., Zhang, Q. Q., Cheng, X., & Huang, S. (2020). α5-nAChR modulates melanoma growth through the Notch1 signaling pathway. *Journal of Cellular Physiology*, *235*(11), 7816–7826. https://doi.org/10.1002/JCP.29435

Dent, R., Trudeau, M., Pritchard, K. I., Hanna, W. M., Kahn, H. K., Sawka, C. A., Lickley, L. A., Rawlinson, E., Sun, P., & Narod, S. A. (2007). Triple-negative breast cancer: Clinical features and patterns of recurrence. *Clinical Cancer Research*, *13*(15), 4429–4434. https://doi.org/10.1158/1078-0432.CCR-06-3045

Donninger, H., Calvisi, D. F., Barnoud, T., Clark, J., Lee Schmidt, M., Vos, M. D., & Clark, G. J. (2015). NORE1A is a Ras senescence effector that controls the apoptotic/senescent balance of p53 via HIPK2. *Journal of Cell Biology*, *208*(6), 777–789. https://doi.org/10.1083/jcb.201408087

Du, T., Zhu, L., Levine, K. M., Tasdemir, N., Lee, A. v., Vignali, D. A. A., Houten, B. van, Tseng, G. C., & Oesterreich, S. (2018). Invasive lobular and ductal breast carcinoma differ in immune response, protein translation efficiency and metabolism. *Scientific Reports*, *8*(1), 7205. https://doi.org/10.1038/s41598-018-25357-0

Duan, L., Yao, J., Wu, X., & Fan, M. (2006). Growth suppression induced by Notch1 activation involves Wnt-beta-catenin down-regulation in human tongue carcinoma cells. *Biology of the Cell*, *98*(8), 479–490. https://doi.org/10.1042/BC20060020

Duffy, M. J., Synnott, N. C., & Crown, · John. (2018). Mutant p53 in breast cancer: potential as a therapeutic target and biomarker. *Breast Cancer Research and Treatment*, *170*, 213–219. https://doi.org/10.1007/s10549-018-4753-7

Enterina, J. R., Enfield, K. S. S., Anderson, C., Marshall, E. A., Ng, K. W., & Lam, W. L. (2017). DLK1-DIO3 imprinted locus deregulation in development, respiratory disease, and cancer. *Http://Dx.Doi.Org/10.1080/17476348.2017.1355241*, *11*(9), 749–761. https://doi.org/10.1080/17476348.2017.1355241

Ferlay, J., Laversanne, M., Ervik, M., Lam, F., Colombet, M., Mery, L., Piñeros, M., Znaor, A., Soerjomataram, I., & Bray, F. (2020). *Global Cancer Observatory: Cancer Tomorrow*. International Agency for Research on Cancer.

Fougner, C., Bergholtz, H., Norum, J. H., & Sørlie, T. (2020). Re-definition of claudin-low as a breast cancer phenotype. *Nature Communications*, *11*(1), 1787. https://doi.org/10.1038/s41467-020-15574-5

Fusté, N. P., Fernández-Hernández, R., Cemeli, T., Mirantes, C., Pedraza, N., Rafel, M., Torres-Rosell, J., Colomina, N., Ferrezuelo, F., Dolcet, X., & Garí, E. (2016). Cytoplasmic cyclin D1 regulates cell invasion and metastasis through the phosphorylation of paxillin. *Nature Communications*, *7*. https://doi.org/10.1038/ncomms11581

Gelmon, K., Dent, R., Mackey, J. R., Laing, K., Mcleod, D., & Verma, S. (2012). Targeting triple-negative breast cancer: Optimising therapeutic outcomes. In *Annals of Oncology* (Vol. 23, Issue 9, pp. 2223–2234). Oxford University Press. https://doi.org/10.1093/annonc/mds067

Ghafouri-Fard, S., & Taheri, M. (2019). Maternally expressed gene 3 (MEG3): A tumor suppressor long non coding RNA. *Biomedicine and Pharmacotherapy*, *118*. https://doi.org/10.1016/J.BIOPHA.2019.109129

Giacinti, C., & Giordano, A. (2006). RB and cell cycle progression. *Oncogene*, *25*, 5220–5227. https://doi.org/10.1038/sj.onc.1209615

González, M. J., Ruiz-García, A., Monsalve, E. M., Sánchez-Prieto, R., Laborda, J., Díaz-Guerra, M. J. M., & Ruiz-Hidalgo, M. J. (2015). DLK1 is a novel inflammatory inhibitor which interferes with NOTCH1 signaling in TLR-activated murine macrophages. *European Journal of Immunology*, *45*(9), 2615–2627. https://doi.org/10.1002/EJI.201545514

Green, M. R., & Sambrook, J. (2016). Precipitation of DNA with ethanol. *Cold Spring Harbor Protocols*, *2016*(12), 1116–1120. https://doi.org/10.1101/pdb.prot093377

Greife, A., Knievel, J., Ribarska, T., Niegisch, G., & Schulz, W. A. (2014). Concomitant downregulation of the imprinted genes DLK1 and MEG3 at 14q32.2 by epigenetic mechanisms in urothelial carcinoma. *Clinical Epigenetics*, *6*(1), 1–13. https://doi.org/10.1186/1868-7083-6-29/FIGURES/6

Gubina, E., Ruiz-Hidalgo, M. J., Baladrón, V., & Laborda, J. (1999). Assignment of DLK1 to human chromosome band 14q32 by in situ hybridization. *Cytogenetic and Genome Research*, *84*(3–4), 206–207. https://doi.org/10.1159/000015259

Hainaut, P., & Pfeifer, G. P. (2016). Somatic TP53 Mutations in the Era of Genome Sequencing. *Cold Spring Harbor Perspectives in Medicine*, *6*(11), a026179. https://doi.org/10.1101/CSHPERSPECT.A026179

Hanahan, D. (2022). Hallmarks of Cancer: New Dimensions. In *Cancer Discovery* (Vol. 12, Issue 1, pp. 31–46). American Association for Cancer Research Inc. https://doi.org/10.1158/2159-8290.CD-21-1059

Hanahan, D., & Weinberg, R. A. (2000). The Hallmarks of Cancer Review evolve progressively from normalcy via a series of pre. In *Cell* (Vol. 100).

Hanahan, D., & Weinberg, R. A. (2011). Hallmarks of cancer: The next generation. In *Cell* (Vol. 144, Issue 5, pp. 646–674). https://doi.org/10.1016/j.cell.2011.02.013

Happo, L., Cragg, M. S., Phipson, B., Haga, J. M., Jansen, E. S., Herold, M. J., Dewson, G., Michalak, E. M., Vandenberg, C. J., Smyth, G. K., Strasser, A., Cory, S., & Scott, C. L. (2010). Maximal killing of lymphoma cells by DNA damage–inducing therapy requires

not only the p53 targets Puma and Noxa, but also Bim. *Blood*, *116*(24), 5256–5267. https://doi.org/10.1182/blood-2010-04-280818

Hayashita, Y., Osada, H., Tatematsu, Y., Yamada, H., Yanagisawa, K., Tomida, S., Yatabe, Y., Kawahara, K., Sekido, Y., & Takahashi, T. (2005a). A polycistronic microRNA cluster, miR-17-92, is overexpressed in human lung cancers and enhances cell proliferation. *Cancer Research*, *65*(21), 9628–9632. https://doi.org/10.1158/0008-5472.CAN-05-2352

Hayashita, Y., Osada, H., Tatematsu, Y., Yamada, H., Yanagisawa, K., Tomida, S., Yatabe, Y., Kawahara, K., Sekido, Y., & Takahashi, T. (2005b). A polycistronic microRNA cluster, miR-17-92, is overexpressed in human lung cancers and enhances cell proliferation. *Cancer Research*, *65*(21), 9628–9632. https://doi.org/10.1158/0008-5472.CAN-05-2352

He, G., Siddik, Z. H., Huang, Z., Wang, R., Koomen, J., Kobayashi, R., Khokhar, A. R., & Kuang, J. (2005). Induction of p21 by p53 following DNA damage inhibits both Cdk4 and Cdk2 activities. *Oncogene*, *24*(18), 2929–2943. https://doi.org/10.1038/sj.onc.1208474

Henning, K., Heering, J., Schwanbeck, R., Schroeder, T., Helmbold, H., Schäfer, H., Deppert, W., Kim, E., & Just, U. (2008). Notch1 activation reduces proliferation in the multipotent hematopoietic progenitor cell line FDCP-mix through a p53-dependent pathway but Notch1 effects on myeloid and erythroid differentiation are independent of p53. *Cell Death and Differentiation*, *15*(2), 398–407. https://doi.org/10.1038/SJ.CDD.4402277

Hermeking, H., Lengauer, C., Polyak, K., He, T.-C., Zhang, L., Thiagalingam, S., Kinzler, K. W., & Vogelstein, B. (1997). 14-3-3σ Is a p53-Regulated Inhibitor of G2/M Progression. *Molecular Cell*, *1*(1), 3–11. https://doi.org/10.1016/S1097-2765(00)80002-7

Huang, C.-C., Cheng, S.-H., Wu, C.-H., Li, W.-Y., Wang, J.-S., Kung, M.-L., Chu, T.-H., Huang, S.-T., Feng, C.-T., Huang, S.-C., & Tai, M.-H. (2019). *Delta-like 1 homologue promotes tumorigenesis and epithelial-mesenchymal transition of ovarian high-grade serous carcinoma through activation of Notch signaling*. https://doi.org/10.1038/s41388-018-0658-5

Huang, J., Zhang, X., Zhang, M., Zhu, J. de, Zhang, Y. L., Lin, Y., Wang, K. S., Qi, X. F., Zhang, Q., Liu, G. Z., Yu, J., Cui, Y., Yang, P. Y., Wang, Z. Q., & Han, Z. G. (2007). Up-regulation of DLK1 as an imprinted gene could contribute to human hepatocellular carcinoma. *Carcinogenesis*, *28*(5), 1094–1103. https://doi.org/10.1093/CARCIN/BGL215

Jin, Z. H., Yang, R. J., Dong, B., & Xing, B. C. (2008). Progenitor gene DLK1 might be an independent prognostic factor of liver cancer. *Http://Dx.Doi.Org/10.1517/14712598.8.4.371*, *8*(4), 371–377. https://doi.org/10.1517/14712598.8.4.371

Kao, S.-H., Wang, W.-L., Chen, C.-Y., Chang, Y.-L., Wu, Y.-Y., Wang, Y.-T., Wang, S.-P., Nesvizhskii, A. I., Chen, Y.-J., Hong, T.-M., & Yang, P.-C. (2015). Analysis of Protein Stability by the Cycloheximide Chase Assay. *Bio-Protocol*, *5*(1). https://doi.org/10.21769/BIOPROTOC.1374

Kim, S., Park, S., Oh, J. H., Lee, S. S., Lee, Y., & Choi, J. (2022). MicroRNA-18a regulates the metastatic properties of oral squamous cell carcinoma cells via HIF-1α expression. *BMC Oral Health*, *22*(1), 378. https://doi.org/10.1186/s12903-022-02425-6

Klein, M. E., Dickson, M. A., Antonescu, C., Li, •, Qin, -Xuan, Scott, •, Dooley, J., Barlas, A., Manova, K., Gary, •, Schwartz, K., Crago, A. M., Singer, • Samuel, Koff, • Andrew, & Tap, W. D. (2018). PDLIM7 and CDH18 regulate the turnover of MDM2 during CDK4/6 inhibitor therapy-induced senescence. *Oncogene*, *37*, 5066–5078. https://doi.org/10.1038/s41388-018-0332-y

Köker, Ş. C. (2018). *Effects of Cholinergic Receptor Nicotinic Alpha 5 (CHRNA5) RNAi on apoptosis, DNA damage response, drug sensitivity, and HSA-MIR-495-3P overexpression in breast cancer*. http://repository.bilkent.edu.tr/handle/11693/48222

Koker, S. C., Jahja, E., Shehwana, H., Keskus, A. G., & Konu, O. (2018). Cholinergic Receptor Nicotinic Alpha 5 (CHRNA5) RNAi is associated with cell cycle inhibition, apoptosis, DNA damage response and drug sensitivity in breast cancer. *PloS One*, *13*(12). https://doi.org/10.1371/JOURNAL.PONE.0208982

Kovatcheva, M., Liao, W., Klein, M. E., Robine, N., Geiger, H., Crago, A. M., Dickson, M. A., Tap, W. D., Singer, S., & Koff, A. (2017). ATRX is a regulator of therapy induced senescence in human cells. *Nature Communications*, *8*(1). https://doi.org/10.1038/S41467-017-00540-5

Kovatcheva, M., Liu, D. D., Dickson, M. A., Klein, M. E., O'Connor, R., Wilder, F. O., Socci, N. D., Tap, W. D., Schwartz, G. K., Singer, S., Crago, A. M., & Koff, A. (2015). MDM2 turnover and expression of ATRX determine the choice between quiescence and senescence in response to CDK4 inhibition. *Oncotarget*, *6*(10), 8226. https://doi.org/10.18632/ONCOTARGET.3364

Kubbutat, M. H. G., Jones, S. N., & Vousden, K. H. (1997). Regulation of p53 stability by Mdm2. *Nature*, *387*(6630), 299–303. https://doi.org/10.1038/387299a0

Laborda, J. (2000). The role of the epidermal growth factor-like protein dlk in cell differentiation. *Histol Histopathol*. https://doi.org/10.14670/HH-15.119

Lane, D. P. (1992). p53, guardian of the genome. *Nature*, *358*(6381), 15–16. https://doi.org/10.1038/358015a0

Lee, D., Yoon, S. H., Lee, H. J., Jo, K. W., Park, B. C., Kim, I. S., Choi, Y., Lim, J. C., & Park, Y. W. (2016). Human soluble delta-like 1 homolog exerts antitumor effects in vitro and in vivo. *Biochemical and Biophysical Research Communications*, *475*(2), 209–215. https://doi.org/10.1016/J.BBRC.2016.05.076

Lehmann, B. D., Bauer, J. A., Chen, X., Sanders, M. E., Chakravarthy, A. B., Shyr, Y., & Pietenpol, J. A. (2011). Identification of human triple-negative breast cancer subtypes and preclinical models for selection of targeted therapies. *Journal of Clinical Investigation*, *121*(7), 2750–2767. https://doi.org/10.1172/JCI45014

Levine, A. J. (2020). p53: 800 million years of evolution and 40 years of discovery. *Nature Reviews Cancer*, *20*(8), 471–480. https://doi.org/10.1038/s41568-020-0262-1

LI, L. T., JIANG, G., CHEN, Q., & ZHENG, J. N. (2015). Ki67 is a promising molecular target in the diagnosis of cancer (Review). *Molecular Medicine Reports*, *11*(3), 1566–1572. https://doi.org/10.3892/mmr.2014.2914

Li, Z., Hu, P., Tu, J., & Yu, N. (2016). Luminal B breast cancer: patterns of recurrence and clinical outcome. *Oncotarget*, *7*(40), 65024–65033. https://doi.org/10.18632/oncotarget.11344

Livak, K. J., & Schmittgen, T. D. (2001). Analysis of Relative Gene Expression Data Using Real-Time Quantitative PCR and the 2−ΔΔCT Method. *Methods*, *25*(4), 402–408. https://doi.org/10.1006/METH.2001.1262

Llanos, S., Clark, P. A., Rowe, J., & Peters, G. (2001). Stabilization of p53 by p14 ARF without relocation of MDM2 to the nucleolus. In *NATURE CELL BIOLOGY* (Vol. 3). https://doi.org/https://doi.org/10.1038/35074506

Loi, S., Sotiriou, C., Haibe-Kains, B., Lallemand, F., Conus, N. M., Piccart, M. J., Speed, T. P., & McArthur, G. A. (2009). Gene expression profiling identifies activated growth factor signaling in poor prognosis (Luminal-B) estrogen receptor positive breast cancer. *BMC Medical Genomics*, *2*(1), 37. https://doi.org/10.1186/1755-8794-2-37

Macdonald, L., Taylor, G. C., Brisbane, J. M., Christodoulou, E., Scott, L., von Kriegsheim, A., Rossant, J., Gu, B., & Wood, A. J. (2022). Rapid and specific degradation of endogenous proteins in mouse models using auxin-inducible degrons. *ELife*, *11*. https://doi.org/10.7554/ELIFE.77987

Matsubara, H., Takeuchi, T., Nishikawa, E., Yanagisawa, K., Hayashita, Y., Ebi, H., Yamada, H., Suzuki, M., Nagino, M., Nimura, Y., Osada, H., & Takahashi, T. (2007). Apoptosis induction by antisense oligonucleotides against miR-17-5p and miR-20a in lung cancers overexpressing miR-17-92. *Oncogene*, *26*(41), 6099–6105. https://doi.org/10.1038/sj.onc.1210425

McManus, M. T. (2003). MicroRNAs and cancer. *Seminars in Cancer Biology*, *13*(4), 253–258. https://doi.org/10.1016/S1044-579X(03)00038-5

Mei, B., Zhao, L., Chen, L., & Sul, H. S. (2002). Only the large soluble form of preadipocyte factor-1 (Pref-1), but not the small soluble and membrane forms, inhibits adipocyte differentiation : role of alternative splicing. *Biochem. J*, *364*, 137–144.

Midgley, C. A., Desterro, J. M., Saville, M. K., Howard, S., Sparks, A., Hay, R. T., & Lane, D. P. (2000). An N-terminal p14ARF peptide blocks Mdm2-dependent ubiquitination in vitro and can activate p53 in vivo. *Oncogene*, *19*(19), 2312–2323. https://doi.org/10.1038/sj.onc.1203593

Mondal, T., Subhash, S., Vaid, R., Enroth, S., Uday, S., Reinius, B., Mitra, S., Mohammed, A., James, A. R., Hoberg, E., Moustakas, A., Gyllensten, U., Jones, S. J. M., Gustafsson, C. M., Sims, A. H., Westerlund, F., Gorab, E., & Kanduri, C. (2015). *MEG3 long noncoding RNA regulates the TGF-β pathway genes through formation of RNA–DNA triplex structures*. https://doi.org/10.1038/ncomms8743

Monti, P., Menichini, P., Speciale, A., Cutrona, G., Fais, F., Taiana, E., Neri, A., Bomben, R., Gentile, M., Gattei, V., Ferrarini, M., Morabito, F., & Fronza, G. (2020). Heterogeneity of TP53 Mutations and P53 Protein Residual Function in Cancer: Does It Matter? *Frontiers in Oncology*, *10*, 2313. https://doi.org/10.3389/FONC.2020.593383/BIBTEX

Morgenstern, J. P., & Land, H. (1990). Advanced mammalian gene transfer: high titre retroviral vectors with multiple drug selection markers and a complementary helper-free packaging cell line. *Nucleic Acids Research*, *18*(12), 3587–3596. https://doi.org/10.1093/NAR/18.12.3587

Nishina, H. (2012). HDlk-1: A cell surface marker common to normal hepatic stem/progenitor cells and carcinomas. *Journal of Biochemistry*, *152*(2), 121–123. https://doi.org/10.1093/jb/mvs069

Nueda, M. L., Naranjo, A. I., Baladrón, V., & Laborda, J. (2017). Different expression levels of DLK1 inversely modulate the oncogenic potential of human MDA-MB-231 breast cancer cells through inhibition of NOTCH1 signaling. *The FASEB Journal*, *31*(8), 3484–3496. https://doi.org/10.1096/FJ.201601341RRR

Nueda, M.-L., Baladrón, V., Sánchez-Solana, B., Ballesteros, M.-Á., & Laborda∗, J. (2006). *The EGF-like Protein dlk1 Inhibits Notch Signaling and Potentiates Adipogenesis of Mesenchymal Cells*. https://doi.org/10.1016/j.jmb.2006.10.043

Peng, Y., & Croce, C. M. (2016). The role of MicroRNAs in human cancer. *Signal Transduction and Targeted Therapy 2016 1:1*, *1*(1), 1–9. https://doi.org/10.1038/sigtrans.2015.4

Perou, C. M., Sørlie, T., Eisen, M. B., van de Rijn, M., Jeffrey, S. S., Rees, C. A., Pollack, J. R., Ross, D. T., Johnsen, H., Akslen, L. A., Fluge, Ø., Pergamenschikov, A., Williams, C., Zhu, S. X., Lønning, P. E., Børresen-Dale, A.-L., Brown, P. O., & Botstein, D. (2000). Molecular portraits of human breast tumours. *Nature*, *406*(6797), 747–752. https://doi.org/10.1038/35021093

Pommier, R. M., Sanlaville, A., Tonon, L., Kielbassa, J., Thomas, E., Ferrari, A., Sertier, A. S., Hollande, F., Martinez, P., Tissier, A., Morel, A. P., Ouzounova, M., & Puisieux, A. (2020). Comprehensive characterization of claudin-low breast tumors reflects the impact of the cell-of-origin on cancer evolution. *Nature Communications*, *11*(1). https://doi.org/10.1038/s41467-020-17249-7

Prat, A., Parker, J. S., Karginova, O., Fan, C., Livasy, C., Herschkowitz, J. I., He, X., & Perou, C. M. (2010). Phenotypic and molecular characterization of the claudin-low intrinsic subtype of breast cancer. *Breast Cancer Research*, *12*(5), R68. https://doi.org/10.1186/bcr2635

Purow, B. W., Sundaresan, T. K., Burdick, M. J., Kefas, B. A., Comeau, L. D., Hawkinson, M. P., Su, Q., Kotliarov, Y., Lee, J., Zhang, W., & Fine, H. A. (2008). Notch-1 regulates transcription of the epidermal growth factor receptor through p53. *Carcinogenesis*, *29*(5), 918–925. https://doi.org/10.1093/CARCIN/BGN079

Qi, R., An, H., Yu, Y., Zhang, M., Liu, S., Xu, H., Guo, Z., Cheng, T., & Cao, X. (2003). Notch1 Signaling Inhibits Growth of Human Hepatocellular Carcinoma through Induction of Cell Cycle Arrest and Apoptosis. *CANCER RESEARCH*, *63*, 8323–8329. http://aacrjournals.org/cancerres/article-pdf/63/23/8323/2510619/zch02303008323.pdf

Riley, M. F., & Lozano, G. (2012). The Many Faces of MDM2 Binding Partners. *Genes & Cancer*, *3*(3–4), 226. https://doi.org/10.1177/1947601912455322

Rocha, S. T. da, Edwards, C. A., Ito, M., Ogata, T., & Ferguson-Smith, A. C. (2008). Genomic imprinting at the mammalian Dlk1-Dio3 domain. *Trends in Genetics*, *24*(6), 306–316. https://doi.org/10.1016/J.TIG.2008.03.011

Rolley, N., Butcher, S., & Milner, J. (1995). Specific DNA binding by different classes of human p53 mutants. *Oncogene*, *11*(4), 763–770. https://europepmc.org/article/med/7651740

Rufini, A., Tucci, P., Celardo, I., & Melino, G. (2013). Senescence and aging: the critical roles of p53. *Oncogene*, *32*, 5129–5143. https://doi.org/10.1038/onc.2012.640

Sáez-Cirión, A., & Manel, N. (2018). Immune Responses to Retroviruses. *Https://Doi.Org/10.1146/Annurev-Immunol-051116-052155*, *36*, 193–220. https://doi.org/10.1146/ANNUREV-IMMUNOL-051116-052155

Samwer, M., Schneider, M. W. G., Hoefler, R., Schmalhorst, P. S., Jude, J. G., Zuber, J., & Gerlich, D. W. (2017). DNA Cross-Bridging Shapes a Single Nucleus from a Set of Mitotic Chromosomes. *Cell*, *170*(5), 956-972.e23. https://doi.org/10.1016/j.cell.2017.07.038

Sarkar, S., Horn, G., Moulton, K., Oza, A., Byler, S., Kokolus, S., & Longacre, M. (2013). Cancer Development, Progression, and Therapy: An Epigenetic Overview. *OPEN ACCESS Int. J. Mol. Sci*, *14*, 14. https://doi.org/10.3390/ijms141021087

Shehwana, H., Keskus, A. G., Ozdemir, S. E., Acikgöz, A. A., Biyik-Sit, R., Cagnan, I., Gunes, D., Jahja, E., Cingir-Koker, S., Olmezer, G., Sucularli, C., & Konu, O. (2021). CHRNA5 belongs to the secondary estrogen signaling network exhibiting prognostic significance in breast cancer. *Cellular Oncology (Dordrecht)*, *44*(2), 453–472. https://doi.org/10.1007/S13402-020-00581-X

Sheikh, M., & Fornace, A. (2000). Death and decoy receptors and p53-mediated apoptosis. *Leukemia*, *14*(8), 1509–1513. https://doi.org/10.1038/sj.leu.2401865

Shu, J., Su, G., Zhang, J., Liu, Z., Chang, R., Wang, Q., & Yang, P. (2021). Analyses of circRNA and mRNA Profiles in Vogt–Koyanagi–Harada Disease. *Frontiers in Immunology*, *12*. https://doi.org/10.3389/fimmu.2021.738760

Skibinski, A., & Kuperwasser, C. (2015). The origin of breast tumor heterogeneity. *Oncogene*, *34*, 5309–5316. https://doi.org/10.1038/onc.2014.475

Slamon, D. J., Clark, G. M., Wong, S. G., Levin, W. J., Ullrich, A., & McGuire, W. L. (1987). Human Breast Cancer: Correlation of Relapse and Survival with Amplification of the HER-2/neu Oncogene. *Science*, *235*(4785), 177–182. https://doi.org/10.1126/science.3798106

Sørlie, T., Perou, C. M., Tibshirani, R., Aas, T., Geisler, S., Johnsen, H., Hastie, T., Eisen, M. B., van de Rijn, M., Jeffrey, S. S., Thorsen, T., Quist, H., Matese, J. C., Brown, P. O., Botstein, D., Lønning, P. E., & Børresen-Dale, A.-L. (2001). Gene expression patterns of breast carcinomas distinguish tumor subclasses with clinical implications. *Proceedings of the National Academy of Sciences*, *98*(19), 10869–10874. https://doi.org/10.1073/pnas.191367098

Sun, M., Xia, R., Jin, F., Xu, T., Liu, Z., De, W., & Liu, X. (2014). Downregulated long noncoding RNA MEG3 is associated with poor prognosis and promotes cell proliferation in gastric cancer. *Tumour Biol*, *35*(2), 1065–1073. https://doi.org/10.1007/s13277-013-1142-z

Sung, H., Ferlay, J., Siegel, R. L., Laversanne, M., Soerjomataram, I., Jemal, A., & Bray, F. (2021). Global Cancer Statistics 2020: GLOBOCAN Estimates of Incidence and Mortality Worldwide for 36 Cancers in 185 Countries. *CA: A Cancer Journal for Clinicians*, *71*(3), 209–249. https://doi.org/10.3322/caac.21660

Tagawa, H., Karube, K., Tsuzuki, S., Ohshima, K., & Seto, M. (2007). Synergistic action of the microRNA-17 polycistron and Myc in aggressive cancer development. *Cancer Science*, *98*(9), 1482–1490. https://doi.org/10.1111/j.1349-7006.2007.00531.x

Takagi, H., Zhao, S., Muto, S., Yokouchi, H., Nishihara, H., Harada, T., Yamaguchi, H., Mine, H., Watanabe, M., Ozaki, Y., Inoue, T., Yamaura, T., Fukuhara, M., Okabe, N., Matsumura, Y., Hasegawa, T., Osugi, J., Hoshino, M., Higuchi, M., … Suzuki, H. (2021). Delta-like 1 homolog (DLK1) as a possible therapeutic target and its application to radioimmunotherapy using 125I-labelled anti-DLK1 antibody in lung cancer models (HOT1801 and FIGHT004). *Lung Cancer*, *153*, 134–142. https://doi.org/10.1016/J.LUNGCAN.2021.01.014

Tanimizu, N., Tsujimura, T., Takahide, K., Kodama, T., Nakamura, K., & Miyajima, A. (2004). Expression of Dlk/Pref-1 defines a subpopulation in the oval cell compartment of rat liver. *Gene Expression Patterns*, *5*(2), 209–218. https://doi.org/10.1016/j.modgep.2004.08.003

Terashima, M., Tange, S., Ishimura, A., & Suzuki, T. (2017). MEG3 long noncoding RNA contributes to the epigenetic regulation of epithelial-mesenchymal transition in lung cancer cell lines. *Journal of Biological Chemistry*, *292*(1), 82–99. https://doi.org/10.1074/JBC.M116.750950

The TP53 Database | ISB-CGC. (n.d.). Retrieved September 9, 2022, from https://tp53.isb-cgc.org/

Tiryaki, R. S. (2019). *Effects of miR-376 family miRNAs on CHRNA5 depleted MCF7 cell line model and co-culture competition studies*. http://repository.bilkent.edu.tr/handle/11693/52395

Tornehave, D., Jansen, P., Teisner, B., Rasmussen, H. B., Chemnitz, J., & Moscoso, G. (1993). Fetal antigen 1 (FA1) in the human pancreas: cell type expression, topological and quantitative variations during development. *Anatomy and Embryology 1993 187:4*, *187*(4), 335–341. https://doi.org/10.1007/BF00185891

Weigelt, B., Horlings, H. M., Kreike, B., Hayes, M. M., Hauptmann, M., Wessels, L. F. A., de Jong, D., van de Vijver, M. J., Van't Veer, L. J., & Peterse, J. L. (2008). Refinement of breast cancer classification by molecular characterization of histological special types. *Journal of Pathology*, *216*(2), 141–150. https://doi.org/10.1002/path.2407

Williams, A. B., & Schumacher, B. (2016). p53 in the DNA-Damage-Repair Process. *Cold Spring Harbor Perspectives in Medicine*, *6*(5), a026070. https://doi.org/10.1101/cshperspect.a026070

Wilson, L. C., Baek, S. J., Call, A., & Eling, T. E. (2003). Nonsteroidal anti-inflammatory drug-activated gene (NAG-1) is induced by genistein through the expression of P53 in colorectal cancer cells. *International Journal of Cancer*, *105*(6), 747–753. https://doi.org/10.1002/IJC.11173

Xu, H., Zhang, B., Yang, Y., Li, Z., Zhao, P., Wu, W., Zhang, H., & Mao, J. (2020). LncRNA MIR4435-2HG potentiates the proliferation and invasion of glioblastoma cells via modulating miR-1224-5p/TGFBR2 axis. *Journal of Cellular and Molecular Medicine*, *24*(11), 6362–6372. https://doi.org/10.1111/jcmm.15280

Yamakuchi, M., Ferlito, M., & Lowenstein, C. J. (2008). *miR-34a repression of SIRT1 regulates apoptosis*. www.pnas.org/cgi/content/full/

Yanai, H., Nakamura, K., Hijioka, S., Kamei, A., Ikari, T., Ishikawa, Y., Shinozaki, E., Mizunuma, N., Hatake, K., & Miyajima, A. (2010). Dlk-1, a cell surface antigen on foetal hepatic stem/progenitor cells, is expressed in hepatocellular, colon, pancreas and breast carcinomas at a high frequency. *Journal of Biochemistry*, *148*(1), 85–92. https://doi.org/10.1093/JB/MVQ034

Ye, J., Coulouris, G., Zaretskaya, I., Cutcutache, I., Rozen, S., & Madden, T. L. (2012). Primer-BLAST: A tool to design target-specific primers for polymerase chain reaction. *BMC Bioinformatics*, *13*(1), 134. https://doi.org/10.1186/1471-2105-13-134

Yersal, O. (2014). Biological subtypes of breast cancer: Prognostic and therapeutic implications. *World Journal of Clinical Oncology*, *5*(3), 412. https://doi.org/10.5306/wjco.v5.i3.412

Zhang, B., Pan, X., Cobb, G. P., & Anderson, T. A. (2007). microRNAs as oncogenes and tumor suppressors. *Developmental Biology*, *302*(1), 1–12. https://doi.org/10.1016/j.ydbio.2006.08.028

Zhang, W.-W., Geng, X., & Zhang, W.-Q. (2019). Downregulation of lncRNA MEG3 attenuates high glucose-induced cardiomyocytes injury by inhibiting mitochondria-mediated apoptosis pathway. *European Review for Medical and Pharmacological Sciences*, *23*(17), 7599–7604. https://doi.org/10.26355/eurrev_201909_18881

Zhao, H. (2021). The prognosis of invasive ductal carcinoma, lobular carcinoma and mixed ductal and lobular carcinoma according to molecular subtypes of the breast. *Breast Cancer*, *28*(1), 187–195. https://doi.org/10.1007/s12282-020-01146-4

Zhou, Y., Zhong, Y., Wang, Y., Zhang, X., Batista, D. L., Gejman, R., Ansell, P. J., Zhao, J., Weng, C., & Klibanski, A. (2007). Activation of p53 by MEG3 Non-coding RNA. *Journal of Biological Chemistry*, *282*(34), 24731–24742. https://doi.org/10.1074/JBC.M702029200